



R. D. RADECKI

PH. D





This is to certify that the

dissertation entitled

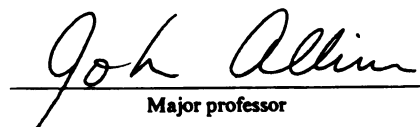
The Gas Phase Chemistry of Metal and Metal-
Containing Ions with Amines and Alkanes

presented by

Barbara Diane Radecki

has been accepted towards fulfillment
of the requirements for

Ph.D. degree in Chemistry


Major professor

Date 14 Aug. 85



RETURNING MATERIALS:

Place in book drop to
remove this checkout from
your record. FINES will
be charged if book is
returned after the date
stamped below.

--	--	--

**THE GAS PHASE CHEMISTRY OF METAL AND METAL-CONTAINING
IONS WITH AMINES AND ALKANES**

by

Barbara Diane Radecki

A DISSERTATION

**Submitted to
Michigan State University
in partial fulfillment of the requirements
for the degree of
DOCTOR OF PHILOSOPHY**

Department of Chemistry

1985

ABSTRACT

THE GAS PHASE CHEMISTRY OF METAL AND METAL-CONTAINING IONS WITH AMINES AND ALKANES

by

Barbara Diane Radecki

The gas phase chemistry of metal and metal-containing ions with amines and alkanes is presented. The three step mechanistic sequence, metal insertion/ β -hydrogen shift/competitive ligand loss, is used to explain the formation of the observed product ions in these reactions.

The reactions of cobalt and cobalt-containing ions with secondary and tertiary amines serve to illustrate the utility of metal ions as chemical ionization reagents. The product ions observed in the reactions of the various amines are found to be dependent upon the structure of the amine being analyzed. Molecular weight information is apparent from ligand substitution reactions.

The metal insertion step as it occurs in the reactions of Fe^+ , Co^+ and Ni^+ with linear alkanes is examined. The relationship between the metal insertion intermediates formed in the first step of the mechanism and final product distributions is presented. Preferential insertion of M^+ into specific C-C bonds in alkanes is noted. A correlation

between preference for insertion into a particular C-C skeletal bond and the ionization potentials of the alkyl radicals formed when the C-C bond is cleaved to form $R-M^+-R'$ is discussed. This correlation suggests that as the $IP(C_nH_{2n+1})$ decreases, $D(M^+-C_nH_{2n+1})$ increases, implying that the insertion intermediates involving those in which the sum of the two M^+-R bonds is largest are formed preferentially.

Finally the chemistry observed with linear and branched alkanes when one or two ligands such as CO or PF_3 are bound to the metal ion is examined. Ion/induced dipole interaction energy calculations are presented. The feasibility of an intact alkane displacing a CO or PF_3 ligand is established. Differences in the chemistry of M^+ and ML^+ ($n=1,2$) are explained on the basis of steric effects. Parallels between gas phase and condensed phase alkane chemistry are discussed.

This dissertation is dedicated
to my husband, Pat, my three
beautiful children, Alicia,
Kathleen and Michael and to my
Mother and Father.

ACKNOWLEDGMENTS

First, the author gratefully acknowledges the assistance and guidance of her research advisor, Dr. John Allison. John has been helpful and conscientious as a research director as well as a good friend. His efforts have always been appreciated.

I would also like to thank Tony, Mac, D.B. and Rich for the friendship and support they provided to me during my ICR years at M.S.U.

TABLE OF CONTENTS

	PAGE
LIST OF TABLES	v
LIST OF FIGURES	viii
LIST OF SCHEMES	ix
CHAPTER 1 - INTRODUCTION	1
CHAPTER 2 - PRINCIPLES OF OPERATION OF ICR	4
CHAPTER 3 - OVERVIEW OF GAS PHASE TRANSITION METAL STUDIES	15
CHAPTER 4 - EXPERIMENTAL	26
CHAPTER 5 - GAS PHASE CHEMISTRY OF $\text{Co}(\text{CO})_3\text{NO}$ WITH SECONDARY AND TERTIARY AMINES	30
CHAPTER 6 - THE PREFERENCE OF Fe^+ , Co^+ and Ni^+ FOR INSERTION INTO THE C-C BONDS OF LINEAR ALKANES	51
CHAPTER 7 - LIGAND EFFECTS	97
CHAPTER 8 - CONCLUSION	147
LIST OF REFERENCES	151

LIST OF TABLES

Table	Page
1 Reactions Observed for Secondary Amines, Tertiary Amines and Analogous Ethers	31
2 Product Distributions Observed in 2:1 Mixture Methane to ML_n	56
3 Product Distributions Observed in 2:1 Mixture Ethane to ML_n	56
4 Product Distributions Observed in 2:1 Mixture Propane to ML_n	57
5 Product Distributions Observed in 2:1 Mixture Butane to ML_n	58
6 Product Distributions Observed in 2:1 Mixture Pentane to ML_n	59
7 Product Distributions Observed in 2:1 Mixture Hexane to ML_n	60
8 Product Distributions Observed in 2:1 Mixture Heptane to ML_n	62
9 Product Distributions Observed in 2:1 Mixture Octane to ML_n	63
10 Product Distributions Observed in 2:1 Mixture Nonane to ML_n	65
11 Product Distributions Observed in 2:1 Mixture Decane to ML_n	67
12 Product Distributions Observed in 2:1 Mixture 2-Methylpropane to ML_n	69
13 Product Distributions Observed in 2:1 Mixture 2,2-Dimethylpropane to ML_n	70
14 Product Distributions Observed in 2:1 Mixture 3-Methylbutane to ML_n	71
15 Product Distributions Observed in 2:1 Mixture 2,3-Dimethylbutane to ML_n	73

Table	Page
16 Product Distributions Observed in 2,2-Dimethylbutane to ML_n :.....	74
17 Product Distributions Observed in 2:1 Mixture 2,2,3,3-Tetramethylbutane to ML_n	75
18 Product Distributions Observed in 2:1 Mixture 3-Methylpentane to ML_n	76
19 Product Distributions Observed in 2:1 Mixture 2,4-Dimethylpentane to ML_n	77
20 Product Distributions Observed in 2:1 Mixture 2,3,4-Trimethylpentane to ML_n	78
21 Product Distributions Observed in 2:1 Mixture 2,2,4-Trimethylpentane to ML_n	80
22 Per Cent (1,2) vs. (1,4) Dehydrogenation in the Reactions of M^+ with Deuterated Butane, Pentane and Hexane.....	84
23 Preference of Fe^+ , Co^+ and Ni^+ for C-C Bond Insertion in Linear Alkanes	87
24 Alkyl Radical Ionization Potentials and Bond Strengths of Various Atomic Cations.....	90
25 Results of Polarizability and Energy Calculations for Linear Alkanes Interacting with a Point Charge	107
26 M^+-L Bond Strengths	109
27 Bond by Bond Breakdown of $U(r)$ for "Arrow Length" of 1 Å	119
28 Bond by Bond Breakdown of $U(R)$ for "Arrow Length" of 2 Å	120
29 Sum of the Energies of Interaction Between a Charge and the three C-C Bonds of Butane.....	122
30 Interaction Energy Between M^+ and the Carbon and Hydrogen Atoms of Butane.....	126

Table	Page
31 Relative Rates in 2:1 Mixtures of Alkane to Co(CO) ₃ NO	138
32 Relative Rates in 2:1 Mixtures of Alkane to Ni(CO) ₄	139
33 Relative Rates in 2:1 Mixtures of Alkane to Ni(PF ₃) ₄	140

LIST OF FIGURES

Figure	Page
1	Block Diagram of ICR Spectrometer for Single Resonance Experiment6
2	The ICR Cell6
3	The Drift Velocity10
4	Correlation Between Priority of Attack and the Ionization Potential Sums91
5	Plot of $-U(r)$ vs. r , Including $D(M^+-L)$110
6	Relationship Between Charge Location and C-C Bonds of Butane116
7	Angle and Distance Measurements for Charge Located at B117
8	Ligand Substitution Patterns127
9	Definition of the Cone Angle134

LIST OF SCHEMES

Page

SCHEME 1	38
SCHEME 2	43
SCHEME 3	49
SCHEME 4	82
SCHEME 5	100

Chapter 1

Introduction

Within the past several years, the gas phase chemistry occurring between several transition metal ions and various organic molecules has been reported.¹⁻⁵ The majority of this work has involved the characterization of the reactions of bare (+1) metal ions with polar organic molecules. Out of this early work came the formulation of a mechanism involving a metal ion insertion / β -H shift/ competitive ligand loss sequence. This mechanism has been used to explain the formation of the majority of the product ions. Its feasibility has been established through both labelling^{6,7} and energetic studies.⁸

Overall, the significance of this work is threefold. In terms of the mechanistic implications, these gas phase reactions allow one to probe the rearrangements of organic molecules on metal centers in the absence of complicating solvent molecules. Secondly, thermochemical information such as bond strengths and metal ion reaction energetics can be inferred from the results. Finally, in terms of the analytical applications, these metal ions can be assessed as chemical ionization (CI) reagents.

Note that ideal CI reagents allow for the determination of both structural and molecular weight information in regard to the analyte species.

To gain further insights into these gas phase processes, Ion Cyclotron Resonance (ICR) spectrometry is used to study the reactions of metal and metal-containing ions with amines and alkanes. First, the reactions of the electron impact fragments of $\text{Co}(\text{CO})_3\text{NO}$ with select secondary and tertiary amines will be discussed. This work represents a continuation in the characterization of the reactions of metal ions with polar organic molecules. These results will be compared to the gas phase reactions of cobalt and cobalt-containing ions with primary amines⁹ and to the chemistry observed for amines in condensed phases¹⁰. Next, the chemistry observed between the electron impact fragments of $\text{Co}(\text{CO})_3\text{NO}$, $\text{Ni}(\text{CO})_4$, $\text{Ni}(\text{PF}_3)_4$ and $\text{Fe}(\text{CO})_5$ and a series of linear and branched alkanes will be examined. The discussion of the alkane chemistry will be divided into two parts. To gain a better understanding of the insertion process, the first part will examine the metal insertion step as it occurs in linear alkanes. An ordering and explanation of the preference of M^+ ($\text{M}^+ = \text{Fe}^+, \text{Co}^+, \text{Ni}^+$) for the C-C bonds of alkanes will be established. Finally, changes observed in the chemistry of bare (+1) metal ions with alkanes

when ligands such as CO, NO or PF₃ are bound to the metal will be discussed. Parallels to condensed phase chemistry will be made.

Overall, the product ions formed in these gas phase studies yield both structural and molecular weight information. Structural information becomes apparent from a knowledge of the mechanism of interaction between metal ions and organic molecules. Molecular weight information can be obtained from ligand displacement reactions. However, before presenting the results, the basis for their interpretation must be established in an understanding of the basic principles of operation of an ICR spectrometer. This understanding, coupled with a knowledge of the pertinent research already carried out in the areas of both gas phase and condensed phase organometallic chemistry, will enable one to extract the structural, mechanistic and thermodynamic information which is inherent to the results.

Chapter 2

Principals of Operation of ICR

ICR spectrometry was developed as a mass spectrometric technique for the study of bimolecular reactions in the gas phase at low pressures. These bimolecular reactions proceed as a result of ion-neutral collisions which occur when the pressure is increased above a low "collision free" pressure of $\sim 2 \times 10^{-6}$ torr (for a reaction time of ~ 1 msec). The ionic products of these reactions manifest themselves as "new" peaks in the mass spectrum. The study of these reactions under "mass spectrometric conditions" allows for an examination of reactive systems in the absence of complicating solvent interferences.

There are several features of ICR spectrometry which make it particularly well suited for the study of these bimolecular or ion/molecule reactions. First of all, the ICR is operated routinely at pressures of less than 1×10^{-5} torr. These low pressures, coupled with reaction times which are on the order of milliseconds, ensure that the predominant reactions taking place are bimolecular in nature. Furthermore these bimolecular reactions are

believed to occur within an order of magnitude of the collision frequency ($\sim 1 \times 10^{-10}$ cm³ molecule⁻¹s⁻¹) which implies that the observed reactions proceed with essentially no activation energy. Furthermore, the observed processes are assumed to arise from exothermic or thermoneutral processes. This assumption allows one to determine limits on heats of formation of products and on bond strengths. Finally, unique to this technique is ion cyclotron double resonance which provides a means of positively identifying precursor ions of reaction products.

Figure 1 represents a block diagram of an ICR spectrometer. Ion formation, focussing, acceleration and detection occur in the ICR "cell". The cell, illustrated in Figure 2, consists of three sections which include an ion source, analyzer, and collector. The ICR cell is housed in a stainless steel vacuum chamber and is located between the poles of an electromagnet.

Thorough reviews of the theory involved in ICR spectrometry have been presented in the literature¹¹⁻¹⁶. A brief review of these principles will be provided here to describe the dynamics of charged particles in electric and magnetic fields.

Ions are formed in the source by electron impact (70eV). Due to the presence of a magnetic field, \vec{B} , the ions are constrained to circular orbits in a plane which is normal to \vec{B} . For an ion of mass m , acceleration a ,

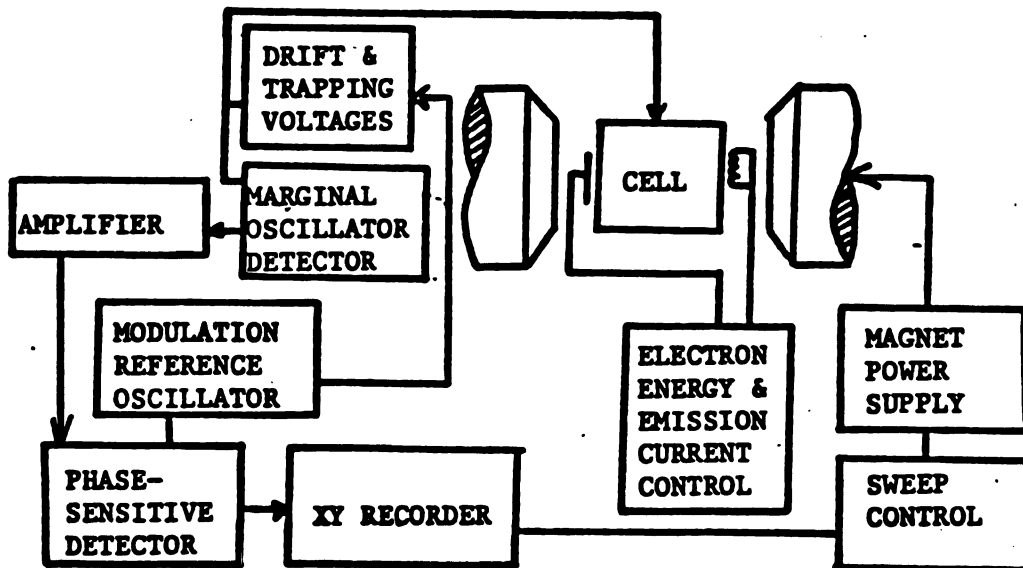


Figure 1.

Block Diagram of ICR Spectrometer for Single Resonance Experiment.

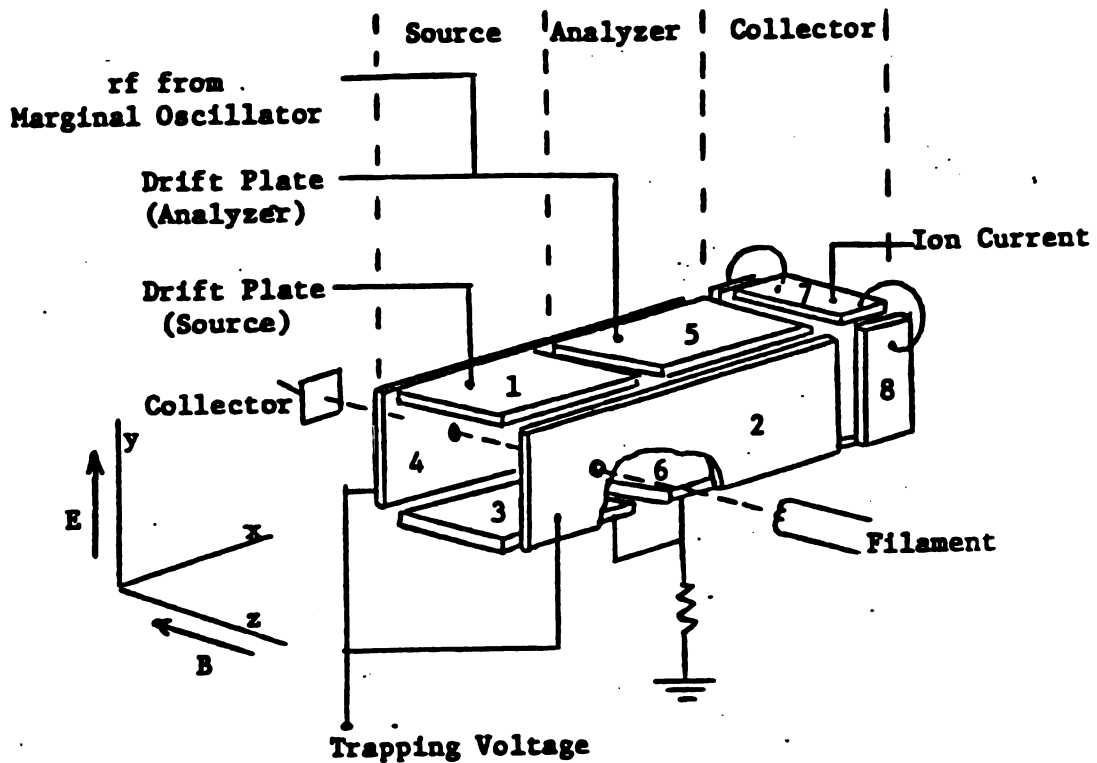


Figure 2.

The ICR Cell

charge q , and velocity \vec{v} which is perpendicular to \vec{B} , the force acting on the ion is presented in equation (1).

$$F = ma = q(\frac{\vec{v} \times \vec{B}}{c}) = \frac{qvB}{c} \quad (1)$$

(where \vec{v} is the velocity normal to \vec{B} , $|\vec{v}| = v$)

This force is perpendicular to B and v . Furthermore, due to the circular motion of the ions

$$a = \frac{v^2}{r} \quad (2)$$

where r is equal to the radius of the ion path. Substituting equation (2) into (1) and rearranging, an expression for the angular frequency, $\frac{v}{r}$, of the ion in rad/s is obtained (equation (3)).

$$\begin{aligned} ma &= \frac{mv^2}{r} = qvb \\ \therefore \omega_c &= \frac{v}{r} = \frac{qB}{m} \end{aligned} \quad (3)$$

ω_c is the natural cyclotron frequency of an ion in the presence of a magnetic field. For example, the cyclotron frequency of a Co^+ ion in a magnetic field strength of 1.0 Tesla is: .

$$\nu_c = \frac{\omega_c}{2\pi} = \frac{1.6 \times 10^{-19} \text{C} \times 1.0 \text{T}}{6.28 \times 59 \text{u} \times 1.66 \times 10^{-27} \text{kg/u}} = 2.6 \times 10^5 \text{ Hz}$$

Note that ω_c is independent of velocity. Furthermore, for a constant ω_c , the mass to charge ratio of the ion varies linearly with B .

The motion of ions in the presence of a magnetic field is not restricted in the plane parallel to \vec{B} . Thus, to constrain the ions in the cell in the XY plane,

a trapping potential, V_{trap} , is applied to the trapping plates. The electric field established by this potential is parallel to \vec{B} and restricts the motion of the ions in the plane perpendicular to \vec{B} by creating a potential energy minimum near the center of the cell. Therefore, when detecting positive ions, small positive voltages ($<0.5V$) are applied to plates 2 and 4 in Figure 2.

To move the ions from the source into the analyzer, a potential difference, V_{drift} , is applied between the plates which are located above and below the electron beam (plates 1, 5, 3 and 6 in Figure 2). The electric field produced by the drift plate potentials is perpendicular to the magnetic field ($\vec{E} \times \vec{B}$). Under these conditions, the ions move at right angles to both \vec{E} and \vec{B} . The force acting on the ion under these circumstances is given in equation (4).

$$\vec{F} = \frac{m \partial \vec{v}}{\partial t} = q \vec{E} + \frac{q \vec{v} \times \vec{B}}{c} \quad (4)$$

Assuming that \vec{E} and \vec{B} are constant, the velocity, \vec{v} , of the ion consists of two components, \vec{v}' , associated with the cyclotron motion and \vec{v}'_d , the drift velocity. The equation for velocity is presented in equation (5).

$$\vec{v} = \vec{v}' + \vec{v}'_d = \vec{v}' + \frac{c \vec{E} \times \vec{B}}{B^2} \quad (5)$$

(Note that \vec{v}'_d is equal to $(c \vec{E} \times \vec{B})/B^2$). Substitution of equation (5) into equation (4) yields a new expression

$$\text{for } \vec{F}: \quad \vec{F} = m \frac{\partial \vec{v}'}{\partial t} = q(\vec{v}' \times \frac{\vec{B}}{c}) \quad (6)$$

From equation (6), it is evident that v' is independent of \vec{E} . Therefore, one can conclude that this component of the velocity is associated with the cyclic motion of the ion occurring about the magnetic field lines, with the ion moving at its cyclotron frequency. The other component of velocity \vec{V}_d is perpendicular to both \vec{E} and \vec{B} . The drift velocity can be simply evaluated¹² by equation (7) where ϵ_{drift} is the magnitude of the electric field. The electric

$$V_d = \frac{\epsilon_{\text{drift}}}{B} \quad (7)$$

field can be obtained by dividing the potential difference between the drift plates by the distance separating the plates. Note that the drift velocity is independent of mass and charge. Typically, the distance between the plates is 1.0 cm and the potential difference between the plates is 0.5 V at $B = 1.0\text{T}$. The drift velocity of an ion calculated by substitution of these parameters into equation (7) is 50 m/s. Considering that the distance between the electron beam (point of ionization) and the far end of the analyzer region is approximately 8.6 cm, we can determine that an ion spends about 2×10^{-3} s in the cell at a magnetic field strength equal to 1T. Furthermore, the total distance travelled by the ion during this time period is approximately 1m. An illustration of the drift velocity is provided in Figure 3.

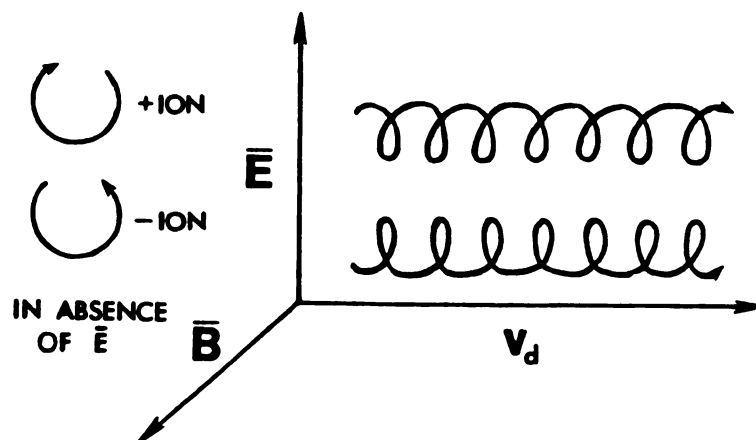


Figure 3. Drift Velocity.

A marginal oscillator with phase sensitive detection is connected to the top and bottom drift plates in the analyzer region. The marginal oscillator serves as the detection system for the ions once they pass into the analyzer region. The output voltage of the marginal oscillator is varied sinusoidally at a frequency which is dependent upon the inductance and capacitance of a tank circuit. The ICR cell serves as a capacitive element in the tank circuit of the marginal oscillator. Detection of an ion occurs when ω_c of the ion is the same as the frequency of the marginal oscillator. When these frequencies match, the ion is said to be in resonance with the applied field. When in resonance, an ion absorbs energy from the radio-frequency, rf, field produced by the marginal oscillator and in doing so generates an electric signal in the circuit.

The power absorbed by an ion from the rf field in the

resonance region can be determined. Since the rf signal is an electromagnetic wave, it has an amplitude of ϵ_{rf} . When interacting with a moving charge, the rf signal can be resolved into two contrarotating circular components, each with an amplitude of $\epsilon_{rf}/2$. When an ion is in resonance, its orbit tracks only one of these circular components. Thus, the frequency of the ion is the same as that of the rf field. When in resonance, the force acting on the ion is given by equation (8).

$$F = ma = \frac{\epsilon_{rf}}{2} q \quad (8)$$

Solving equation (8) for a , equation (9) is obtained.

$$a = \frac{\epsilon_{rf} q}{2m} \quad (9)$$

Integration of equation (9) with respect to time yields an expression for velocity. Therefore, after an ion has been in resonance for a time period of t , its velocity is

$$v = \int_0^t a dt = \frac{\epsilon_{rf} q}{2m} t \quad (10)$$

The instantaneous power absorbed, $A(t)$, by an ion is a product of the force acting on the ion (equation 9) and its velocity (equation 10).

$$A(t) = Fv = \frac{\epsilon_{rf}^2 q^2}{4m} t \quad (11)$$

To calculate the average power absorbed by an ion during the time, τ ($0 < t < \tau$), the ion spends in the detector, equation (11) is integrated with respect to time from 0 to τ .

$$A(\tau) = \overline{A(t)} = \frac{1}{\tau} \int_0^{\tau} A(t) dt = \frac{\epsilon_{rf}^2 q^2 \tau}{8m} \quad (12)$$

Equation (12) yields the power absorbed by one ion at resonance. Power absorption is inversely proportional to mass.

During the course of a typical single resonance experiment, the magnetic field strength is scanned from 0 to 1.8 T (18kG) while the frequency, $\omega_{m.o.}$, of the marginal oscillator is held constant and chosen such that one atomic mass unit corresponds to a change of 0.01 T (100 Gauss):

$$\nu_{m.o.} = \frac{\omega_{m.o.}}{2\pi} = \frac{1.6021 \times 10^{-19} \text{C} \times 0.01 \text{ T}}{6.2832 \times 10^{-27} \text{Kg/u}} = 1.5357 \times 10^5 \text{Hz}$$

Recall that from equation (3), the m/q ratio varies linearly with B at a constant frequency. Thus by setting the marginal oscillator frequency at 153.57 kHz and scanning B, each ion is brought into resonance, one at a time, with the marginal oscillator and detected. A plot of absorption versus B, which is linear in mass, is obtained.

To enhance the signal-to-noise ratio, S/N, the ion signal is modulated by applying a 27Hz square wave on one of the trapping plates (plate 2, Figure 2). When the potential on the plate is negative, all of the positively charged ions are swept out of the cell. As a result, the rf level of the marginal oscillator varies at this same frequency. Using a lock-in amplifier in conjunction with the marginal oscillator, the S/N is greatly improved. Under these circumstances, the marginal oscillator is

modulated at the same frequency as the square wave on the trapping plate. Thus, the marginal oscillator generates a signal only when ions are present in the cell. Theoretically, a marginal oscillator can detect as few as 14 ions.¹²

Following the analyzer is a collector region. The collector plates are all connected to ground. When the ions drift into these plates, an ion current is produced. The total ion current can be measured using an electrometer. The total ion current is on the order of 10^{-12} Amperes.

Ion-neutral collisions resulting in the formation of products occur when the pressure in the cell is increased above a "collision free" pressure of $\sim 2 \times 10^{-6}$ torr. To identify the reaction sequences involving the product ions formed in ion-molecule reactions, ion cyclotron double resonance (ICDR) is utilized. This technique is unique to ICR spectrometry and it allows one to unambiguously assign the precursors of a product ion.

During ICDR, the frequency of a variable rf oscillator is scanned in the source thus adding energy to potential reactant ions. At the same time, the product ion under consideration is kept in resonance with the marginal oscillator in the analyzer. Thus, its intensity is continuously being monitored. When the ω_c of a potential reactant ion equals the frequency of the

secondary oscillator in the source, the ion absorbs energy and is swept from the cell. If the ejected ion corresponds to a precursor, a decrease in the intensity of the peak representing the product ion being monitored is observed. Since the magnetic field strength is kept constant during ICDR, the following relationship holds:

$$B = \frac{\omega_{\text{product}} m_{\text{product}}}{q} c = \frac{\omega_{\text{precursor}} m_{\text{precursor}}}{q} c \quad (13)$$

Therefore, the mass of the precursor is readily determined from equation (13) when the frequency ratio is known.

$$\frac{\omega_{\text{product}}}{\omega_{\text{precursor}}} = \frac{m_{\text{precursor}}}{m_{\text{product}}}$$

Detailed descriptions of the ICDR experiment ^{11,12} and thorough discussions concerning the interpretation of double resonance results^{16,17} can be found in the literature.

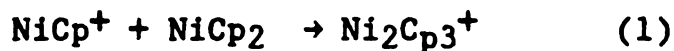
Chapter 3

Overview of Gas Phase Transition Metal Studies

Early work^{18,19} done with transition metal compounds in gas phase studies involved volatile carbonyl containing species, $M(CO)_x$ (where $M = Ni, x = 4$; $M = Fe, x = 5$; $M = Cr, Mo, W, x = 6$). Transition metal carbonyls were of interest due to the fact that metal carbonyls play an important structural role in many organometallic complexes. Gas phase studies allowed for an examination of the intrinsic properties of a metal complex in the absence of complications from the interference of solvent. The fragmentation patterns observed for these metal carbonyls following ionization via electron impact was used to determine the ionization potential of MCO_x and the appearance potentials of the remaining fragment ions. Using this information, the energetics involved in ionization and dissociation of the ions was determined.

The first ion/molecule reactions observed for mononuclear organometallic compounds were reported by Schumaker and Taubenest.²⁰ They observed peaks corresponding to the formation of bimetallic ions in their mass spectrometer. They used reaction (1) to

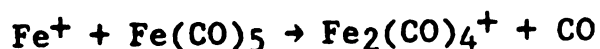
account for their results



(where Cp = C₅H₅).

Another early investigation by Müller²¹ revealed that polynuclear metal complexes were formed from ion/molecule reactions in CpV(CO)₄, Cr(CO)₆, Ni(PF₃)₄, Cr(C₆H₆)₂, CpCrCONO and (C₆H₆)Cr(CO)₃. Furthermore, Müller reported ion/molecule reactions occurring between ionized transition metal complexes such as CpCo(CO)₂⁺ or CpNiNO⁺ and a number of σ and π donor molecules including H₂O, NH₃ and benzene. Emerging from these investigations was the realization that ion/molecule reactions of organometallic complexes in the gas phase yielded useful information regarding the formation and stability of metal-metal and metal-ligand bonds.

During the time in which Müller was conducting his studies, the ICR technique was being developed. The utility of ICR in the study of gas phase ion/molecule reactions was soon realized.²² Foster and Beauchamp were the first to use this technique to study the reactions of ions formed by electron impact on Fe(CO)₅ with neutral Fe(CO)₅ and in binary mixtures with molecules such as CH₃F, H₂O, NH₃ and HCl.²³ They observed the formation of binuclear iron species. Using ICDR, they were able to unambiguously determine that this binuclear iron species was formed from Fe⁺ and Fe(CO)₅:

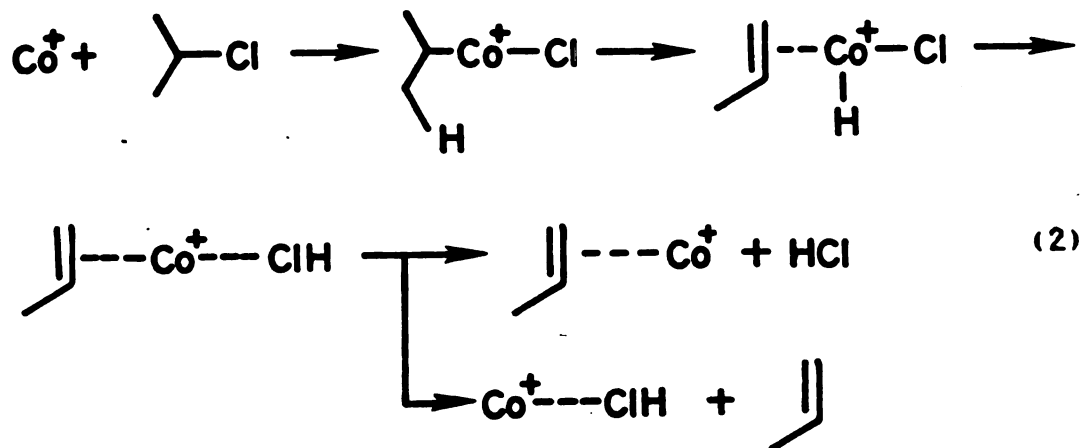


Results from the experiments involving binary mixtures enabled them to determine bond energies and the relative rates of ligand substitution in Fe(CO)_n^+ ($n = 0-5$). From these studies, it was evident that ICR could serve as a useful tool in the characterization of the thermodynamic and intrinsic chemical properties of ions and molecules in the absence of solvent.

In addition to the formation of polynuclear clusters and ligand substitution reactions, many transition metal complexes were found to exhibit rich chemistries with organic molecules in the gas phase.²⁴⁻⁷⁵ For example, Ridge et al. were the first to report the formation of metal to carbon bonds in the reactions of the electron impact fragments of $\text{Co(CO)}_3\text{NO}$ and Fe(CO)_5 with alkyl halides⁷ and alcohols.^{1,6} Tricarbonylnitrosylcobalt(0) and other metal carbonyl compounds were chosen for study because of their volatility and because CO and NO serve as important ligands in transition metal chemistry. The formation of metal to carbon bonds was explained by the oxidative addition of M^+ , formed from electron impact on ML_n ($\text{M} = \text{Fe, Co, Ni, Cr}$), to C-X bonds (where X = halide or OH) in saturated polar organic neutral molecules.

Essentially all of the polar organic molecules that have been studied to date react with transition metal ions such as Fe^+ , Co^+ or Ni^+ in the gas phase. Reaction (2) illustrates the dominant mechanism believed to be

operative in these gas phase studies. This mechanism involves a metal insertion / β -H shift/ competitive ligand loss sequence.

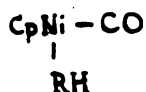


Thus, Co^+ inserts into the polar C-Cl bond followed by the shift of a β -hydrogen²⁸. Isopropyl chloride is "rearranged" on the ionic metal center into HCl and propene. HCl and propene then compete as ligands on the metal. Similarly for alcohols, Ridge and coworkers reported that the metal ion inserts into the C-OH bond to eliminate H_2O .¹ In general, Fe^+ , Co^+ and Ni^+ were all found to dehydrate alcohols and dehydrohalogenate alkyl halides.^{1,6}

Many other polar organic molecules have been studied with various metal containing compounds. Ridge and coworkers also studied mixtures of TiCl_4 with small olefins³⁰ and oxygen containing organic compounds.³³ These reactions were of interest due to the catalytic

participation of TiCl_4 in the Ziegler-Natta scheme for the polymerization of olefins in solution. Ridge et al. found that the electron impact fragments of TiCl_4 (including Ti^+ , TiCl^+ , TiCl_2^+ , TiCl_3^+ and TiCl_4^+) exhibited specific chemistry with organic compounds.^{30,33} Furthermore, different chemistry was observed depending upon how many chlorines were bound to Ti^+ . For example, TiCl_2^+ and TiCl_3^+ were both found to eliminate HCl and smaller olefins from larger olefins, Ti^+ was found only to eliminate H_2 , and TiCl_4^+ was unreactive.

Beauchamp et al. have reported the decarbonylation of aldehydes by $(\eta^5\text{-C}_5\text{H}_5)\text{Ni}^+$ in the gas phase.²⁷ The mechanism they proposed involved a reaction intermediate such as



from which the competitive elimination of RH or CO could occur. Decarbonylation of aldehydes in solution and on solid surfaces has been reported in the literature.⁷⁶

Beauchamp and his coworkers at Cal Tech have made other significant contributions to the area of gas phase transition metal chemistry. They have studied cobalt and chromium carbenes^{2,42} in an effort to characterize these metal carbenes in the gas phase. Transition metal carbenes are of interest because they may serve as intermediates in the Fischer-Tropsch synthesis and in

olefin metathesis. Furthermore, Beauchamp et al. have examined the basicity of iron pentacarbonyl,²⁴ ferrocene²⁵ and nickelocene²⁶ in the gas phase using ICR and have reported the proton affinities of a number of organotransition metal complexes.⁴⁴ They have determined the metal-ligand bond dissociation energies of some π -donor ligands to cyclopentadienylnickel cation⁷⁹ and have described the methodology involved in the determination of metal-hydrogen, metal-carbon and metal-ligand bond dissociation energies in the gas phase.^{37,77,78} The purpose of these studies was to gain information relating to the intrinsic reactivity of transition metal complexes in the absence of solvent.

Freiser and coworkers at Purdue reported the cleavage of C-C, C-H, and C-O bonds in the gas phase reactions of Fe^+ with ketones and ethers.⁴⁸ They observed the formation of alkyl-, acyl- and alkoxide Fe^+ species arising from oxidative addition reactions. They also observed decarbonylation for a few small ketones. Dehydrogenation was reported for unbranched ketones and reductive elimination of methane occurred in ketones which were branched at the α carbon. They also reported the gas phase chemistry of Cu^+ with esters and ketones.³⁸

The gas phase chemistry of Cu^+ with alkyl chlorides⁴⁰ was reported by Staley et al. Halide transfer onto Cu^+ followed by dehydrochlorination was

observed. The mechanism they used to account for their results once again involved oxidative addition of Cu^+ to the polar carbon-halide bond.

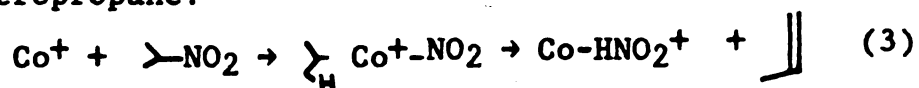
Work done in the Allison lab at MSU has involved the characterization of the reactions occurring between iron or chromium containing ions and polyethers.⁶⁰ The chemistry occurring between the 70eV electron impact fragments of $\text{Co}(\text{CO})_3\text{NO}$ and various bifunctional organic molecules has also been reported.^{5,59} These results indicated that bifunctional molecules exhibit a much richer chemistry than monofunctional compounds due to the interaction of the metal ion with two polar functional groups instead of one. Also, the reactions of nitroalkanes and cobalt-containing compounds have been reported recently by Allison et al.⁷²

From the brief overview presented above, it is evident that the chemistry of many transition metal ions and transition metal complexes has been studied. The results illustrate the rich chemistry occurring with various types of organic molecules in the gas phase. Furthermore, the mechanism which has been found to be operative in these reactions is one involving an oxidative addition of the metal ion followed by the shift of a hydrogen and competitive ligand loss.^{6,7}

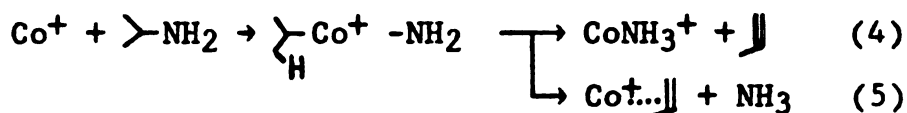
In an effort to characterize the reactions of metal ions with select nitrogen containing compounds, a study of the reactions of cobalt-containing ions with secondary

and tertiary amines was carried out as the first part of this Ph.D. project. This particular part of the project represents a continuation of work done earlier with primary amines by this author for a Master's thesis.

In investigating the chemistry of metal ions with organic compounds containing C-N bonds, it was determined in our lab that nitroalkanes react with Co^+ to yield products indicative of initial Co^+ insertion into the C-N bond. For example, reaction (3) was reported for Co^+ and 2-nitropropane.



The trend established by the earlier work done with polar compounds (reaction(1)) and by reaction (3) suggested that primary amines would undergo similar reactions. Therefore, for the reaction of Co^+ with isopropylamine, reactions (4) and (5) were expected:



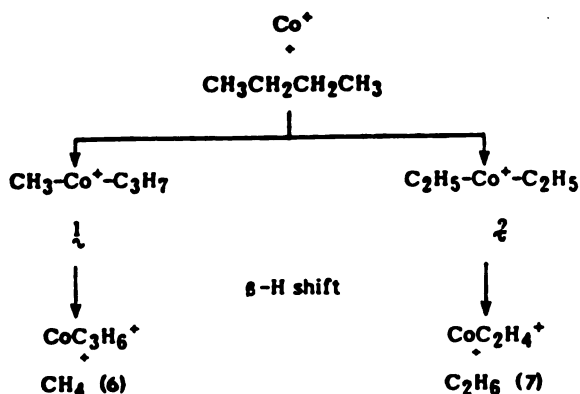
However, products indicative of Co^+ insertion into the C-N bond of primary amines were never observed. Instead, only products indicative of metal ion insertion into C-C and C-H bonds were observed. Thus, Co^+ reacted with primary amines to induce the elimination of H_2 , small alkanes and small alkenes.⁷¹

These results were not totally unexpected since they were similar to results observed by Müller for metal-containing ions such as $\text{C}_6\text{H}_6\text{V}^+$ and $\text{C}_5\text{H}_5\text{NiNO}^+$ with diethylamine and dimethylamine. 80, 81 He reported reaction products corresponding to the elimination of one or more molecules of hydrogen or of small hydrocarbons.

In Chapter 5 of this dissertation, the chemistry of the $\text{Co}(\text{CO})_x^+$ ($x=0-2$) and $\text{Co}(\text{CO})\text{NO}^+$ ($x=0-3$) ions formed by electron impact on $\text{Co}(\text{CO})_3\text{NO}$ with secondary and tertiary amines will be discussed. It will become apparent, that the reactions observed for secondary amines parallel those observed for primary amines and those observed by Müller, whereas the products formed in the reaction of metal ions with tertiary amines are suggestive of a mechanism involving metal ion insertion into C-N bonds. These results will be compared to those observed in condensed phases.

Chapters 6 and 7 will be devoted to the gas phase chemistry of metal-containing ions and alkanes.⁴³ In 1979, first row transition metal ions were reported to interact with alkanes in bimolecular gas phase reactions. These initial results indicated that it was energetically feasible for ions such as Fe^+ , Co^+ and Ni^+ to insert into any of the skeletal bonds of most alkanes in an exothermic process. 43,52,57 For example, in the reaction of Co^+ with n-butane, products indicative of initial insertion into both the terminal and internal C-C

bond were observed:⁴³ (reactions (6) and (7))



Twelve percent of the products of this reaction were attributed to CoC_3H_6^+ . The CoC_2H_4^+ product represented fifty-nine per cent of the products. The remainder of the products (twenty-nine per cent) arose through hydrogen elimination resulting in the formation of CoC_4H_8 .

The product distributions observed in the reaction of Co^+ and butane, along with subsequent studies of the mechanisms involved in H_2 elimination^{51,52} suggested that the formation of products from intermediate **2** are favored over intermediate **1**. A number of attempts were made to explain why some products are formed in greater abundance than others. (These attempts will be discussed in Chapter 6). We believe that the insertion process plays a dominant role in determining the final product distributions. Based on work performed in our laboratory, along with product distributions reported previously in the litera-

ture, 6, 36, 43, 52, 53, 57 a direct correlation between the C-C bonds of normal alkanes preferred by M^+ for insertion and the ionization potentials (IP's) of the alkyl group bound to M^+ ($M=Fe, Co, Ni$) upon its insertion is reported and rationalized in Chapter 6. It is suggested that this correlation is indicative of reactions where the most stable insertion intermediate is formed preferentially thus leading to the greatest abundance of products. Therefore, the distribution of insertion intermediates reflects their relative stabilities.

Finally, Chapter 7 will examine the changes which occur in the chemistry of Fe Co and Ni with straight-chained and branched alkanes as up to two ligands (including CO, NO or PF) are bound to the metal. Previous studies 6, 36, 43, 52, 53, 57 have focussed on the reactions of the bare (+1) metal ions with alkanes. However, in condensed phases, the organometallic reactions of interest involve metal complexes. 86, 87

In the gas phase, with the addition of ligands, a number of pathways may be taken, depending upon the number and nature of the ligands. These pathways will be discussed and compared to those observed in condensed phase chemistry.

Chapter 4

Experimental

This chapter will consist of three parts. The first part will describe the specifications of the ICR spectrometer used in this study. The second part will list the chemicals utilized along with their manufacturers. The last part will briefly describe how the data were acquired.

ICR Specifications

All experiments were performed on an ICR spectrometer of conventional design⁸⁴ which was constructed at Michigan State University. The ICR cell consists of a source, analyzer and collector region. The overall dimensions of the cell are 0.88 inch by 0.88inch by 6.25 inches. The source region is 2.00 inches long, the analyzer region is 3.75 inches long, and the collector is 0.50 inch long. Ions are formed in the source by electron impact with 70eV electrons. The electron filament is emission regulated. Both the filament controller and plate voltage controller for the ICR cell were designed and constructed at MSU. The

instrument is operable in either the pulsed or drift ICR modes. All data for this study were obtained under normal drift-mode conditions by using trapping voltage modulation and phase sensitive detection. A marginal oscillator detection system based on the design of Warnick, Anders and Sharp⁸⁵ was used. Ion cyclotron double resonance experiments¹¹ were performed using a Wavetek Model 144 sweep generator as the secondary oscillator. The ICR cell is contained in a stainless steel vacuum system and sits between the polecaps of a Varian 12 inch electromagnet (1.5 in. gap). A varian V-7800, 13 kW power supply and a Fieldial Mark I Magnetic Field Regulator are used to operate the electromagnet.

The instrument is pumped by a 4-inch diffusion pump with a liquid nitrogen cold trap and an Ultek 20 liter per second ion pump. Samples are admitted by Varian 951-5106 precision leak valves. The approximate sample pressures are measured with a Veeco RG1000 ionization gauge.

Chemicals

Tricarbonylnitrosylcobalt(0) and tetrakis(trifluorophosphine)nickel were obtained from Alfa Inorganics. Iron pentacarbonyl, 2,2,3,3-tetramethylbutane and butane were purchased from Aldrich Chemical Co. Piperidine, pyrrolidine, tetrahydrofuran, diethyl ether, diethylamine and triethylamine were obtained from Chem-Service Inc.

Tetrahydrofuran-d₈ was purchased from Norell Chemical Co., Inc. Ethylbutylamine, propane, 2-methylpropane, 2,2-dimethylpropane, butane, 2,3-dimethylbutane, 2,2-dimethylbutane, pentane, 3-methylpentane, 2,4-dimethylpentane, 2,3,4-trimethylpentane, 2,2,4-trimethylpentane, hexane, heptane, octane, nonane and decane were obtained from Fluka Chemical Corporation. Methane and ethane were purchased from Matheson Company, Inc. All samples were degassed three times by freeze-pump-thaw cycles. After degassing, the vapor pressure of a liquid sample (typically around 6 torr) was admitted into an evacuated glass bulb and was used without further purification.

Data Acquisition

Data were acquired in the following manner. High- and low-pressure (1×10^{-5} torr versus 1×10^{-6} torr) spectra of each compound were obtained. Any ions formed by ion/molecule reactions in the organic compound alone and in the metal compound alone were determined. Next, a 1:2 mixture (by pressure) of metal compound to alkane or amine was introduced into the cell at a total pressure of $\sim 8 \times 10^{-6}$ torr. Spectra were taken up to a mass to charge ratio (m/z) of 260 and all product ions characteristic of the mixture were identified.

Conventional double resonance techniques were used








to identify the ionic precursors of the ion/molecule reaction products. (Note, that if $A^+ \rightarrow B^+$ and $B^+ \rightarrow C^+$, then the precursors of C^+ as determined by ICDR will be A^+ and B^+). Branching ratios were calculated to determine product distributions and were taken to be accurate to within $\pm 10\%$. The reported reactions are facile and occur within an order of magnitude of the collision frequency ($k \approx 1 - 10 \times 10^{-10} \text{ cm}^3 \text{ molecule}^{-1} \text{ s}^{-1}$). An approximate lower limit for the rate constant for processes not observed is $5 \times 10^{-11} \text{ cm}^3 \text{ molecule}^{-1} \text{ s}^{-1}$.

(Note that when working with metal carbonyls in these experiments caution must be used in interpreting results and suggesting product compositions. This is due to the fact that both C_2H_4 and CO have a nominal mass of 28u. Yet, following a careful analysis of all precursors of each product and a comparison of these results to the results of similar studies, the processes reported in this dissertation are thought to represent a self-consistent set).

Chapter 5
Gas Phase Chemistry of $\text{Co}(\text{CO})_3\text{NO}$
with Secondary and Tertiary Amines

In this chapter, the reactions of the 70eV electron impact fragments of $\text{Co}(\text{CO})_3\text{NO}$ (Co^+ , CoCO^+ , CoNO^+ , $\text{Co}(\text{CO})_2^+$, CoCONO^+ , $\text{Co}(\text{CO})_2\text{NO}^+$ and $\text{Co}(\text{CO})_3\text{NO}^+$) with diethylamine, pyrrolidine, piperidine, ethylbutylamine and triethylamine will be presented. A summary of these reactions, in terms of the neutral losses, is presented in Table 1 along with the branching ratios. Also included in Table 1 are the reactions observed for a few analogous oxygen containing compounds. (Note that labelled tetrahydrofuran was used to unambiguously identify products because in the reactions of unlabelled tetrahydrofuran, loss of ($\text{H}_2\text{O}+\text{CO}$) could not be distinguished from loss of ($\text{C}_2\text{H}_6\text{O}$) (C_2H_4 and CO both correspond to 28u)). The discussion of these results will consist of four parts. The first part will examine the formation of CoH as a neutral product and will present evidence indicating that metal-induced H_2 elimination from amines occurs with Co^+ insertion into an N-H bond as a first step. The second part will discuss intermediates involving metal-amide bonds. A comparison to the chemistry occurring in condensed phases will be

Table I. Reactions observed for Secondary Amines, Tertiary Amines and Analogous Ethers (Reactions proceed via indicated neutral losses)

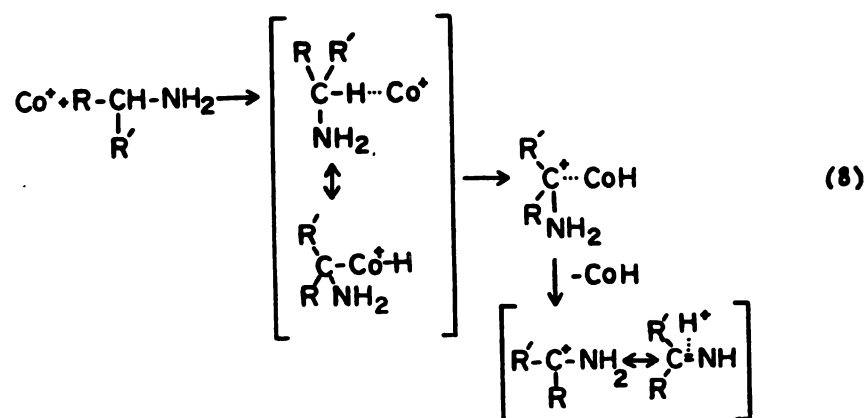
Reactant Ion	Reactant Neutral							
Co^+		CoH (1.0)	C_2H_4 (0.30)	CoH (1.0)	H_2O (0.26)	2H_2 (0.11)	H_2 (0.10)	C_2H_4 (0.08)
			C_2H_6 (0.01)		CH_2O (0.38)	CoH (0.89)	C_2H_4 (0.08)	C_2H_6 (0.06)
			$\text{C}_2\text{H}_6\text{O}$ (0.45)		CoH (0.36)		C_2H_6 (0.18)	CoH (0.86)
			CoH (0.24)			C_3H_8 (0.19)		
						CoH (0.45)		
CoCO^+		H_2 (0.14)	$\text{C}_2\text{H}_4 + \text{CO}$ (0.07)	H_2 (0.52)	$\text{H}_2\text{O} + \text{CO}$ (0.17)	H_2 (0.11)	$\text{H}_2 + \text{CO}$ (0.65)	C_2H_6 (0.12)
		$\text{H}_2 + \text{CO}$ (0.48)	CO (0.93)	CO (0.47)	$\text{CH}_2\text{O} + \text{CO}$ (0.05)	2H_2 (0.03)	$\text{C}_2\text{H}_4 + \text{CO}$ (0.18)	
		CO (0.38)			CO (0.78)	$\text{H}_2 + \text{CO}$ (0.53)	CO (0.17)	$\text{C}_2\text{H}_6 + \text{CO}$ (0.05)
						$2\text{H}_2 + \text{CO}$ (0.07)		CO (0.06)
						CO (0.26)		CoH (0.77)
$\text{Co}(\text{CO})_2^+$	CO (0.73)	CO (1.0)	CO (0.48)	CO (0.48)	CO (0.93)	CO (0.61)	CO (0.71)	CO (0.48)
	2CO (0.27)		2CO (0.52)	2CO (0.52)	2CO (0.07)	2CO (0.39)	2CO (0.29)	2CO (0.52)
Substitution Reactions: $\text{Co}(\text{CO})_x\text{MO}^+ + \text{A} \rightarrow \text{Co}(\text{CO})_{x-a}\text{MO}(\text{A})^+ + a\text{CO}$								
CoCoMo^+	a = 1	a = 1	a = 1	a = 1	a = 1	a = 1	a = 1	a = 1
$\text{Co}(\text{CO})_2\text{MO}^+$	2	2	2	2	2	2	2	2
$\text{Co}(\text{CO})_3\text{MO}^+$	3,2	2	3,2	3,2	2	2	2,3	N.R.

* N.R. = No Reaction Observed

made. The third part will examine the differences with the addition of CO and NO ligands on the metal. The last part will compare and contrast the reactions of cobalt and cobalt-containing ions with analogous oxygen containing compounds.

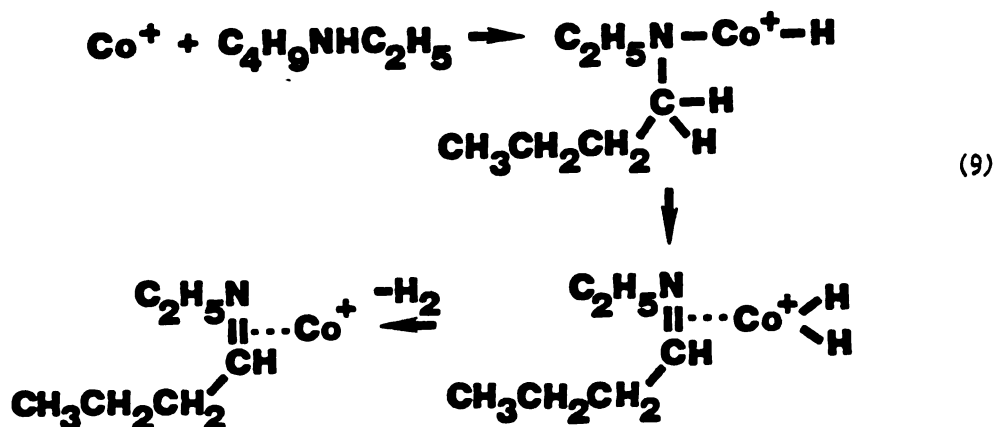
The data presented in Table 1 coupled with the results previously reported for primary amines⁷¹ suggests that both the N-H bond and the α -C-H bond of amines are attacked by Co^+ . Attack of the α -C-H bond results in the loss of the CoH neutral and formation of the (amine-1)⁺ ion. Insertion of Co^+ into the N-H bond leads to H_2 elimination.

Consider first the formation of CoH. Co^+ reacts with all of the secondary and tertiary amines in Table 1 to form CoH. Co^+ also reacts with methyl-, ethyl-, propyl-, isopropyl-, butyl-, isobutyl-, and sec-butylamine to form CoH.⁷¹ It does not react with tert-butylamine to form CoH. Thus, this process occurs for triethylamine (which does not contain an N-H bond) and for methylamine (which contains only α -C-H bonds and N-H bonds) but not for tert-butylamine which has no α -C-H. These results suggest that the reaction is predominantly an α -hydride abstraction. A general mechanism for this process is provided in reaction(8).



Thermodynamic conclusions based on this reaction type are difficult to make due to the fact that accurate thermodynamic data on the possible (amine-1)⁺ ions are not available. Also, bond strengths for Co-H reported in the literature have values ranging from 40 to 70 kcal/mol.⁸⁸ However, the driving force of this reaction may be the stability of the product ion. For example, when Co⁺ reacts with CH₃NH₂ to abstract a hydrogen, CH₄N⁺ is formed. While the structure of CH₄N⁺ formed in this manner is unknown, available thermochemical data⁸² suggests that the protonated amide, CH₄N⁺, is a highly stable ion.

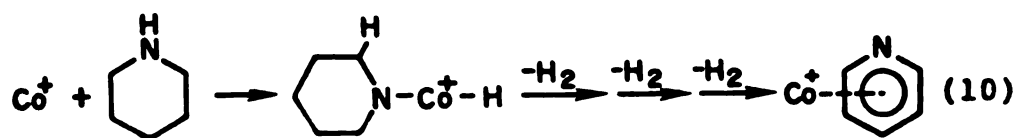
Table 1 also shows that H_2 is eliminated in the reactions of Co^+ with piperidine and ethylbutylamine. Furthermore, it is evident that Co^+ does not react with triethylamine to induce the elimination of H_2 . Note that all of the primary amines previously studied, except tert-butylamine, reacted with Co^+ by elimination of H_2 . Overall, these results suggest that H_2 elimination occurs following Co^+ insertion into the N-H bond. H_2 elimination is illustrated for ethylbutylamine in reaction(9). Several observations support this mechanism. First, H_2 elimination occurs in the reaction of Co^+ and methylamine in which only a C=N double bond can be formed (for a 1,2 elimination). Also, H_2 elimination is not observed for tert-butylamine. This negative result is expected based on the proposed mechanism since, following Co^+ insertion into the N-H bond, no β -H is available to shift. Furthermore, in terms of primary amines, labelling experiments with



$\text{C}_2\text{H}_5\text{ND}_2$ are consistent with the proposed mechanism in that HD elimination predominates. Finally, Table 1 shows that H_2 elimination occurs for secondary amines which contain an N-H bond but not for triethylamine which has no N-H bond. If H_2 elimination occurred following insertion into the $\alpha\text{-C-H}$ bond, then H_2 elimination resulting in the formation of a C=C double bond would be expected for triethylamine. Since this is not observed, this suggests that insertion into the N-H bond leads to H_2 elimination.

Note that H_2 elimination is not observed in the reaction of Co^+ and pyrrolidine, a secondary amine consisting of a five-membered ring. Based on the proposed mechanism, H_2 elimination would result in the formation of a double bond in the ring. The 120° bond angles associated with a double bond are much larger than the 105° angles associated with a stable five-membered ring (based on cyclopentane).⁸⁹ Compression of these 120° bond angles to satisfy the angle requirements of the ring would result in tremendous strain. A product ion involving this strained configuration would not be expected and was not observed.

Interestingly, in the case of piperidine, up to three molecules of hydrogen can be eliminated to form a "metal-pyridine" complex (reaction (10)).



The driving force of this reaction may be the formation of a conjugated system which can complex strongly with the cobalt ion. Note that the proposed product structure involves pyridine which is known to be very stable. Similarly, in primary amines, when the skeletal chain consists of four or more atoms, the elimination of two molecules of hydrogen is observed. This results in the formation of the metal-butadiene like complex illustrated in reaction(11).⁷¹ Again, the driving force of reaction (11) may be the formation of the butadiene-like ligand which can strongly complex to Co^+ .

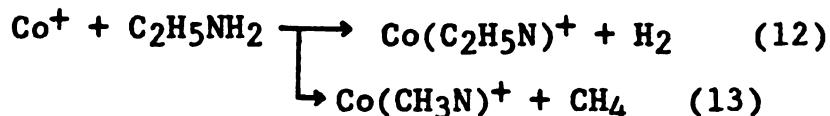


A comparison of the chemistry of diethylamine and ethylbutylamine shows that Co^+ reacts with ethylbutylamine to form a larger variety of products than when it reacts with diethylamine. The only product formed in the reaction of Co^+ and diethylamine is CoH . Products indicative of initial Co^+ insertion into C-C or N-H bonds of diethylamine are not observed. These results suggest that the products observed for ethylbutylamine arise from initial Co^+ insertion into the

C-C bonds of the butyl portion of the molecule. These reactions are illustrated in Scheme 1 (omitting, for simplicity, H₂ elimination and hydride abstraction). Thus, Co⁺ inserts into a C-C bond, a β-hydrogen shifts onto the metal and finally two molecules compete as ligands on the metal. Previous work indicates that the bond strengths between Co⁺ and a variety of ligands can be correlated to the proton affinities of the ligands.⁵ Therefore, the larger the proton affinity, the stronger the bond to the metal ion. In general, proton affinities take the following order:⁸³

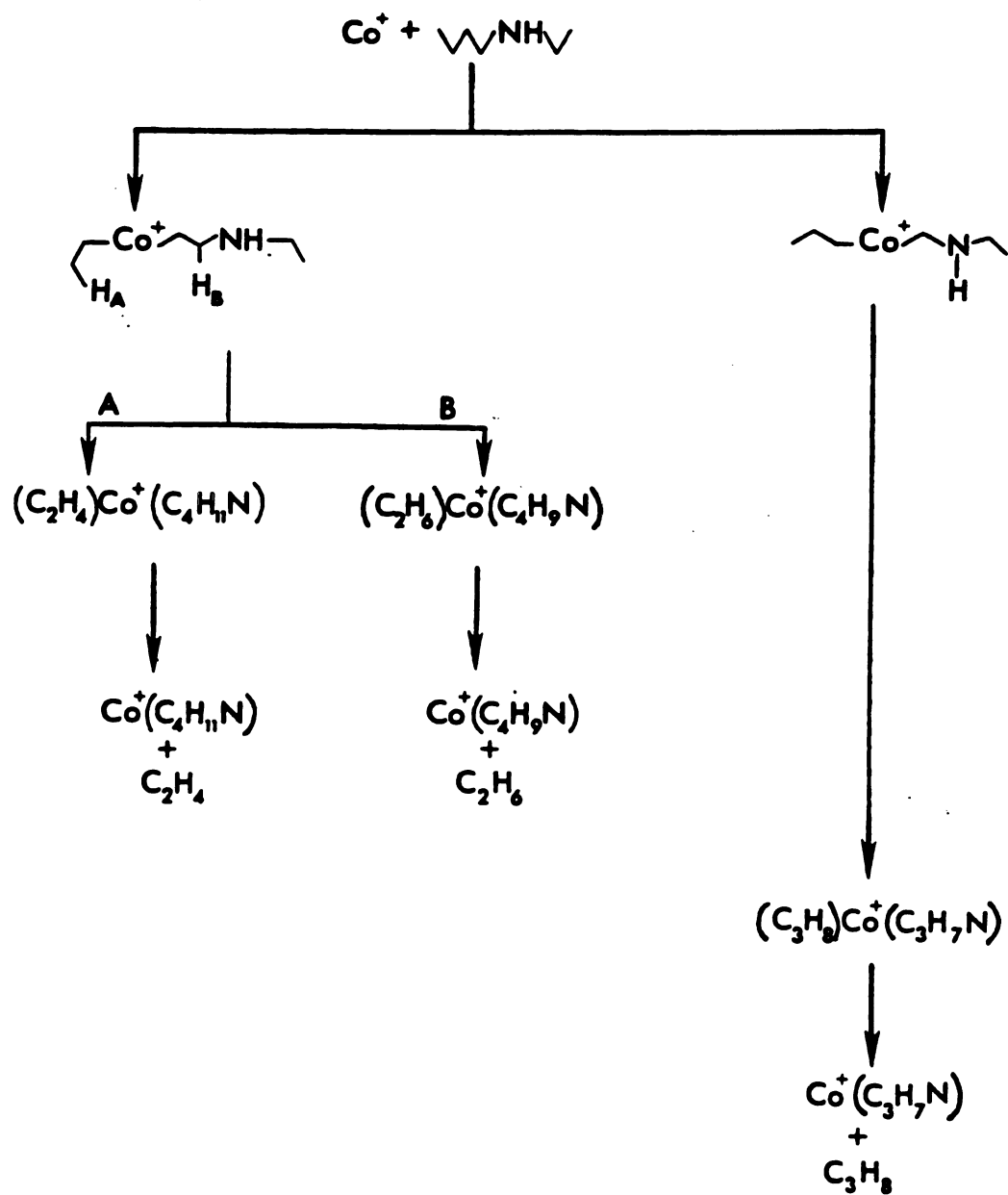
Amines, Imines > Alkenes > Alkanes

Thus, in each reaction sequence in Scheme 1, the more weakly bound ligands are lost to form the final products. Therefore, we believe that the products observed for ethylbutylamine are not indicative of initial insertion into the C-N bonds. These results are consistent with those reported for primary amines.⁷¹ For example, the reactions of ethylamine are typical of primary amines (reactions (12) and (13))

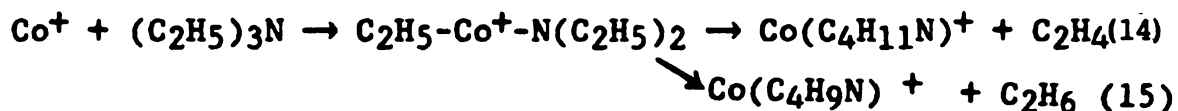


Products resulting from Co⁺ insertion into N-H bonds (reaction (12)) and into C-C bonds (reaction (13)) are observed. No reactions appear to occur via initial insertion into the C-N bond.

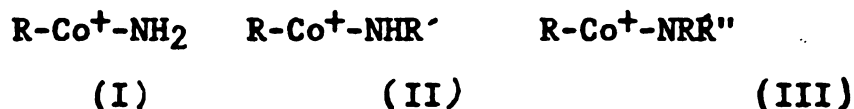
Scheme 1



In contrast to the results for primary and secondary amines, triethylamine does form products indicative of Co^+ insertion into the C-N bond. These reactions are shown in (14) and (15).



A comparison of the structures which would result from Co^+ insertion into the C-N bond of primary, secondary and tertiary amines reveals an interesting parallel to condensed phase chemistry.



Structure (I) would result from insertion of Co^+ into the C-N bond of primary amines and represents a primary amide. Co^+ insertion into the C-N bond of secondary amines would give rise to structure (II) which is analogous to a secondary amide. Structure (III) corresponds to Co^+ insertion into tertiary amines and represents a tertiary amide. Products indicative of the formation of structures (I) and (II) in the gas phase are never observed. However, products indicative of the formation of structure (III) in the gas phase are observed for triethylamine. Note that in condensed phases, transition metal primary amides and secondary amides are rare while tertiary amides of cobalt are common.¹⁰ The increasing stability of amides with

increasing N-alkyl substitution is not well understood. Primary and secondary amides may condense with the loss of NH_3 or $\text{NH}_2\text{-R}$ to yield



unless there is steric hindrance contributing to the "kinetic stabilization" of the metal amide species.¹⁰ Alternatively, primary and secondary amides may be difficult to isolate in condensed phases due to an ability to undergo "β decompositions" in which M-H bonds are formed in a process similar to that occurring for metal alkyls.¹⁰

Furthermore, in condensed phases, transition metal-tertiary amide bonds are considered moderately strong:¹⁰



It is interesting to note that in the series $\text{C}_2\text{H}_5\text{NH}_2$, $(\text{C}_2\text{H}_5)_2\text{NH}$, $(\text{C}_2\text{H}_5)_3\text{N}$ the strength of the C-N bond increases from 77 to 89 kcal/mol.⁸² Despite this, Co^+ inserts into the C-N bond of triethylamine. This may be interpreted as an indication of an increasing metal-amide bond strength as the extent of N-alkyl substitution increases. In general, the gas phase results suggest that, just as in solution, the formation of a tertiary amide is preferred over the formation of secondary and primary amides. Also, it is interesting to note that in

solution, amines prefer to react to form amides when the oxidation state of the metal is low¹⁰ and in this study gaseous Co^+ was utilized.

Interesting ligand effects are observed in the the reactions of CoCO^+ with diethylamine and pyrrolidine. Recall that Co^+ reacts with these secondary amines only to form CoH . However, CoCO^+ reacts with diethylamine and pyrrolidine to induce the elimination of H_2 . One possible explanation of these results involves the formulation of a mechanism in which CoCO^+ inserts into the C-N bond of diethylamine and pyrrolidine. This explanation is based on a series of reactions observed for ethylamine and confirmed by labelling experiments:⁷¹



By what is formally considered to be a ligand substitution process, a complex between Co^+ and ethylamine is formed in reaction (16). Note that the further reactions of a product ion are useful in gaining insights into its structure.¹ Thus, the further reaction of the product in (16), reaction (17), implies that the product of (16) exists as:



Structure IV apparently is not formed when Co^+ reacts with ethylamine. The formation of IV would require the insertion of Co^+ into a C-N bond of this primary amine. In reaction (16) however, the reactant ion is CoCO^+ . This

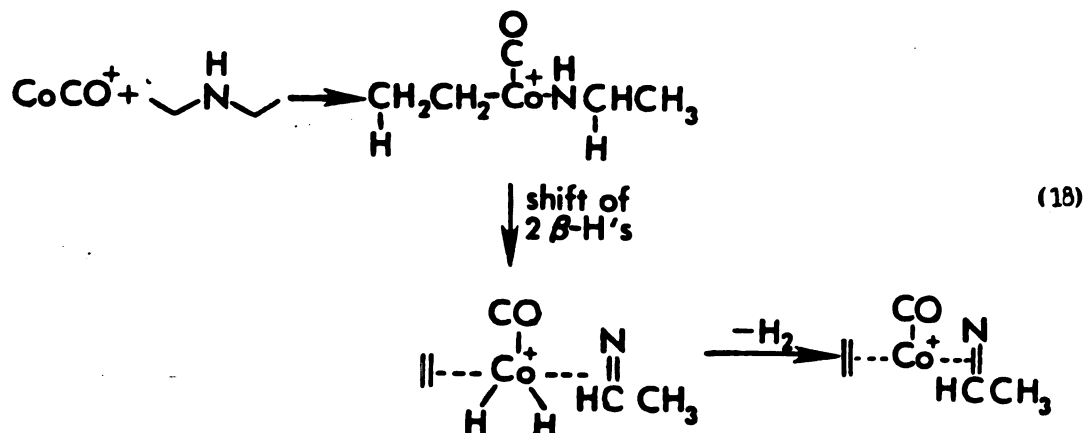
seemingly contradictory set of reactions can be understood by considering the potential set of processes which can occur between CoCO^+ and ethylamine if CoCO^+ inserts into C-C, N-H and C-N bonds. These processes are shown in Scheme 2.

Assuming that all four intermediates (V' , V'' , VI' , IV) are formed, it is evident that a variety of ligands are attached to Co^+ before the dissociation to final products occurs. Proton affinities suggest that the bond strength between Co^+ and the following series of molecules takes the following order:⁸³

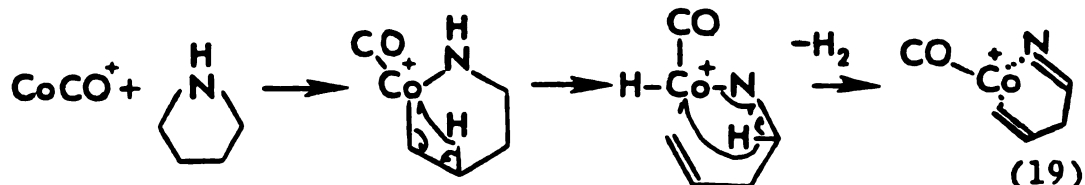


Thus in each reaction sequence in Scheme 2, the more weakly bound ligands are lost to form the final products. The product formed via intermediate IV'' contains two strongly bound ligands, NH_3 and C_2H_4 , which are retained while CO is lost. Other possible structures for $\text{Co}(\text{C}_2\text{H}_7\text{N})^+$ such as $\text{Co}(\text{C}_2\text{H}_5\text{N})(\text{H}_2)^+$ and $\text{Co}(\text{CH}_3\text{N})(\text{CH}_4)^+$ would not be expected since the intermediate through which they would be formed would lose H_2 or CH_4 rather than retain these electron-poor ligands. Thus, the $\text{Co}(\text{C}_2\text{H}_7\text{N})^+$ ion formed in reaction (16) has the structure $\text{Co}(\text{C}_2\text{H}_4)(\text{NH}_3)^+$, and it reacts further in (17) by a ligand substitution in which a second molecule of ethylamine displaces the more weakly bound C_2H_4 from the metal center.

Based on this analysis for ethylamine, we believe that CoCO^+ inserts into the C-N bond of diethylamine and pyrrolidine to induce the elimination of H_2 . Reaction (18) illustrates this mechanism for diethylamine. Note



that the dehydrogenation process occurring in reaction (18) involves the shift of two hydrogens which are located β to the metal ion. H_2 elimination resulting from the shift of two $\beta\text{-H's}$ onto the metal in a manner similar to that illustrated in reaction (18) has been previously reported in the gas phase reactions of Fe^+ , Co^+ and Ni^+ with alkanes.^{51,52,57,58} The dehydrogenation reaction occurring for pyrrolidine is illustrated in reaction (19). This reaction involves the insertion of Co^+ into a C-N bond thus forming a six membered ring followed by the cleavage of this ring:



The question that remains to be answered is: why would CoCO^+ insert into C-N bonds in primary and secondary amines when Co^+ does not? Note that in the

insertion process



the sum of the strengths of the two bonds formed, (M^+-A) and (M^+-B) , must be greater than the sum of the strength of the bond which is broken, $(A-B)$ and the promotion energy (PE)⁹⁰ of M^+ for the process to be exothermic. Since products indicative of Co^+ insertion into C-N bonds in primary and secondary amines are never observed, one can conclude that it is not energetically feasible for Co^+ to insert into the C-N bond because the energy associated with the formation of the bonds RH_2C-Co^+ and Co^+-NHR' is not sufficient to overcome the promotion energy needed to place Co^+ in its proper configuration for bonding and the energy required to break the C-N bond. Perhaps $CoCO^+$ forms stronger bonds to RH_2C- and/or $-NHR'$ than does Co^+ thus making the insertion of $CoCO^+$ into C-N possible.

There are several observations which lend support to the claim that $CoCO^+$ forms stronger bonds than Co^+ . First, data reported in the literature indicates that this claim is true for the bond between a metal ion and CO. $D(MCO^+-CO) > D(M^+-CO)$ for similar first row transition metal ions where $M = Cr, Fe$ and Ni and for $M = W$.⁸² Also, it has been reported recently for scandium, that $D(LSc^+ - CH_3) > D(Sc^+-CH_3)$ for $L = H, CH_3$. Thus ScL^+ forms a stronger bond to methyl than Sc^+ alone.⁹¹

Furthermore, Co^+ reacts with ethylamine and ethylbutylamine to eliminate H_2 via insertion into N-H. Note that the N-H bond in diethylamine is approximately 15 kcal/mol stronger than the N-H bond in both ethylamine and ethylbutylamine.⁸² No reaction is observed for Co^+ with diethylamine except hydride abstraction. However, H_2 elimination occurs when CoCO^+ reacts with diethylamine. This suggests that higher energy intermediates can be formed with CoCO^+ than with Co^+ . Thus, the sum of the bonds formed in IV' is larger than the C-N bond strength in ethylamine and the insertion becomes energetically accessible.

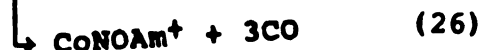
Unfortunately, RCo^+-NH_2 and RCo^+-NHR bond strengths are not available. Thus a precise evaluation of the thermodynamic influence on insertion into such C-N bonds by Co^+ cannot be made. Nonetheless, these experimental results indicate that Co^+-NH_2 and Co^+-NHR bonds may be weak, and $\text{D}(\text{Co}^+-\text{NR}_2)$ is largely dependent upon the extent of N-alkyl substitution.

Also reported in Table 1 are the reactions observed for $\text{Co}(\text{CO})_x^+$ and $\text{Co}(\text{CO})_x\text{NO}^+$ ions with secondary and tertiary amines. In general, as the number of carbonyls present on the metal center increase, the observed chemistry involves almost exclusively ligand substitution reactions in which one or more CO's are displaced by an amine. For example, the following ligand substitutions

were observed for all of the amines studied. (Note: "Am" stands for the parent amine).



With the presence of a nitrosyl ligand on the metal, the only reactions observed are ligand substitutions.



Note that all ligand substitutions involved only the displacement of carbonyl ligands. Never was the nitrosyl ligand displaced. The energy needed to displace the CO's comes from the energy released in the formation of the new bond formed between the metal and the complexing amine. Therefore, the number of CO's displaced is a rough indication of the cobalt-ligand bond strengths.

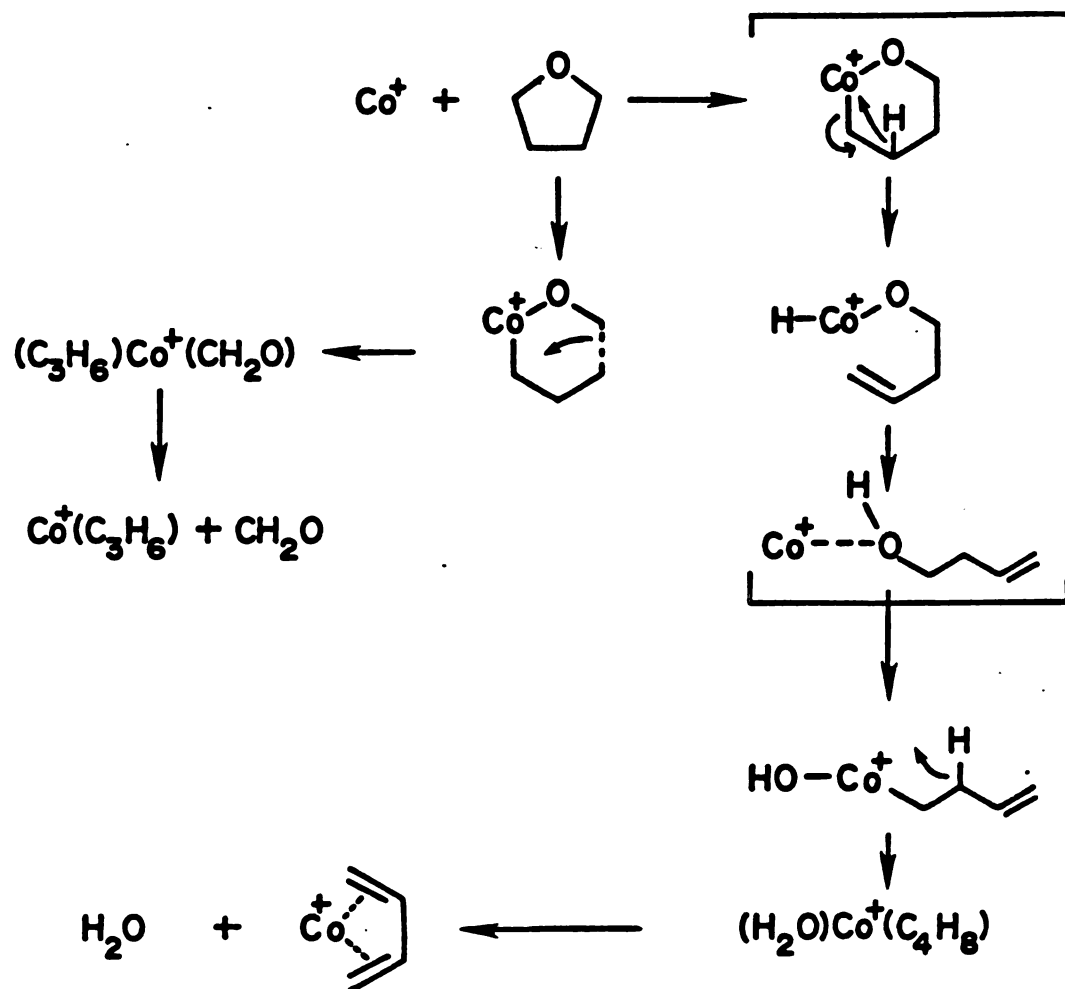
Finally, the products observed in the chemistry of Co^+ with secondary amines are much different than those observed for analogous ethers. Oxygen is a very good "director" for the site of metal attack in the organic molecule; only insertion into the C-O bond occurs. Thus, diethyl ether and tetrahydrofuran react to form products indicative of exclusive Co^+ insertion into the C-O bond.

These products are listed in Table 1. The processes leading to the formation of products for Co^+ and tetrahydrofuran are indicated in Scheme 3. H_2O elimination is shown to occur by first inducing the isomerization of the ether to the ene-ol. Following Co^+ insertion into the C-O bond of tetrahydrofuran, there may be attack of the carbon which is bonded to the β carbon to facilitate CH_2O elimination. These results are similar to those reported for small alcohols in which only insertion into the C-OH bond is observed. For example, isopropyl alcohol reacts with Co^+ by H_2O elimination but not by CH_4 or H_2 elimination pathways.^{1,6}

The results observed for the analogous ethers contrast with those observed for diethylamine and pyrrolidine. These two secondary amines only react with Co^+ to form hydride abstraction products. Furthermore, the products observed for ethylbutylamine appear to be typical H_2 and small-hydrocarbon eliminations as a result of metal insertion into C-C and N-H bonds. These results also contrast to those for the ethers. Interestingly, triethylamine does react with Co^+ to form products analogous to diethyl ether. Co^+ readily inserts into the polar C-N bond of triethylamine.

In conclusion, this study has allowed for an examination of the basic chemistry of the isolated Co^+ metal center with a series of amines and a determination

Scheme 3



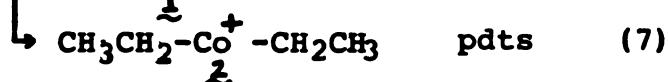
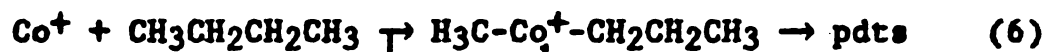
of how this chemistry changes as the available orbitals on the metal became occupied with CO and NO ligands. Furthermore, this study has shown that the chemistry which occurs for secondary and tertiary amines depends heavily upon the structure of the amine. A mechanism involving a metal insertion/ β -hydrogen shift and competitive ligand loss was proposed consistent with the observed results. Ligand substitution reactions were reported. Since structural information is obtained by knowledge of the mechanism of interaction and molecular weight information can be obtained from ligand substitution reactions, this study has illustrated the potential of $\text{Co}(\text{CO})_3\text{NO}$ as chemical ionization reagent.

Chapter 6

The Preference of Fe^+ , Co^+ and Ni^+ for Insertion into the C-C Bonds of Linear Alkanes

If each step in the metal insertion / β -H shift/ competitive ligand loss sequence were fully understood, products and branching ratios could be predicted a priori. This would render metal ions as ideal reagents in chemical ionization mass spectrometry. The least understood step in this sequence is the metal insertion process, yet it appears to be the dominant factor affecting product distributions.⁴³ To better understand the insertion process, a specific ordering of the preference of M^+ ($\text{M} = \text{Fe}^+$, Co^+ , Ni^+) for insertion into the C-C bonds of linear alkanes up to and including decane will be determined. To achieve this end, first other attempts which have been made to rationalize product distributions will be presented. Next, a procedure for establishing an ordering of the preference of M^+ for C-C bonds in alkanes will be presented followed by that ordering. Finally, an explanation of the factors which render certain C-C bonds in nonpolar alkanes more susceptible to metal ion attack than others will be provided.

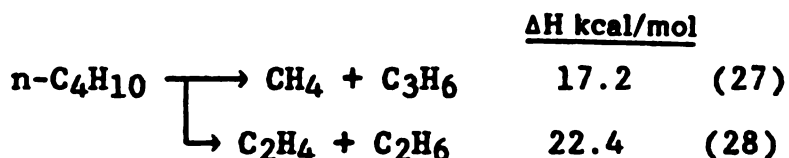
Several attempts have been made to explain why some products are formed in greater abundance than others. Most of these explanations have focused on the various thermochemical aspects of the mechanism. Before going into these thermochemical aspects, one must be aware that evidence indicative of random or nonselective metal insertion is never observed.⁵⁷ If insertion were predominantly a random process, then for the reaction of Co^+ with butane, products arising from intermediate 1 would outnumber products arising from intermediate 2



by a frequency of two to one. However, recall from Chapter 3, that the majority of the products observed in the reaction of Co^+ and butane are attributed to intermediate 2 and not 1. Product distributions indicative of a random trend have never been observed for alkanes or for any other class of compounds.

In terms of the thermochemistry involved in these gas phase reactions, one might expect the stability of the final products to be the dominant factor in determining product distributions. In the reaction of Co^+ and butane, this stability can be assessed upon consideration of the energies involved in the organic decomposition of

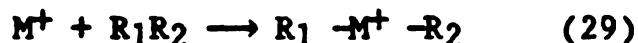
butane and the metal-ligand bond strengths in the products. The energies required for the necessary organic decompositions are shown here:⁸²



Unfortunately, the necessary metal-ligand bond strengths have not been determined experimentally. However, we can apply the correlation⁵ between metal ligand bond strengths and the proton affinities⁸³ of the ligands. The proton affinity of propene is 185 kcal/mol. The proton affinity of ethylene is 164 kcal/mol. Thus, since less energy is required to form propene from butane than ethylene from butane, and because the resulting Co^+ -propene bond is stronger than the Co^+ -ethylene bond (based on the proton affinities) one might expect that reaction (6) would be favored over reaction (7). However, as we have seen earlier, the experimental results indicate that the products of reaction (7) are formed in a greater abundance than those of reaction (6). Thus, this analysis, as well as similar analyses for many other reactions, shows that the final product stabilities for these thermoneutral/exothermic reactions do not determine the product distributions.

Another approach used to explain product distributions focuses on the metal insertion step. Recall that for a

metal to successfully insert into a bond



both the energy required to cleave that bond $D(R_1-R_2)$ and the energy of the two M^+-R bonds formed must be considered. Since accurate thermodynamic information is available only for the $M^+ - CH_3$ bonds (M = first row transition metal)^{77,78}, discussions have focused on a correlation of product distributions with the bond strength of the C-C bond which is cleaved. A consideration of n-butane reveals that the terminal C-C bond strength is ~3 kcal/mol greater than that for the internal C-C bond.⁸² This suggests that M^+ selectively inserts into the weakest skeletal bond of butane to yield the largest fraction of products. However, a difference in bond strength of only 3 kcal/mol may not be expected to produce such a dramatic selectivity. Furthermore, in the larger alkanes, the difference in energy of the internal C-C bonds becomes negligible. Therefore, based on this type of analysis, the trends observed for large alkanes cannot be rationalized. Thus, no correlation between $D(R_1-R_2)$ and product distributions can be accurately made for the metal ion/alkane reaction results in the literature.

The thermochemistry involved in both bond breaking and bond making has also been considered to explain the failure of M^+ to insert into terminal C-C bonds of longer alkanes. Freiser et al. suggest that the higher energy of

the terminal C-C bond coupled with an increase in the metal-alkyl bond energy as the length of the alkyl chain increases, results in selective insertion into internal bonds in alkanes.⁵⁷ They suggest that the increase in metal-alkyl bond energies is due to "electronic considerations".⁵⁷

We suggest here that, since the C-C bond strengths in the n-alkanes are all approximately equal,⁸² the M^+-R bonds formed in reaction (29) determine which insertion intermediates are most stable. Based on work performed in our laboratory along with product distributions reported previously^{5,6,43,36,51,57}, we report here a direct correlation between the C-C bonds of normal alkanes preferred by M^+ for insertion and the ionization potentials (IP's), of the alkyl groups bound to M^+ upon its insertion. We suggest that this correlation is indicative of reactions where the most stable insertion intermediate is formed preferentially.

Before a procedure for establishing an ordering of the preference of M^+ for the C-C bonds in alkanes can be presented, both the experimentally determined product distributions and the mechanism of interaction leading to product formation must be known. The products (both neutral and ionic and branching ratios obtained in the reactions of $Co(CO)^+_n$, $Ni(PF_3)^+_n$, $Ni(CO)_n^+$ and $Fe(CO)^+_n$ [$n = 0,1,2$] with linear and branched alkanes are presented in Tables 2 thru 21. These branching ratios are

TABLE 2. Product Distributions Observed in 2:1 Mixture Methane to ML_n

$\text{Co}(\text{CO})_n^+$	+	CH_4	\longrightarrow	CoCH_4^+	+	$n\text{CO}$	$\frac{n=0}{-}$	$\frac{n=1}{1.0}$	$\frac{n=2}{-}$
$\text{Ni}(\text{CO})_n^+$	+	CH_4	\longrightarrow	N.R.			-	-	-
$\text{Ni}(\text{PF}_3)_n^+$	+	CH_4	\longrightarrow	N.R.			-	-	-

TABLE 3. Product Distributions Observed in 2:1 Mixture Ethane to ML_n

$\text{Co}(\text{CO})_n^+$	+	C_2H_6	\longrightarrow	CoC_2H_6^+	+	$n\text{CO}$	$\frac{n=0}{-}$	$\frac{n=1}{1.0}$	$\frac{n=2}{-}$
$\text{Ni}(\text{CO})_n^+$	+	C_2H_6	\longrightarrow	N.R.			-	-	-
$\text{Ni}(\text{PF}_3)_n^+$	+	C_2H_6	\longrightarrow	N.R.			-	-	-

TABLE 4. Product Distributions Observed in 2:1 Mixture Propane to ML_n

		$\frac{n=0}{1.0}$	$\frac{n=1}{-}$	$\frac{n=2}{-}$
$Co(CO)_n^+ + C_3H_8$	$\rightarrow CoC_3H_6^+ + H_2 + nCO$	-	1.0	-
	$\rightarrow CoC_3H_8^+ + nCO$			
$Ni(CO)_n^+ + C_3H_8$	$\rightarrow NiC_3H_4^+ + 2H_2 + nCO$	-	0.35	-
	$\rightarrow NiC_3H_6^+ + H_2 + nCO$			
	$\rightarrow NiC_2H_4^+ + CH_4 + nCO$			
	$\rightarrow NiC_3H_8^+ + nCO$			
	$\rightarrow NiOOC_3H_8^+ + (n-1)CO$			
$Ni(PF_3)_n^+ + C_3H_8$	$\rightarrow NiC_2H_4^+ + CH_4 + nPF_3$	1.0	-	-
	$\rightarrow NiC_3H_8^+ + nPF_3$			
	$\rightarrow NiPF_3C_3H_8^+ + (n-1)PF_3$			

TABLE 5, Product Distributions Observed in 2:1 Mixture Butane to ML_n

		$\frac{n=0}{-}$	$\frac{n=1}{-}$	$\frac{n=2}{-}$
$Co(CO)_n^+ + C_4H_{10}$	$\rightarrow CoC_2H_4^+ + C_2H_6 + nCO$	0.52	-	-
	$\rightarrow CoC_3H_6^+ + CH_4 + nCO$	0.09	-	-
	$\rightarrow CoC_4H_8^+ + H_2 + nCO$	0.39	0.22	-
	$\rightarrow CoC_4H_{10}^+ + nCO$	-	0.78	-
	$\rightarrow CoCoC_4H_{10}^+ + (n-1)CO$	-	-	1.0
$Ni(CO)_n^+ + C_4H_{10}$	$\rightarrow NiC_2H_4^+ + C_2H_6 + nCO$	0.96	-	-
	$\rightarrow NiC_4H_8^+ + H_2 + nCO$	0.04	0.19	-
	$\rightarrow NiC_4H_{10}^+ + nCO$	-	0.81	-
	$\rightarrow NiCoC_4H_{10}^+ + (n-1)CO$	-	-	1.0
$Ni(PF_3)_n^+ + C_4H_{10}$	$\rightarrow NiC_2H_4^+ + C_2H_6 + nPF_3$	0.73	0.23	-
	$\rightarrow NiC_4H_8^+ + H_2 + nPF_3$	0.11	0.05	-
	$\rightarrow NiC_4H_{10}^+ + nPF_3$	0.16	0.72	-
	$\rightarrow NiPF_3C_4H_{10}^+ + (n-1)PF_3$	-	-	1.0

TABLE 6. Product Distributions Observed in 2:1 Mixture Pentane to ML_n

		$\frac{n=0}{0.12}$	$\frac{n=1}{-}$	$\frac{n=2}{-}$
$Co(CO)_n^+ + C_5H_{12}$	$\rightarrow CoC_2H_4^+ + C_3H_8 + nCO$			
	$\rightarrow CoC_3H_6^+ + C_2H_6 + nCO$	0.65	0.28	-
	$\rightarrow CoC_5H_{10}^+ + H_2 + nCO$	0.23	0.04	-
	$\rightarrow CoC_5H_{12}^+ + nCO$	-	0.68	-
	$\rightarrow CoOOC_5H_{12} + (n-1)CO$	-	-	1.0
$Ni(CO)_n^+ + C_5H_{12}$	$\rightarrow NiC_2H_4^+ + C_3H_8 + nCO$	0.11	-	-
	$\rightarrow NiC_3H_6^+ + C_2H_6 + nCO$	0.54	0.18	-
	$\rightarrow NiC_5H_{10}^+ + H_2 + nCO$	0.35	0.35	-
	$\rightarrow NiC_5H_{12}^+ + nCO$	-	0.47	-
	$\rightarrow NiOOC_5H_{12} + (n-1)CO$	-	-	1.0
$Ni(PF_3)_3^+ + C_5H_{12}$	$\rightarrow NiC_2H_4^+ + C_3H_8 + nPF_3$	0.28	-	-
	$\rightarrow NiC_3H_6^+ + C_2H_6 + nPF_3$	0.40	-	-
	$\rightarrow NiC_5H_{10}^+ + H_2 + nPF_3$	0.32	-	-
	$\rightarrow NiC_5H_{12}^+ + nPF_3$	-	1.0	-

TABLE 7. Product Distributions Observed in 2:1 Mixture Hexane to ML_n

	$n=0$	$n=1$	$n=2$
$Co(CO)_n^+ + \text{Hexane}$ $\rightarrow CoC_3H_6^+ + C_3H_8 + nCO$ $\rightarrow CoC_4H_6^+ + C_2H_6 + H_2 + nCO$ $\rightarrow CoC_4H_8^+ + C_2H_6 + nCO$ $\rightarrow CoC_6H_{12}^+ + H_2 + nCO$ $\rightarrow CoC_6H_{14}^+ + nCO$ $\rightarrow CoCOC_6H_{14}^+ + (n-1)CO$	0.36 0.13 0.29 0.22 - -	0.09 - 0.69 - 0.22 -	- - - - 0.35 0.65
$Ni(CO)_n^+ + \text{Hexane}$ $\rightarrow NiC_3H_6^+ + C_3H_8 + nCO$ $\rightarrow NiC_4H_6^+ + C_2H_6 + H_2 + nCO$ $\rightarrow NiC_6H_{14}^+ + nCO$ $\rightarrow NiCOC_6H_{14}^+ + (n-1)CO$	0.54 0.46 - -	0.32 - 0.68 -	- - 0.73 0.27

TABLE 7

(continued)

	$\frac{n=0}{}$	$\frac{n=1}{}$	$\frac{n=2}{}$
$\text{Nl}(\text{PF}_3)_n^+ + \text{Zigzag}$			
$\rightarrow \text{NlC}_3\text{H}_6^+ + \text{C}_3\text{H}_8 + \text{nPF}_3$	0.36	-	-
$\rightarrow \text{NlC}_4\text{H}_6^+ + \text{C}_2\text{H}_6 + \text{H}_2 + \text{nPF}_3$	0.08	-	-
$\rightarrow \text{NlC}_4\text{H}_8^+ + \text{C}_2\text{H}_6 + \text{nPF}_3$	0.24	-	-
$\rightarrow \text{NlC}_4\text{H}_{10}^+ + \text{C}_2\text{H}_4 + \text{nPF}_3$	0.04	0.15	-
$\rightarrow \text{NlC}_6\text{H}_{12}^+ + \text{H}_2 + \text{nPF}_3$	0.28	-	-
$\rightarrow \text{NlC}_6\text{H}_{14}^+ + \text{nPF}_3$	-	0.85	-
$\rightarrow \text{NlPF}_3\text{C}_6\text{H}_{14}^+ + (\text{n}-1)\text{PF}_3$	-	-	1.0

TABLE 8. Product Distributions Observed in 2:1 Mixture Heptane to ML_n

$Co(CO)_n^+ + \text{heptane}$	$\frac{n=0}{0.56}$	$\frac{n=1}{0.15}$	$\frac{n=2}{-}$
$\rightarrow CoC_3H_6^+ + C_4H_{10} + nCO$			
$\rightarrow CoC_4H_8^+ + C_3H_8 + nCO$	0.16	0.16	-
$\rightarrow CoC_5H_{10}^+ + C_2H_6 + nCO$	0.17	0.27	-
$\rightarrow CoC_7H_{14}^+ + H_2 + nCO$	0.11	0.10	-
$\rightarrow CoC_7H_{16}^+ + nCO$	-	0.32	1.0
$Ni(CO)_n^+ + \text{heptane}$			
$\rightarrow NiC_3H_6^+ + C_4H_{10} + nCO$	0.55	-	-
$\rightarrow NiC_4H_8^+ + C_3H_8 + H_2 + nCO$	0.12	-	-
$\rightarrow NiC_4H_8^+ + C_3H_8 + nCO$	0.10	-	-
$\rightarrow NiC_5H_{10}^+ + C_2H_6 + nCO$	0.14	-	-
$\rightarrow NiC_7H_{14}^+ + H_2 + nCO$	0.09	0.31	-
$\rightarrow NiC_7H_{16}^+ + nCO$	-	0.69	-
$\rightarrow NiOC_7H_{16}^+ + (n-1)CO$	-	-	1.0
$Ni(PF_3)_3^+ + \text{heptane}$			
$\rightarrow NiC_4H_8^+ + C_3H_8 + nPF_3$	0.67	-	-
$\rightarrow NiC_7H_{14}^+ + H_2 + nPF_3$	0.33	-	-
$\rightarrow NiC_7H_{16}^+ + nPF_3$	-	1.0	1.0

TABLE 9. Product Distributions Observed in 2:1 Mixture Octane to ML_n



	<u>n=0</u>	<u>n=1</u>	<u>n=2</u>
$Co(CO)_n^+ + $  $\rightarrow CoC_3H_6^+ + C_5H_{12} + nCO$ $\rightarrow CoC_4H_8^+ + C_4H_{10} + nCO$ $\rightarrow CoC_5H_{10}^+ + C_3H_8 + nCO$ $\rightarrow CoC_6H_{12}^+ + C_2H_6 + nCO$ $\rightarrow CoC_8H_{16}^+ + H_2 + nCO$ $\rightarrow CoC_8H_{18}^+ + nCO$	0.46	0.19	-
	0.15	0.13	-
	0.22	0.23	-
	0.10	0.17	0.05
	0.07	0.28	-
	-	-	0.95
$Ni(CO)_n^+ + $  $\rightarrow NiC_3H_6^+ + C_5H_{12} + nCO$ $\rightarrow NiC_4H_8^+ + C_4H_{10} + nCO$ $\rightarrow NiC_5H_{10}^+ + C_3H_8 + nCO$ $\rightarrow NiC_8H_{18}^+ + nCO$	0.39	0.47	-
	0.13	-	-
	0.48	0.53	-
	-	-	1.0

TABLE 9
(continued)

	$\frac{n=0}{n=1}$	$\frac{n=1}{n=2}$
$\text{Ni}(\text{PF}_3)_n^+ + \text{---} \rightarrow \text{NiC}_3\text{H}_6^+ + \text{C}_5\text{H}_{12} + n\text{PF}_3$	0.37	-
$\rightarrow \text{NiC}_4\text{H}_8^+ + \text{C}_4\text{H}_{10} + n\text{PF}_3$	0.18	-
$\rightarrow \text{NiC}_5\text{H}_{10}^+ + \text{C}_3\text{H}_8 + n\text{PF}_3$	0.36	0.10
$\rightarrow \text{NiC}_8\text{H}_{16}^+ + \text{H}_2 + n\text{PF}_3$	0.09	0.14
$\rightarrow \text{NiC}_8\text{H}_{18}^+ + n\text{PF}_3$	-	0.76
		1.0
$\text{Fe}(\text{CO})_n^+ + \text{---} \rightarrow \text{FeC}_2\text{H}_4^+ + \text{C}_6\text{H}_{14} + n\text{CO}$	0.11	-
$\rightarrow \text{FeC}_3\text{H}_6^+ + \text{C}_5\text{H}_{12} + n\text{CO}$	0.36	0.17
$\rightarrow \text{FeC}_4\text{H}_6^+ + \text{C}_4\text{H}_{10} + \text{H}_2 + n\text{CO}$	0.22	-
$\rightarrow \text{FeC}_4\text{H}_8^+ + \text{C}_4\text{H}_{10} + n\text{CO}$	0.11	-
$\rightarrow \text{FeC}_5\text{H}_8^+ + \text{C}_3\text{H}_8 + \text{H}_2 + n\text{CO}$	0.02	-
$\rightarrow \text{FeC}_5\text{H}_{10}^+ + \text{C}_3\text{H}_8 + n\text{CO}$	0.18	0.02
$\rightarrow \text{FeC}_8\text{H}_{16}^+ + \text{H}_2 + n\text{CO}$	-	0.16
$\rightarrow \text{FeC}_8\text{H}_{18}^+ + n\text{CO}$	-	0.65
$\rightarrow \text{FeCOC}_8\text{H}_{18}^+ + (n-1)\text{CO}$	-	0.19
		0.81

TABLE 10. Product Distributions Observed in 2:1 Mixture Nonane to ML_n

$Co(CO)_n^+ + \text{Nonane}$	$n=0$	$n=1$	$n=2$
$\rightarrow CoC_3H_6^+ + C_6H_{14} + nCO$	0.29	0.06	-
$\rightarrow CoC_4H_8^+ + C_5H_{12} + H_2 + nCO$	0.03	-	-
$\rightarrow CoC_4H_8^+ + C_5H_{12} + nCO$	0.31	0.16	-
$\rightarrow CoC_5H_{10}^+ + C_4H_{10} + nCO$	0.19	0.12	0.04
$\rightarrow CoC_6H_{12}^+ + C_3H_8 + nCO$	0.09	0.13	0.08
$\rightarrow CoC_7H_{14}^+ + C_2H_6 + nCO$	0.03	0.07	-
$\rightarrow CoC_9H_{18}^+ + H_2 + nCO$	0.03	0.07	-
$\rightarrow CoC_9H_{20}^+ + nCO$	0.03	0.26	0.33
$\rightarrow CoCOC_9H_{20}^+ + (n-1)CO$	-	0.13	0.55
$Ni(CO)_n^+ + \text{Nonane}$			
$\rightarrow NiC_3H_6^+ + C_6H_{14} + nCO$	0.20	0.16	-
$\rightarrow NiC_4H_8^+ + C_5H_{12} + nCO$	0.05	0.08	-
$\rightarrow NiC_5H_{10}^+ + C_4H_{10} + nCO$	0.63	0.44	-
$\rightarrow NiC_6H_{12}^+ + C_3H_8 + nCO$	0.07	-	-
$\rightarrow NiC_7H_{14}^+ + C_2H_6 + nCO$	0.05	-	-
$\rightarrow NiC_9H_{18}^+ + H_2 + nCO$	-	0.14	-
$\rightarrow NiC_9H_{20}^+ + nCO$	-	0.18	0.44
$\rightarrow NiCOC_9H_{20}^+ + (n-1)CO$	-	-	0.56

TABLE 10
(continued)

$\text{Fe}(\text{CO})_n^+ + \text{C}_n\text{H}_{2n+2}$	$\text{Fe}(\text{CO})_n^+ + \text{C}_n\text{H}_{2n+2} + \text{nCO}$	$\frac{n=0}{n=1}$	$\frac{n=1}{n=2}$
$\rightarrow \text{FeC}_2\text{H}_4^+ + \text{C}_7\text{H}_{16} + \text{nCO}$	0.11	-	-
$\rightarrow \text{FeC}_3\text{H}_6^+ + \text{C}_6\text{H}_{14} + \text{nCO}$	0.20	0.10	-
$\rightarrow \text{FeC}_4\text{H}_8^+ + \text{C}_5\text{H}_{12} + \text{H}_2 + \text{nCO}$	0.17	-	-
$\rightarrow \text{FeC}_4\text{H}_8^+ + \text{C}_5\text{H}_{12} + \text{nCO}$	0.16	0.06	-
$\rightarrow \text{FeC}_5\text{H}_{10}^+ + \text{C}_4\text{H}_{10} + \text{nCO}$	0.18	0.06	-
$\rightarrow \text{FeC}_6\text{H}_{12}^+ + \text{C}_3\text{H}_8 + \text{nCO}$	0.04	-	-
$\rightarrow \text{FeC}_7\text{H}_{14}^+ + \text{C}_2\text{H}_6 + \text{nCO}$	0.05	0.04	-
$\rightarrow \text{FeC}_9\text{H}_{18}^+ + \text{H}_2 + \text{nCO}$	0.09	0.34	-
$\rightarrow \text{FeC}_9\text{H}_{20}^+ + \text{nCO}$	-	0.40	0.25
$\rightarrow \text{FeCOC}_9\text{H}_{20}^+ + (\text{n}-1)\text{CO}$	-	-	0.75
$\rightarrow \text{NiC}_3\text{H}_6^+ + \text{C}_6\text{H}_{14} + \text{nPF}_3$	0.22	-	-
$\rightarrow \text{NiC}_4\text{H}_8^+ + \text{C}_5\text{H}_{12} + \text{nPF}_3$	0.08	0.02	-
$\rightarrow \text{NiC}_5\text{H}_{10}^+ + \text{C}_4\text{H}_{10} + \text{nPF}_3$	0.56	-	-
$\rightarrow \text{NiC}_6\text{H}_{12}^+ + \text{C}_3\text{H}_8 + \text{nPF}_3$	0.12	0.04	-
$\rightarrow \text{NiC}_7\text{H}_{14}^+ + \text{C}_2\text{H}_6 + \text{nPF}_3$	0.02	0.01	-
$\rightarrow \text{NiC}_9\text{H}_{18}^+ + \text{H}_2 + \text{nPF}_3$	-	0.16	-
$\rightarrow \text{NiC}_9\text{H}_{20}^+ + \text{nPF}_3$	-	0.77	0.45
$\rightarrow \text{NiPF}_3\text{C}_9\text{H}_{20}^+ + (\text{n}-1)\text{PF}_3$	-	-	0.55

TABLE 11. Product Distributions Observed in 2:1 Mixture Decane to ML_n

	$n=0$	$n=1$	$n=2$
$Co(CO)_n^+ + \text{decane} \rightarrow CoC_3H_6^+ + C_7H_{16} + nCO$	0.18	0.04	-
$\rightarrow CoC_4H_8^+ + C_6H_{14} + nCO$	0.28	0.17	-
$\rightarrow CoC_5H_{10}^+ + C_5H_{12} + nCO$	0.16	0.10	-
$\rightarrow CoC_6H_{12}^+ + C_4H_{10} + nCO$	0.17	0.16	-
$\rightarrow CoC_7H_{14}^+ + C_3H_8 + nCO$	0.07	0.09	-
$\rightarrow CoC_8H_{16}^+ + C_2H_6 + nCO$	0.05	0.06	-
$\rightarrow CoC_{10}H_{20}^+ + H_2 + nCO$	0.05	0.10	-
$\rightarrow CoC_{10}H_{22}^+ + nCO$	0.04	0.21	0.47
$\rightarrow CoCOC_{10}H_{22}^+ + (n-1)CO$	-	0.07	0.53
$Ni(CO)_n^+ + \text{decane} \rightarrow NiC_3H_6^+ + C_7H_{16} + nCO$	0.30	0.18	-
$\rightarrow NiC_4H_8^+ + C_6H_{14} + nCO$	0.07	-	-
$\rightarrow NiC_5H_{10}^+ + C_5H_{12} + nCO$	0.17	0.12	-
$\rightarrow NiC_6H_{12}^+ + C_4H_{10} + nCO$	0.28	-	-
$\rightarrow NiC_7H_{14}^+ + C_3H_8 + nCO$	0.15	0.08	-
$\rightarrow NiC_{10}H_{20}^+ + H_2 + nCO$	0.03	0.19	-
$\rightarrow NiC_{10}H_{22}^+ + nCO$	-	0.43	0.45
$\rightarrow NiCOC_{10}H_{22}^+ + (n-1)CO$	-	-	0.55

TABLE 11
(continued)

$\text{Ni}(\text{PF}_3)_n^+ + \text{zigzag}$	n=0	n=1	n=2
$\rightarrow \text{NiC}_3\text{H}_6^+ + \text{C}_7\text{H}_{16} + \text{nPF}_3$	0.41	-	-
$\rightarrow \text{NiC}_4\text{H}_8^+ + \text{C}_6\text{H}_{14} + \text{nPF}_3$	0.20	-	-
$\rightarrow \text{NiC}_5\text{H}_{10}^+ + \text{C}_5\text{H}_{12} + \text{nPF}_3$	0.13	0.05	-
$\rightarrow \text{NiC}_6\text{H}_{12}^+ + \text{C}_4\text{H}_{10} + \text{nPF}_3$	0.14	-	-
$\rightarrow \text{NiC}_7\text{H}_{14}^+ + \text{C}_3\text{H}_8 + \text{nPF}_3$	0.12	-	-
$\rightarrow \text{NiC}_{10}\text{H}_{22}^+ + \text{nPF}_3$	-	0.95	0.51
$\rightarrow \text{NiPF}_3\text{C}_3\text{H}_6^+ + (\text{n-1})\text{PF}_3$	-	-	0.49
$\text{Fe}(\text{CO})_n^+ + \text{zigzag}$			
$\rightarrow \text{FeC}_3\text{H}_6^+ + \text{C}_7\text{H}_{16} + \text{nCO}$	0.15	-	-
$\rightarrow \text{FeC}_4\text{H}_8^+ + \text{C}_6\text{H}_{14} + \text{nCO}$	0.16	-	-
$\rightarrow \text{FeC}_5\text{H}_{10}^+ + \text{C}_5\text{H}_{12} + \text{nCO}$	0.24	-	-
$\rightarrow \text{FeC}_6\text{H}_{12}^+ + \text{C}_4\text{H}_{10} + \text{nCO}$	0.09	-	-
$\rightarrow \text{FeC}_7\text{H}_{14}^+ + \text{C}_3\text{H}_8 + \text{nCO}$	0.12	-	-
$\rightarrow \text{FeC}_{10}\text{H}_{20}^+ + \text{H}_2 + \text{nCO}$	0.14	0.83	-
$\rightarrow \text{FeC}_{10}\text{H}_{22}^+ + \text{nCO}$	0.10	0.17	-
$\rightarrow \text{FeCOC}_{10}\text{H}_{22}^+ + (\text{n-1})\text{CO}$	-	-	1.0

TABLE 12. Product Distributions Observed in 2:1 Mixture 2-Methylpropane to ML_n

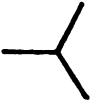
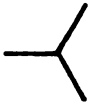
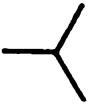
	$n=0$	$n=1$	$n=2$
$Co(CO)_n^+ +$  $\rightarrow CoC_3H_6^+ + CH_4 + nCO$ $\rightarrow CoC_4H_8^+ + H_2 + nCO$ $\rightarrow CoC_4H_{10}^+ + nCO$ $\rightarrow CoCOC_4H_{10}^+ + (n-1)CO$	0.75	0.25	-
	0.25	-	-
	-	0.75	-
	-	-	1.0
$Ni(CO)_n^+ +$  $\rightarrow NiC_3H_6^+ + CH_4 + nCO$ $\rightarrow NiC_4H_{10}^+ + nCO$ $\rightarrow NiCOC_4H_{10}^+ + (n-1)CO$	1.0	0.38	-
	-	0.39	-
	-	0.23	-
$Ni(PF_3)_n^+ +$  $\rightarrow NiC_3H_6^+ + CH_4 + nPF_3$ $\rightarrow NiC_4H_{10}^+ + nPF_3$ $\rightarrow NiPF_3C_4H_{10}^+ + (n-1)PF_3$	1.0	0.14	-
	-	0.77	-
	-	0.09	1.0

TABLE 13. Product Distributions Observed in 2:1 Mixture 2,2-Dimethylpropane to ML_n




		$\frac{n=0}{-}$	$\frac{n=1}{-}$	$\frac{n=2}{-}$
$Co(CO)_n^+ +$ 	$\rightarrow CoC_4H_8^+ + CH_4 + nCO$	1.0	0.62	-
	$\rightarrow CoCOC_4H_8^+ + CH_4 + (n-1)CO$	-	0.38	0.33
	$\rightarrow CoCOC_5H_{12}^+ + (n-1)CO$	-	-	0.67
$Ni(CO)_n^+ +$ 	$\rightarrow NiC_4H_8^+ + CH_4 + nCO$	1.0	0.73	-
	$\rightarrow NiC_5H_{12}^+ + nCO$	-	0.27	0.09
	$\rightarrow NiCOC_5H_{12}^+ + (n-1)CO$	-	-	0.91
$Ni(PF_3)_n^+ +$ 	$\rightarrow NiC_4H_8^+ + CH_4 + nPF_3$	1.0	0.36	-
	$\rightarrow NiC_5H_{12}^+ + nPF_3$	-	0.64	-
	$\rightarrow NiPF_3C_5H_{12}^+ + (n-1)PF_3$	-	-	1.0

TABLE 14. Product Distributions Observed in 3:1 Mixture 2-Methylbutane to ML_n

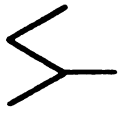
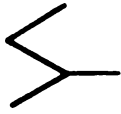
	$\frac{n=0}{}$	$\frac{n=1}{}$	$\frac{n=2}{}$
$Co(CO)_n^+ + $ 			
$\rightarrow CoC_3H_6^+ + C_2H_6 + nCO$	0.46	0.43	-
$\rightarrow CoC_4H_6^+ + CH_4 + H_2 + nCO$	0.33	-	-
$\rightarrow CoC_5H_{10}^+ + H_2 + nCO$	0.21	-	-
$\rightarrow CoC_5H_{12}^+ + nCO$	-	0.57	-
$\rightarrow CoCOC_5H_{12}^+ + (n-1)CO$	-	-	1.0
$Ni(CO)_n^+ + $ 			
$\rightarrow NiC_2H_4^+ + C_3H_8 + nCO$	0.10	-	-
$\rightarrow NiC_3H_6^+ + C_2H_6 + nCO$	0.49	0.35	-
$\rightarrow NiC_4H_6^+ + CH_4 + H_2 + nCO$	0.28	-	-
$\rightarrow NiC_5H_{10}^+ + H_2 + nCO$	0.13	0.18	-
$\rightarrow NiC_5H_{12}^+ + nCO$	-	0.47	-
$\rightarrow NiCOC_5H_{12}^+ + (n-1)CO$	-	-	1.0

TABLE 14
(continued)

	$\frac{n=0}{n=1}$	$\frac{n=1}{n=2}$
$\text{Ni}(\text{PF}_3)_n^+ + \text{C}_3\text{H}_8 + \text{nPF}_3$	0.20	0.14
$\text{Ni}(\text{PF}_3)_n^+ + \text{C}_2\text{H}_6 + \text{nPF}_3$	0.36	0.23
$\text{Ni}(\text{PF}_3)_n^+ + \text{CH}_4 + \text{H}_2 + \text{nPF}_3$	0.13	-
$\text{Ni}(\text{PF}_3)_n^+ + \text{CH}_4 + \text{nPF}_3$	0.17	-
$\text{Ni}(\text{PF}_3)_n^+ + \text{H}_2 + \text{nPF}_3$	0.14	-
$\text{Ni}(\text{PF}_3)_n^+ + \text{nPF}_3$	-	0.63
$\text{Ni}(\text{PF}_3)_n^+ + (\text{n}-1)\text{PF}_3$	-	1.0

TABLE 15. Product Distributions Observed in 2:1 Mixture 2,3-dimethylbutane to ML_n

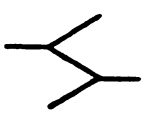
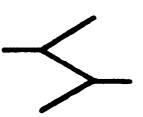
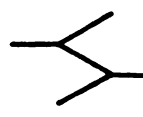
		$n=0$	$n=1$	$n=2$
$Co(CO)_n^+ + $ 	$\rightarrow CoC_3H_6^+ + C_3H_8 + nCO$	0.49	0.50	-
	$\rightarrow CoC_4H_6^+ + 2CH_4 + nCO$	0.23	-	-
	$\rightarrow CoC_5H_8^+ + CH_4 + H_2 + nCO$	0.15	-	-
	$\rightarrow CoC_5H_{10}^+ + CH_4 + nCO$	0.13	0.50	-
$Ni(CO)_n^+ + $ 	$\rightarrow NiC_3H_6^+ + C_3H_8 + nCO$	0.57	0.74	-
	$\rightarrow NiC_4H_6^+ + 2CH_4 + nCO$	0.20	0.06	-
	$\rightarrow NiC_5H_8^+ + CH_4 + H_2 + nCO$	0.15	0.04	-
	$\rightarrow NiC_5H_{10}^+ + CH_4 + nCO$	0.08	0.16	0.27
	$\rightarrow NiCOC_6H_{14}^+ + (n-1)CO$	-	-	0.73
$Ni(PF_3)_n^+ + $ 	$\rightarrow NiC_3H_6^+ + C_3H_8 + nPF_3$	0.89	-	-
	$\rightarrow NiC_6H_{12}^+ + H_2 + nPF_3$	0.11	-	-
	$\rightarrow NiC_6H_{14}^+ + nPF_3$	-	1.0	-
	$\rightarrow NiPF_3C_6H_{14}^+ + (n-1)PF_3$	-	-	1.0

TABLE 16. Product Distributions Observed in 2:1 Mixture 2,2-Dimethylbutane to ML_n



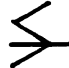
$Co(CO)_n^+ +$ 		$\frac{n=0}{}$	$\frac{n=1}{}$	$\frac{n=2}{}$
\rightarrow $CoC_3H_6^+ + C_3H_8 + nCO$		0.09	-	-
\rightarrow $CoC_4H_6^+ + C_2H_6 + H_2 + nCO$		0.29	-	-
\rightarrow $CoC_4H_8^+ + C_2H_6 + nCO$		0.31	0.20	-
\rightarrow $CoC_5H_8^+ + CH_4 + H_2 + nCO$		0.11	-	-
\rightarrow $CoC_5H_{10}^+ + CH_4 + nCO$		0.14	0.14	-
\rightarrow $CoC_6H_{12}^+ + H_2 + nCO$		0.06	0.50	-
\rightarrow $CoCOC_5H_{10}^+ + CH_4 + (n-1)CO$		-	0.16	-
$Ni(CO)_n^+ +$ 				
\rightarrow $NiC_2H_4^+ + C_4H_{10} + nCO$		0.12	-	-
\rightarrow $NiC_4H_6^+ + C_2H_6 + H_2 + nCO$		0.30	0.19	-
\rightarrow $NiC_4H_8^+ + C_2H_6 + nCO$		0.33	0.62	-
\rightarrow $NiC_5H_8^+ + CH_4 + H_2 + nCO$		0.18	-	-
\rightarrow $NiC_5H_{10}^+ + CH_4 + nCO$		0.07	0.05	-
\rightarrow $NiC_6H_{14}^+ + nCO$		-	0.14	-
\rightarrow $NiCOC_6H_{14}^+ + (n-1)CO$		-	-	1.0
$Ni(PF_3)_n^+ +$ 				
\rightarrow $NiC_4H_6^+ + C_2H_6 + H_2 + nPF_3$		0.27	-	-
\rightarrow $NiC_4H_8^+ + C_2H_6 + nPF_3$		0.73	-	-

TABLE 17. Product Distributions Observed in 2:1 Mixture 2,2,3,3-Tetramethylbutane to ML_n


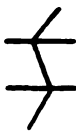

		$\frac{n=0}{}$	$\frac{n=1}{}$	$\frac{n=2}{}$
$Co(CO)_n^+ + $ 	$\rightarrow CoC_4H_8^+ + C_4H_{10} + nCO$	0.33	0.10	-
	$\rightarrow CoCOC_4H_8^+ + C_4H_{10} + (n-1)CO$	-	0.26	0.52
	$\rightarrow CoC_6H_{10}^+ + 2CH_4 + nCO$	0.67	0.16	-
	$\rightarrow CoC_8H_{16}^+ + H_2 + nCO$	-	0.19	-
	$\rightarrow CoC_8H_{18}^+ + nCO$	-	0.29	-
	$\rightarrow CoCOC_8H_{18}^+ + (n-1)CO$	-	-	0.48
$Ni(CO)_n^+ + $ 	$\rightarrow NiC_4H_8^+ + C_4H_{10} + nCO$	-	0.12	-
	$\rightarrow NiC_6H_{10}^+ + 2CH_4 + nCO$	1.0	0.40	-
	$\rightarrow NiC_8H_{18}^+ + nCO$	-	0.48	-
$Ni(PF_3)_n^+ + $ 	$\rightarrow NiC_4H_8^+ + C_4H_{10} + nPF_3$	0.48	0.33	-
	$\rightarrow NiC_6H_{10}^+ + 2CH_4 + nPF_3$	0.52	0.22	-
	$\rightarrow NiC_8H_{18}^+ + nPF_3$	-	0.45	-

TABLE 18. Product Distributions Observed in 2:1 Mixture 3-Methylpentane to ML_n




$Co(CO)_n^+ + $ 		$\frac{n=0}{}$	$\frac{n=1}{}$	$\frac{n=2}{}$
$\rightarrow CoC_2H_4^+ + C_4H_{10} + nCO$		0.14	-	-
$\rightarrow CoC_4H_6^+ + C_2H_6 + H_2 + nCO$		0.40	-	-
$\rightarrow CoC_4H_8^+ + C_2H_6 + nCO$		0.35	0.41	-
$\rightarrow CoC_6H_{12}^+ + H_2 + nCO$		0.11	0.18	-
$\rightarrow CoC_5H_8^+ + CH_4 + H_2 + nCO$		-	0.18	-
$\rightarrow CoC_6H_{14}^+ + nCO$		-	0.23	-
$Ni(CO)_n^+ + $ 				
$\rightarrow NiC_4H_6^+ + C_2H_6 + H_2 + nCO$		0.35	0.16	-
$\rightarrow NiC_4H_8^+ + C_2H_6 + nCO$		0.65	0.35	-
$\rightarrow NiC_6H_{12}^+ + H_2 + nCO$		-	0.26	-
$\rightarrow NiC_6H_{14}^+ + nCO$		-	0.23	-
$\rightarrow NiCOC_6H_{14}^+ + (n-1)CO$		-	-	1.0
$Ni(PF_3)_n^+ + $ 				
$\rightarrow NiC_4H_6^+ + C_2H_6 + H_2 + nPF_3$		0.39	0.03	-
$\rightarrow NiC_4H_8^+ + C_2H_6 + nPF_3$		0.43	0.37	-
$\rightarrow NiC_6H_{12}^+ + H_2 + nPF_3$		0.18	-	-
$\rightarrow NiC_6H_{14}^+ + nPF_3$		-	0.60	-
$\rightarrow NiPF_3C_6H_{14}^+ + (n-1)PF_3$		-	-	1.0

TABLE 19. Product Distributions Observed in 2:1 Mixture 2,4-Dimethylpentane to ML_n

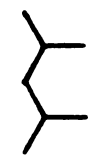
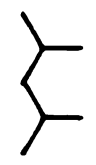
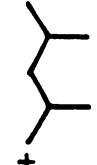
		$n=0$	$n=1$	$n=2$
$Co(CO)_n^+ + $ 	$\rightarrow CoC_3H_6^+ + C_4H_{10} + nCO$	0.31	-	-
	$\rightarrow CoC_4H_8^+ + C_3H_8 + nCO$	0.35	0.29	-
	$\rightarrow CoC_6H_{12}^+ + CH_4 + nCO$	0.18	0.20	0.30
	$\rightarrow CoC_7H_{14}^+ + H_2 + nCO$	0.16	0.13	-
	$\rightarrow CoC_7H_{16}^+ + nCO$	-	0.38	-
	$\rightarrow CoCOC_7H_{16}^+ + (n-1)CO$	-	-	0.70
$Ni(CO)_n^+ + $ 	$\rightarrow NiC_3H_6^+ + C_4H_{10} + nCO$	0.38	-	-
	$\rightarrow NiC_4H_8^+ + C_3H_8 + nCO$	0.46	-	-
	$\rightarrow NiC_7H_{14}^+ + H_2 + nCO$	0.16	0.57	-
	$\rightarrow NiC_7H_{16}^+ + nCO$	-	0.43	0.38
	$\rightarrow NiCOC_7H_{16}^+ + (n-1)CO$	-	-	0.62
$Ni(PF_3)_n^+ + $ 	$\rightarrow NiC_3H_6^+ + C_4H_{10} + nPF_3$	0.12	-	-
	$\rightarrow NiC_4H_8^+ + C_3H_8 + nPF_3$	0.63	-	-
	$\rightarrow NiC_7H_{14}^+ + H_2 + nPF_3$	0.25	0.36	-
	$\rightarrow NiC_7H_{16}^+ + nPF_3$	-	0.64	-
	$\rightarrow NiPF_3C_7H_{16}^+ + (n-1)PF_3$	-	-	1.0

TABLE 20. Product Distributions Observed in 2:1 Mixture 2,3,4-Trimethylpentane to M_L^n

	$n=0$	$n=1$	$n=2$
$\text{Co}(\text{CO})_n^+ + \text{2,3,4-Trimethylpentane} \rightarrow \begin{cases} \text{CoC}_3\text{H}_6^+ + \text{C}_5\text{H}_{12} + \text{nCO} \\ \text{CoC}_4\text{H}_6^+ + \text{CH}_4 + \text{C}_3\text{H}_8 + \text{nCO} \\ \text{CoC}_4\text{H}_8^+ + \text{C}_4\text{H}_{10} + \text{nCO} \\ \text{CoC}_5\text{H}_{10}^+ + \text{C}_3\text{H}_8 + \text{nCO} \\ \text{CoC}_7\text{H}_{14}^+ + \text{CH}_4 + \text{nCO} \\ \text{CoC}_8\text{H}_{16}^+ + \text{H}_2 + \text{nCO} \\ \text{CoC}_8\text{H}_{18}^+ + \text{nCO} \end{cases}$	0.18	-	-
	0.29	-	-
	0.11	0.09	-
	0.27	0.36	-
	0.10	0.30	-
	0.05	0.09	-
	-	0.16	1.0
$\text{Ni}(\text{CO})_n^+ + \text{2,3,4-Trimethylpentane} \rightarrow \begin{cases} \text{NiC}_3\text{H}_6^+ + \text{C}_5\text{H}_{12} + \text{nCO} \\ \text{NiC}_4\text{H}_6^+ + \text{CH}_4 + \text{C}_3\text{H}_8 + \text{nCO} \\ \text{NiC}_5\text{H}_{10}^+ + \text{C}_3\text{H}_8 + \text{nCO} \\ \text{NiC}_7\text{H}_{14}^+ + \text{CH}_4 + \text{nCO} \\ \text{NiC}_8\text{H}_{16}^+ + \text{H}_2 + \text{nCO} \end{cases}$	0.64	-	-
	0.23	-	-
	0.13	0.14	-
	-	0.41	-
	-	0.45	1.0

TABLE 20
(continued)

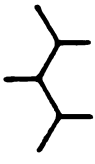
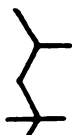
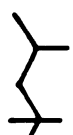

$\text{Ni}(\text{PF}_3)_n^+ +$ 	$\text{NiC}_3\text{H}_6^+ + \text{C}_5\text{H}_{12} + \text{nPF}_3$	n=0	n=1	n=2
\rightarrow	$\text{NiC}_4\text{H}_6^+ + \text{CH}_4 + \text{C}_3\text{H}_8 + \text{nPF}_3$	0.36	0.07	-
\rightarrow	$\text{NiC}_5\text{H}_{10}^+ + \text{C}_3\text{H}_8 + \text{nPF}_3$	0.18	-	-
\rightarrow	$\text{NiC}_8\text{H}_{16}^+ + \text{H}_2 + \text{nPF}_3$	0.31	0.09	-
\rightarrow	$\text{NiC}_8\text{H}_{18}^+ + \text{nPF}_3$	0.15	0.38	-
\rightarrow	$\text{NiPF}_3\text{C}_8\text{H}_{18}^+ + (\text{n-1})\text{PF}_3$	-	0.46	-
		-	-	1.0

TABLE 21. Product Distributions Observed in 2:1 Mixture 2,2,4-Trimethylpentane to M_n

	$n=0$	$n=1$	$n=2$
$\text{Co}(\text{CO})_n^+ + $ 			
$\rightarrow \text{CoC}_3\text{H}_6^+ + \text{C}_5\text{H}_{12} + \text{nCO}$	0.46	-	-
$\rightarrow \text{CoC}_4\text{H}_8^+ + \text{C}_4\text{H}_{10} + \text{nCO}$	0.41	0.05	-
$\rightarrow \text{CoCOC}_4\text{H}_8^+ + \text{C}_4\text{H}_{10} + (n-1)\text{CO}$	-	0.11	0.38
$\rightarrow \text{CoC}_7\text{H}_{14}^+ + \text{CH}_4 + \text{nCO}$	0.06	0.06	-
$\rightarrow \text{CoC}_8\text{H}_{16}^+ + \text{H}_2 + \text{nCO}$	0.07	0.07	-
$\rightarrow \text{CoC}_8\text{H}_{18}^+ + \text{nCO}$	-	0.68	-
$\rightarrow \text{CoCOC}_8\text{H}_{18}^+ + (n-1)\text{CO}$	-	0.03	0.62
$\text{Ni}(\text{CO})_n^+ + $ 			
$\rightarrow \text{NiC}_3\text{H}_6^+ + \text{C}_5\text{H}_{12} + \text{nCO}$	0.26	0.16	-
$\rightarrow \text{NiC}_4\text{H}_8^+ + \text{C}_4\text{H}_{10} + \text{nCO}$	0.70	0.43	-
$\rightarrow \text{NiC}_4\text{H}_6^+ + 2\text{C}_2\text{H}_6 + \text{nCO}$	-	0.04	-
$\rightarrow \text{NiC}_7\text{H}_{14}^+ + \text{CH}_4 + \text{nCO}$	-	0.06	-
$\rightarrow \text{NiC}_8\text{H}_{16}^+ + \text{H}_2 + \text{nCO}$	0.04	0.31	-
$\text{Ni}(\text{PF}_3)_n^+ + $ 			
$\rightarrow \text{NiC}_3\text{H}_6^+ + \text{C}_5\text{H}_{12} + \text{nPF}_3$	0.35	-	-
$\rightarrow \text{NiC}_4\text{H}_8^+ + \text{C}_4\text{H}_{10} + \text{nPF}_3$	0.65	0.13	-
$\rightarrow \text{NiC}_8\text{H}_{16}^+ + \text{H}_2 + \text{nPF}_3$	-	0.47	-
$\rightarrow \text{NiC}_8\text{H}_{18}^+ + \text{nPF}_3$	-	0.40	1.0

consistent with those previously reported^{5,6,43,36,51,57} and represent the product distributions. Knowledge of the mechanism allows for correlation between specific insertion intermediates and specific products. When mechanistic information is coupled to product distributions, a direct relationship between product and intermediate abundances can be established.

Consider the reaction of Co^+ and heptane as an example. Heptane is composed of three pairs of chemically indistinguishable bonds, labelled here as a, b and c:



In the reaction of Co^+ with heptane, Co^+ has a choice of inserting into three "distinct" C-C bonds: a, b and c. Based on Scheme 4, which involves the accepted metal insertion / β -H shift/ competitive ligand loss sequence, and the branching ratios taken from Table 8, an ordering of the preference of Co^+ for a, b and c can be determined. Thus, disregarding H_2 elimination, intermediate **3** accounts for zero per cent of the products, **4** accounts for seventeen per cent of the products and **5** accounts for seventy-two per cent of the products, suggesting bond (c) is preferred over (b) which is preferred over (a) by Co^+ .

This initial analysis has assumed that H_2 elimination occurs exclusively through Co^+ insertion into C-H bonds followed by the shift of a β -hydrogen (1,2

Scheme 4



<u>Intermediates</u>		<u>Products</u>	<u>Product Distributions</u>
CH ₃ -Co ⁺ -C ₆ H ₁₃ 3	H-shift	CoC ₆ H ₁₂ ⁺ + CH ₄	0%
C ₂ H ₅ -Co ⁺ -C ₅ H ₁₁ 4	H-Shift	CoC ₅ H ₁₀ ⁺ + C ₂ H ₆ CoC ₂ H ₄ ⁺ + C ₅ H ₁₂	17% 0%
C ₃ H ₇ -Co ⁺ -C ₄ H ₉ 5	H-shift	CoC ₄ H ₈ ⁺ + C ₃ H ₈ CoC ₄ H ₆ ⁺ + H ₂ CoC ₃ H ₆ ⁺ + C ₄ H ₁₀	16% 0% 56%
H-Co ⁺ -C ₇ H ₁₅ 6	H-shift	CoC ₇ H ₁₄ ⁺ + H ₂	10%

dehydrogenation). However, the literature reports that H_2 elimination can also be induced by M^+ insertion into C-C bonds followed by the shift of two hydrogens which are β to the metal^{51,57} (1,4 dehydrogenation). Therefore, to accurately assess the preference of M^+ for the C-C bonds of alkanes, differentiation between H_2 elimination resulting from initial insertion into C-H and into C-C bonds must be established.

Two approaches have been used to distinguish between 1,2 and 1,4 dehydrogenation. These include labelling experiments⁵³ and collision-induced dissociation (CID) experiments.⁵⁷ By examining the branching ratios associated with H_2 , HD and D_2 elimination in the reactions of M^+ and strategically deuterated alkanes, the percentage of M^+ insertion into each of the various C-H and C-C bonds should become apparent. The reactions of specifically deuterated butane, pentane and hexanes with Fe^+ , Co^+ and Ni^+ were studied.⁵³ The percentages of both 1,2 and 1,4 dehydrogenation observed in these reactions are summarized in Table 22. For example, the results for the reaction of Co^+ with $CD_3CH_2CH_2CD_3$ suggest that fifty-one percent of the H_2 elimination products result from initial insertion into the internal C-C bond and forty-nine per cent from insertion into C-H bonds. The results obtained for the reactions of Fe^+ and Co^+ with deuterated pentane and hexane are inconclusive. The products observed in these cases can be attributed to

TABLE 22. Per Cent (1,2) vs. (1,4) Dehydrogenation in the
Reactions of M^+ with Deuterated Butane, Pentane and Hexane ^a

Reactant Alkane M^+	Butane $CD_3CH_2CH_2CD_3$		Pentane $CH_3CD_2CD_2CD_2CH_3$		Hexane $CH_3CD_2CH_2CH_2CH_2CD_2CH_3$			
	% (1,2)	% (1,4)	% (1,2)	% (1,4)	% (1,2)	% (1,4)	% (1,2)	% (1,4)
Fe^+	77	23	≥17	b	b	b	≥43	≥10
Co^+	49	51	≥12	b	b	b	≥21	≥33
Ni^+	0	100	0	100	b	b	b	≥45

a. Based on product distributions in Table III in Ref. 53.

b. Formation of observed products can be attributed to either (1,2) or (1,4) dehydrogenation.

either 1,2 or 1,4 dehydrogenation or both. Furthermore, the authors note that caution must be used in interpreting the results of these labelling experiments due to potential deuterium isotope effects which may be significant in all or some of the individual steps of the mechanism.⁵³

Also, some products observed in the reactions of Fe^+ with deuterated alkanes are indicative of the occurrence of β -methyl shifts.⁵³ However, these products are representative of only a small fraction of the total reaction products. Therefore, the ordering of the preference of Fe^+ for the C-C bonds of alkanes should be unaffected by the occurrence of β -methyl shifts.

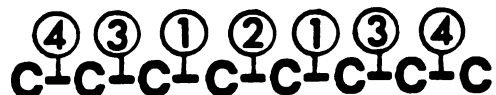
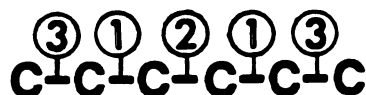
Jacobson and Freiser have utilized CID to probe the structures of the ionic products formed in the dehydrogenation reactions occurring between M^+ and select alkanes.⁵⁷ Their results suggest that thirty per cent of the dehydrogenation occurs via insertion into C-C bonds and seventy per cent by insertion into C-H bonds in alkanes for Fe^+ . For Co^+ , ninety per cent of the dehydrogenation occurs through a 1,4 process and ten per cent by insertion into C-H bonds. Ni^+ appears to insert exclusively into C-C bonds to eliminate H_2 .

When dehydrogenation can result from M^+ insertion into more than one C-C bond of a particular alkane, structurally different product ions of the same mass to charge ratio may be formed. The CID results of Jacobson

and Freiser further suggest which of the C-C bonds in hexane and heptane are preferred for insertion by Co^+ or Ni^+ in dehydrogenation reactions. For example, of the dehydrogenation products resulting from the reaction of Co^+ with heptane, sixty-two per cent would suggest a $\text{Co}^+(\text{propene})(\text{butene})$ complex and thirty-eight per cent a $\text{Co}^+(\text{ethylene})(\text{pentene})$ complex.⁵⁷ These results indicate that bond c is preferred over b for insertion by Co^+ to eliminate H_2 from heptane. Reassessing the abundances of intermediates 3,4,5 and 6 in Scheme 4 based on this information, the overall ordering of the preference of Co^+ for insertion into heptane is $c > b > a$. Note further, that according to the results in Tables 5 thru 11, as the length of the alkyl chain increases from butane to decane, the total percentage of H_2 elimination significantly decreases. Thus consideration of H_2 elimination resulting from insertion into C-C bonds in determining the abundances of the various intermediates becomes unnecessary for alkanes larger than heptane.

Using the product distributions provided in Tables 5 thru 11 in conjunction with Freiser's results for 1,4 dehydrogenation occurring in hexane and heptane,⁵⁷ an ordering of the preferred sites of Co^+ and Ni^+ insertion into the C-C bonds of normal alkanes from butane to decane is presented in Table 23. Note that the trends observed for these two metal ions are identical. Furthermore, an analysis of the product distributions

Table 23. Preference ^a of Fe⁺, Co⁺ and Ni⁺ for C-C Bond Insertion in Linear Alkanes ^b



- a. As determined by the method discussed in the text. The ordering is consistent with ICR results from our laboratory and previously reported results^{2,3} within experimental uncertainty.
- b. Double circles indicate that a different preference for these two bonds was observed for the metal ions studied. In the case of decane, Fe⁺ exhibited equal preference for the two bonds indicated by double circles. In the case of Co⁺ the order is as shown. In the case of Ni⁺ the order of the bonds labelled ① and ② is reversed.

observed in the reactions of Fe^+ and $n\text{-C}_n\text{H}_{2n+2}$ ($n = 4-7$) previously reported in the literature^{52,53,57} along with the Fe^+ data provided in Tables 9 thru 11 indicates that Fe^+ exhibits the same trends as Co^+ and Ni^+ . In general, terminal C-C bonds have the lowest priority for insertion in each case.

Why are some C-C bonds in nonpolar alkanes more susceptible to insertion than others? As we have seen, for successful insertion to occur, the energy associated with bond breaking (plus the promotion energy of M^+)⁹⁰ must be compensated for by the energy released during bond formation. Of these two processes, direct correlation between C-C bond strengths in alkanes and the preferred sites of M^+ insertion is indeterminate. Pertinent experimental data regarding the heats of formation of alkyl radicals which are needed to calculate C-C bond strengths are either lacking or else are indicative of differences which are quite small ($<5\text{kcal}$) and may be insufficient to explain the dramatic selectivity observed. Any correlation between the bond making process and the ordering could be determined through a knowledge of $\text{M}^+\text{-R}$ bond strengths. Experimental values of these bond strengths are unavailable for $\text{R} > \text{CH}_3$. However, we believe they can be assessed upon consideration of polarizabilities.

A comparison of the experimentally determined values of $D(M^+-H)$ and $D(M^+-CH_3)$ reveals that M^+ forms a stronger bond to a methyl group than to a hydrogen^{43,53}. This trend is opposite to that observed for the neutral metal species and has been explained on the basis of polarizability. Since CH_3 is more polarizable than H , CH_3 can better stabilize the positive charge on the metal and in doing so forms a stronger bond to the metal ion. Building on this example, the polarizability of an alkyl group (C_nH_{2n+1}) would be expected to increase as n gets larger. We suggest that an increase in polarizability parallels an increase in $D(M^+-C_nH_{2n+1})$.

Unfortunately, experimentally determined alkyl group polarizabilities are not available. However, ionization potentials, which in part reflect polarizabilities, are available. In general, the smaller the IP, the larger the polarizability. Table 24 lists the IP's of C_nH_{2n+1} from $n = 4$ to $n = 10$. Note that the IP's decrease as n increases. Therefore, we suggest that the polarizability increases leading to an increase in $D(M^+-C_nH_{2n+1})$ as n gets larger. This is apparently true for $D^+(Hg^+-R)$, $D^+(Cl^+-R)$ and $D^+(HO^+-R)$ as is shown in Table 24. As $IP(C_nH_{2n+1})$ decreases, each of these bond strengths increases. (This does not appear to be the case for the analogous neutral species).⁹ Furthermore, as $IP(C_nH_{2n+1})$ decreases, the $HOMO(C_nH_{2n+1}) - LUMO(M^+)$ gap may decrease

Table 24. Alkyl Radical Ionization Potentials and Bondstrengths to Various Atomic Cations

Radical (R·)	IP (kcal/mol)	$D^{\circ}(\text{Cl}^{+}\text{-R})$, kcal/mole	$D^{\circ}(\text{HO}^{+}\text{-R})$, kcal/mole	$D^{\circ}(\text{Hg}^{+}\text{-R})$, kcal/mole
CH ₃	226.0 ± 0.5 ^a	119.7	137.0	53.2
C ₂ H ₅	193.5 ± 0.5 ^a	123.4	144.7	57.0
n-C ₃ H ₇	187.5 ± 1.0 ^b	130.4	148.7	65.8 ^f
n-C ₄ H ₉	184.7 ± 1.0 ^b	132.4	150.7	
n-C ₅ H ₁₁	183.1 ± 1.4 ^c			
n-C ₆ H ₁₃	182.6 ± 1.4 ^c			
n-C ₇ H ₁₅	182.2 ± 1.4 ^c			
n-C ₈ H ₁₇	182.2 ^d			
n-C ₉ H ₁₉	182.2 ^d			

^a Data taken from Ref. 91. ^b Data taken from Ref. 92. ^c Data taken from Ref. 93. ^d Extrapolated from a plot of the known IP's (as given in this table) vs. number of carbons. ^e Data taken from Ref. 9. ^f Bondstrength for Hg⁺-(i-C₃H₇).

thus facilitating bonding.⁹⁶

Upon consideration of the bond making process, direct correlation is found between the sum of the IP's of the alkyl groups bound to M^+ after insertion and the ordering of the preference of M^+ for the C-C bonds of alkanes. Figure 4 graphically illustrates this correlation. Note that within the experimental error of the thermodynamic information available, the preference of attack is largest when the sum of the corresponding alkyl IP's is lowest. Priority decreases as the sum of the IP's increases. For example in heptane, the sums of the IP's associated with the alkyl groups involved in the various intermediates can be ranked as follows:

$$\begin{aligned} & [\text{IP}(\text{CH}_3) + \text{IP}(\text{C}_6\text{H}_{13})] > [\text{IP}(\text{C}_2\text{H}_5) + \text{IP}(\text{C}_5\text{H}_{11})] \\ & > [\text{IP}(\text{C}_3\text{H}_7) + \text{IP}(\text{C}_4\text{H}_9)] \end{aligned}$$

Based on the experimental results, the smallest sum is associated with intermediate C which accounts for the majority of the products. Thus, the third C-C bond in heptane, designated as c, is given a priority of attack of ①. The largest sum corresponds to A which accounts for the smallest number of products. Therefore, the terminal C-C bond in heptane is given a priority of ③ in Figure 4. This correlation suggests that when more than one metal insertion intermediate of the type $R-M^+-R'$ is possible, the one in which the M^+-R bonds are strongest is formed preferentially. We believe that the

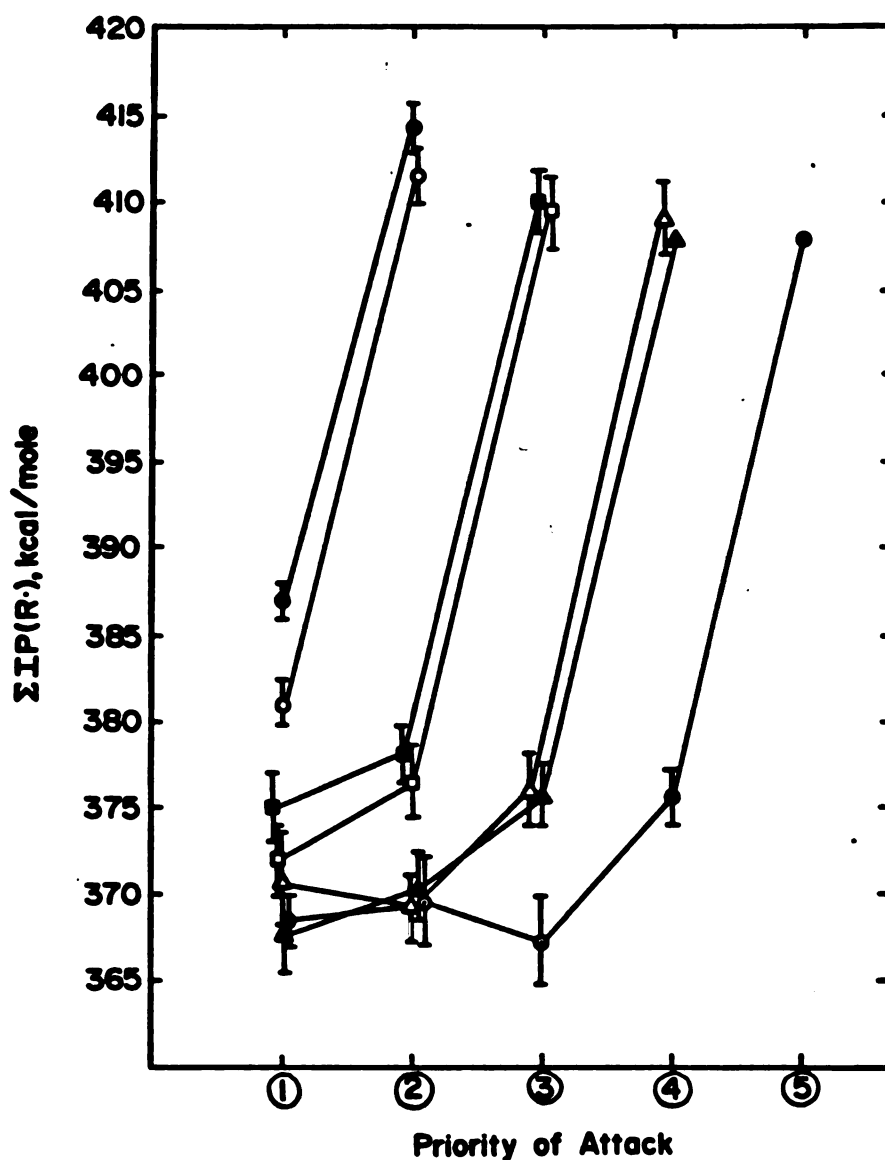


Figure 4. Correlation between priority of attack and the radical ionization potential sums. The C-C bond for which insertion by M^+ ($M = \text{Fe, Co, Ni}$) occurs to the greatest extent is given a priority of ①. The bond next most favored is priority ②, etc. When a C-C bond is cleaved, two alkyl radicals are formed. The sum of the ionization potentials of these two radicals correlates with the extent to which M^+ inserts into that bond. The correlation is shown for butane (●), pentane (○), hexane (■), heptane (□), octane (△), nonane (▲) and decane (⊙).

distribution of insertion intermediates reflects their relative stabilities. For heptane, then, we suggest that ζ is favored over β which is favored over α because:

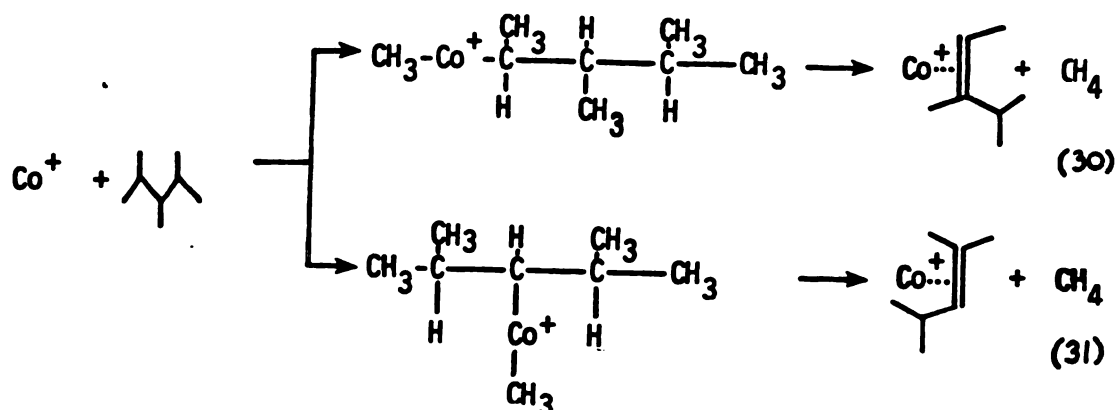
$$[D^\circ(M^+-C_3H_7) + D^\circ(C_3H_7M^+-C_4H_9)] > [D^\circ(M^+-C_2H_5) + D^\circ(C_2H_5M^+-C_5H_{11})] \\ > [D^\circ(M^+-CH_3) + D^\circ(CH_3M^+-C_6H_{13})]$$

A slight discrepancy is seen in the trend observed for decane in Figure 4. The insertion intermediate involving the lowest sum of IP's is ranked third (priority III) in preference. This discrepancy can be understood on the basis of the uncertainty associated with the experimental values of the alkyl group IP's. This uncertainty causes overlap in the values of the sums of the IP's associated with the three most preferred C-C bonds in decane by M^+ . Furthermore, as the number of carbons in the alkyl chain increases, the difference in the IP of (C_nH_{2n+1}) and $(C_{n+1}H_{2(n+1)+1})$ decreases until it eventually becomes negligible. Thus, it would appear that, as in the case of $D^\circ(Cl^+-R)$, the difference in bond strengths, $[D^\circ(M^+-C_nH_{2n+1}) - D^\circ(M^+-C_{(n+1)}H_{2(n+1)+1})]$, should also decrease with increasing n . Thus, metal ion-alkyl bond strengths would be expected to converge when n is sufficiently large. This convergence would contribute further to overlap in the sums of the IP's as the chain length of the alkyl groups bound to M^+ get larger. Perhaps then decane marks the transition where

direct correlation between the sum of the IP's and priority of attack cannot be established.

Using this model, the fact that M^+ rarely inserts into terminal C-C bonds^{53,57} can be explained on the basis of the relatively high IP of the methyl radical which in turn suggests that the M^+-CH_3 bond may be the weakest of the M^+ -alkyl bonds. Also, it must be noted that this model does not appear to hold for the reactions of transition metal ions and polar molecules (RX). The functional group, (X), in polar molecules may have a strong effect in "directing" the site of attack of the metal ion to certain skeletal bonds which would not be attacked in the corresponding alkanes, (RH).¹⁹

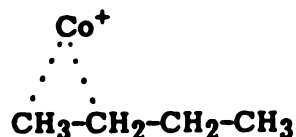
Two major problems arise when one attempts to apply this type of analysis to branched alkanes. First, a significant number of IP's of the radicals associated with branched alkanes are not available. Secondly, due to the presence of the branched sites, metal ion insertion into several chemically nonequivalent C-C bonds can result in the loss of the same small neutral molecule. For example, in the reaction of M^+ with 2,3,4-trimethylpentane, there are two insertion intermediates which could be responsible for the observed methane elimination. Reactions (30) and (31) illustrate this point.



Both of the ionic products in reactions (30) and (31) correspond to an $m/z = 157$ and therefore cannot be distinguished in the mass spectrum. Due to complications such as these, a similar analysis for branched alkanes will not be attempted.

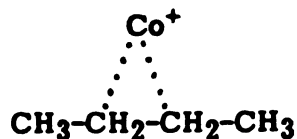
Finally, we realize that there may be other explanations for the observed correlation. We believe that the distribution of observed products reflects the distribution of intermediates which are formed "early" in the reaction. This prompts us to ask how the initial distribution of insertion intermediates is established. There are at least two possibilities. Perhaps rapid insertion/"deinsertion" occurs, allowing the metal ion to

"sample" all possibilities. A second explanation may involve the formation of the most stable ion-alkane complexes. Thus, for butane, consider intermediates 7 and 8.



7

~



8

~

A consideration of alkyl polarizabilities may predict that 8 is more stable than 7. Therefore, the distribution of initial complex structures may determine which bonds are attacked, rather than the stabilities of the insertion intermediates which follow.

Chapter 7

Ligand Effects

Several studies have appeared in the literature yielding useful insights into the reactions of bare (+1) metal ions and alkanes. As discussed in Chapter 6, product formation in these gas phase reactions can be rationalized by a mechanism involving the metal insertion / β -H shift/ competitive ligand loss mechanistic sequence. Furthermore metal insertion into the C-C bonds of alkanes was shown to be favored by Fe^+ , Co^+ , and Ni^+ over insertion into C-H bonds.

In condensed phases, organometallic chemistry involves metal complexes.^{86,87,97-103} Ligands such as CO, NO and PF_3 are frequently utilized in these metal complexes and serve as important ligands in organometallic chemistry.¹⁰⁴ Therefore, it would be useful to investigate the changes which occur in the chemistry of Fe^+ , Co^+ and Ni^+ with alkanes when one or two of these ligands are bound to the metal, and compare this chemistry to that observed for organometallic complexes in condensed phases. Thus, in this chapter, the chemistry of $\text{Fe}(\text{CO})_n^+$, $\text{Co}(\text{CO})_n^+$, CoNO^+ , $\text{Ni}(\text{CO})_n^+$, and $\text{Ni}(\text{PF}_3)_n^+$ [$n = 1,2$] with a series of linear and branched alkanes will be examined. The products and branching ratios associated with these reactions are summarized in Tables 2 through 21. These results will be compared to those observed for the bare metal

ions. Parallels to solution chemistry will be discussed.

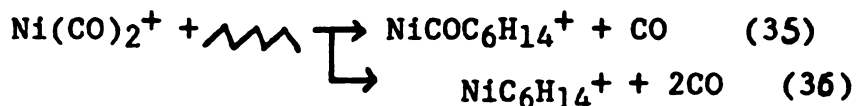
With the addition of ligands to the metal, several different types of reactions are observed depending upon the number and nature of the ligands. FeCO^+ , CoCO^+ and NiPF_3^+ all react with alkanes to form some of the same products as the corresponding bare metal ion. In this case, the addition of a ligand has no apparent effect on the reactivity of the metal. We refer to this situation as one where the ligand acts as a spectator. For example, both Co^+ and CoCO^+ react with 2-methylbutane to form CoC_3H_6^+ :



In contrast to this is the CoNO^+ ion which is totally unreactive. The presence of the nitrosyl ligand apparently deactivates the metal ion. In addition, FeCO^+ , CoCO^+ , NiCO^+ and NiPF_3^+ all react with alkanes to form "ligand substitution" products. This process is illustrated for NiPF_3^+ and 2-methylbutane in reaction (34).



A metal ion complex containing two ligands only reacts with alkanes to form "ligand substitution" products in which one or both ligands are lost. For hexane and Ni(CO)_2^+ , reactions (35) and (36) are observed.

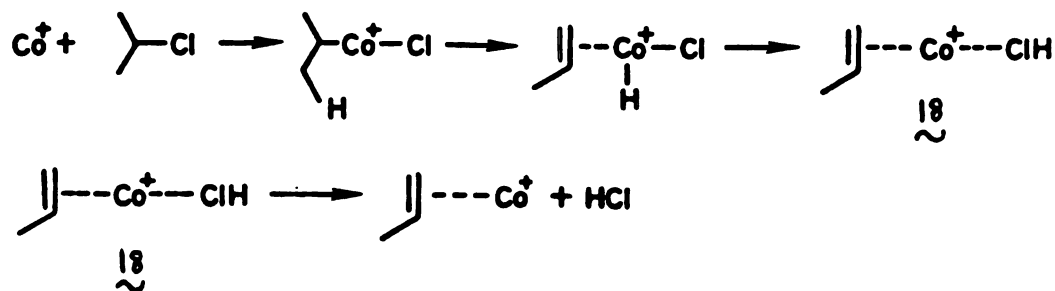


Thus, in general ML^+ reacts to form many of the same products as M^+ ; both ML^+ and ML_2^+ are involved in ligand substitution reactions.

There are several considerations which must be taken into account in order to evaluate any ligand effects which may be associated with these reactions. First, it would be useful to know at which point in the mechanism the ligand is lost in these reactions. Assuming that the same mechanism operative for M^+ also applies to ML^+ , Scheme 5 illustrates a potential series of reactions occurring between $CoCO^+$ and hexane. Note that there are at least four different points in Scheme 5 where CO could be lost. Furthermore, it is evident from Scheme 5 that the structure of the ligand substitution product depends upon where in the overall reaction sequence the CO is lost. Thus, if there was sufficient energy associated with intermediate 9, the initially formed $CoCO(alkane)^+$ complex, simple ligand substitution could occur. In this case the structure of complex 10, the ligand substitution product would involve a Co^+ and an intact hexane molecule. Alternatively, if it is energetically feasible, $CoCO^+$ could insert into a C-C bond of hexane to form an intermediate such as 13. In this case, loss of CO could occur either before the alkane has a chance to rearrange on the metal center (intermediate 14) or after alkane rearrangement (intermediates 15 and 17). Note that if there is any excess energy present in these ligand substitution products, they may form products which are

identical to those observed for Co^+ alone. These processes would account for the spectator type reactions observed for CoCO^+ and hexane. Before correlating the branching ratios for CoCO^+ with intermediates as we did with Co^+ in Chapter 6, it is necessary to determine whether the ligand substitution product is best represented by a complex such as 10 ($\text{M}^+-\text{RR}'$) or by an insertion complex such as 14 ($\text{R}-\text{M}^+-\text{R}'$).

Note that previous studies in the area of gas phase organometallic chemistry have concentrated heavily on the reactions of metal and metal containing ions with polar organic molecules such as isopropyl chloride. It has been determined, that Co^+ reacts with isopropyl chloride to form an intermediate in which propene and HCl compete as ligands on the metal:¹



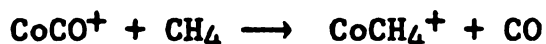
Following its formation, Intermediate 18 loses HCl to form the final product. It has been noted in these reactions that when two ligands such as HCl and propene compete as ligands on the metal, the ligand with the largest proton affinity (PA) is preferentially retained on the metal. According to

the PA rule⁵, the larger the PA of a ligand, the better its electron donating ability. Thus, since M^+ is electron deficient, it retains the ligands which are the best bases in these reactions. Since the PA of HCl is less than that of propene, HCl is lost in the above reaction. Furthermore, the PA rule also applies to the ligand substitution reactions observed for these polar organic molecules. Thus when $CoCO^+$ reacts with a polar organic molecule such as methyl iodide



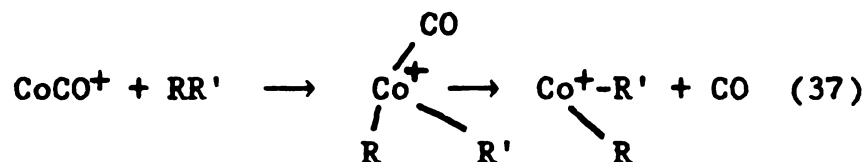
CH_3I and CO compete as ligands on the metal. Since the PA of CH_3I is approximately 171 kcal/mol and that of CO is 142 kcal/mol⁸³, CO is preferentially lost in this reaction to form the ligand substitution product.

Apparent ligand substitution products are also observed in the reactions of metal-containing ions and alkanes. The following reaction is observed for methane:



However, the PA of methane is only 132 kcal/mol which is less than the PA of CO . Therefore, the observed loss of CO in this reaction is in violation of the PA rule. This would suggest that either the PA rule does not apply to the reactions of metal-containing ions and alkanes or the ligand substitution product formed in the above reaction with methane does not involve an intact alkane molecule. If the latter were the case, the general process presented in reaction (37) would illustrate the apparent ligand

substitution process occurring for alkanes, where the final product involves a metal ion bound to two alkyl ligands or in the case of CH_4 , the product would be $(\text{HCo}^+\text{CH}_3)$.

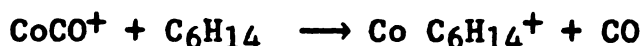


To evaluate the feasibility of the formation of a metal ion-intact alkane complex such as 10 in Scheme 5, the first part of this discussion will examine the energy associated with the interaction of a positively charged metal ion and a polarizable alkane. Next, a comparison of the chemistry of M^+ and ML^+ with alkanes will be made; their "reactivities" will be compared and contrasted. (Note that reactivity is frequently defined in such studies by the number of different products which are formed, since this is generally indicative of the number of bonds into which a given metal will insert in an organic molecule). Product distributions will be evaluated to determine whether the observed ordering of preference of ML^+ for the C-C bonds of alkanes parallels that observed for M^+ . Differences in this ordering will be assessed in terms of both steric effects and the bond strengths associated with the ligands on the metal. Obvious steric effects may provide evidence supporting the existence of a metal ion complex such as 13 in Scheme 5. For example, if the ML^+ insertion complexes involving the least amount of steric hindrance are formed preferentially, then the number of bonds into which ML^+ inserts may be limited.

Under these circumstances, the reactivity of ML^+ would be expected to be different than that observed for M^+ . In comparison, one would expect any steric effects associated with the formation of a complex such as 10 to be less significant than those associated with the ML^+ insertion complex (13) since L is lost before the insertion step. Finally, parallels between the gas phase chemistry observed and solution chemistry will be made.

ALKANE POLARIZABILITIES

If the energy released during the initial interaction of a positively charged metal ion (ML^+) and a polarizable alkane is greater than the M^+-L bond strength, then the formation of a metal ion-intact alkane is feasible and reactions such as



can be considered to be ligand substitutions. To calculate this energy, alkane polarizabilities must be known. Therefore, methods of obtaining alkane polarizabilities followed by the energy calculations based on these polarizabilities will now be presented. (Note that we are assuming here that the presence of L on M^+ does not alter the charge on M^+ . Thus we are assuming that the energy associated with the interaction between ML^+ and the alkane is the same as that for M^+ and an alkane).

Empirical methods have been established for calculating average molecular polarizabilities.^{105,106} The values of the alkane polarizabilities, α , which are utilized in this study can be calculated using equation (14) which was formulated by Miller and Savchik.¹⁰⁵

$$\alpha_{(ahc)} = \frac{4}{N} \left[\sum_A \tau_A \right]^2 \quad (14)$$

N in this equation equals the number of electrons in the molecule and τ_A represents the atomic hybrid component (ahc) of polarizability for each atom, A , in the molecule. Each atom in the molecule is represented by one value of τ_A in equation (14). These values have been determined by Miller and Savchik and are provided in reference 105. The value of τ_A coinciding with a particular atom depends upon the hybridization of that atom. For example, there are three different values of τ_A for carbon because carbon can be either sp^3 , sp^2 or sp hybridized.

The polarizabilities calculated from equation (14) have been found to be within one per cent of the experimentally determined values for most alkanes.¹⁰⁵ Therefore, the advantages of using this method lie in its simplicity —only a few parameters are necessary, and in its accuracy. However, one of the major shortcomings of this approach lies in the fact that τ_A does not depend on the atoms which are bonded to A. As a result, the polarizabilities calculated for isomers such as pentane and neopentane are identical. For the purpose of this discussion, the values calculated for α are taken to be the average molecular polarizabilities of the linear alkanes.¹⁰⁵ These values are listed in Table 25.

The potential, U , associated with a positively charged ion separated from a polarizable alkane by a distance of r can now be calculated using equation (15) where ZE is the charge

$$U(r) = -\frac{\alpha Z^2 \epsilon^2}{2r^4} \quad (15)$$

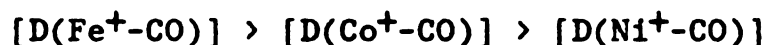
of the ion. (Note that equation (15) is valid for $r \gg$ radius of the molecule).¹⁰⁷ For simplicity, let us first assume that we are calculating the potential energy of a point charge separated from a spherically symmetric polarizable

Table 25. Results of Polarizability and Energy Calculations
for Linear Alkanes Interacting with a Point Charge

ALKANE	$\alpha(\text{cm}^3/\text{mol})$	$-U(r)$ kcal/mol					
		$r=1\text{\AA}$	$r=1.5\text{\AA}$	$r=2\text{\AA}$	$r=3\text{\AA}$	$r=5\text{\AA}$	$r=10\text{\AA}$
Methane	1.57	432	85.4	27.0	5.33	0.692	0.0432
Ethane	2.67	735	145	46.0	9.08	1.18	0.0735
Propane	3.79	1043	206	65.2	12.9	1.67	0.104
Butane	4.90	1349	266	84.3	16.7	2.16	0.135
Pentane	6.01	1655	327	103	20.4	2.65	0.166
Hexane	7.12	1960	387	123	24.2	3.14	0.196
Heptane	8.24	2269	448	142	28.0	3.63	0.227
Octane	9.35	2574	508	161	31.8	4.12	0.257
Nonane	10.46	2880	569	180	35.6	4.61	0.288
Decane	11.57	3186	629	199	39.3	5.10	0.319

point by distances between 1 and 10 angstroms. The results of these energy calculations are tabulated in Table 25 along with the polarizabilities. It is apparent from the average molecular polarizabilities that, the larger the alkane, the greater the polarizability. Furthermore, it is evident from $U(r)$ that these ion/molecule interactions fall off rapidly with distance and thus cannot be considered long range. However, at distances less than 3\AA , interaction energies greater than 100 kcal/mol are calculated for alkanes larger than butane.

Table 26 lists the M^+-L bond strengths which have been reported in the literature. (Note based on the available heats of formation reported for Ni^+ , $Ni-CO^+$ and CO , $D(Ni^+-CO)$ was calculated to be only 6.6 kcal/mol. This seems unreasonably low compared to the bond dissociation energies of the other metal carbonyls presented in Table 26 which were determined experimentally. Nonetheless, this value is included in the Table. Furthermore, the trends reported ⁷⁷ for $D(M^+-CH_3)$ and $D(M^+-H)$ [where $M^+ = Fe^+, Co^+, Ni^+$] would suggest that



[Trends for M^+-H may not be relevant to M^+-CO depending on the nature of the M^+-CO bonding which is currently not well understood]. Therefore, $D(Ni^+-CO)$ is probably less than 40 but greater than 6.6 kcal/mol]. The information provided in Figure 5, which graphically illustrates the information contained in Tables 25 and 26, suggests that at least one CO

Table 26. M^+-L Bond Strengths

<u>$M^+ - L$</u>	<u>Bond Strength(kcal/mol)</u>
$Fe^+ - CO$	63 ^a
$Co^+ - CO$	40 ^b
$Ni^+ - CO$	6.6 ^c
$Ni^+ - PF_3$	75 ^d

a. Taken from Ref. 29

b. Taken from Ref. 108

c. Taken from Ref. 82

d. Taken from Ref. 109

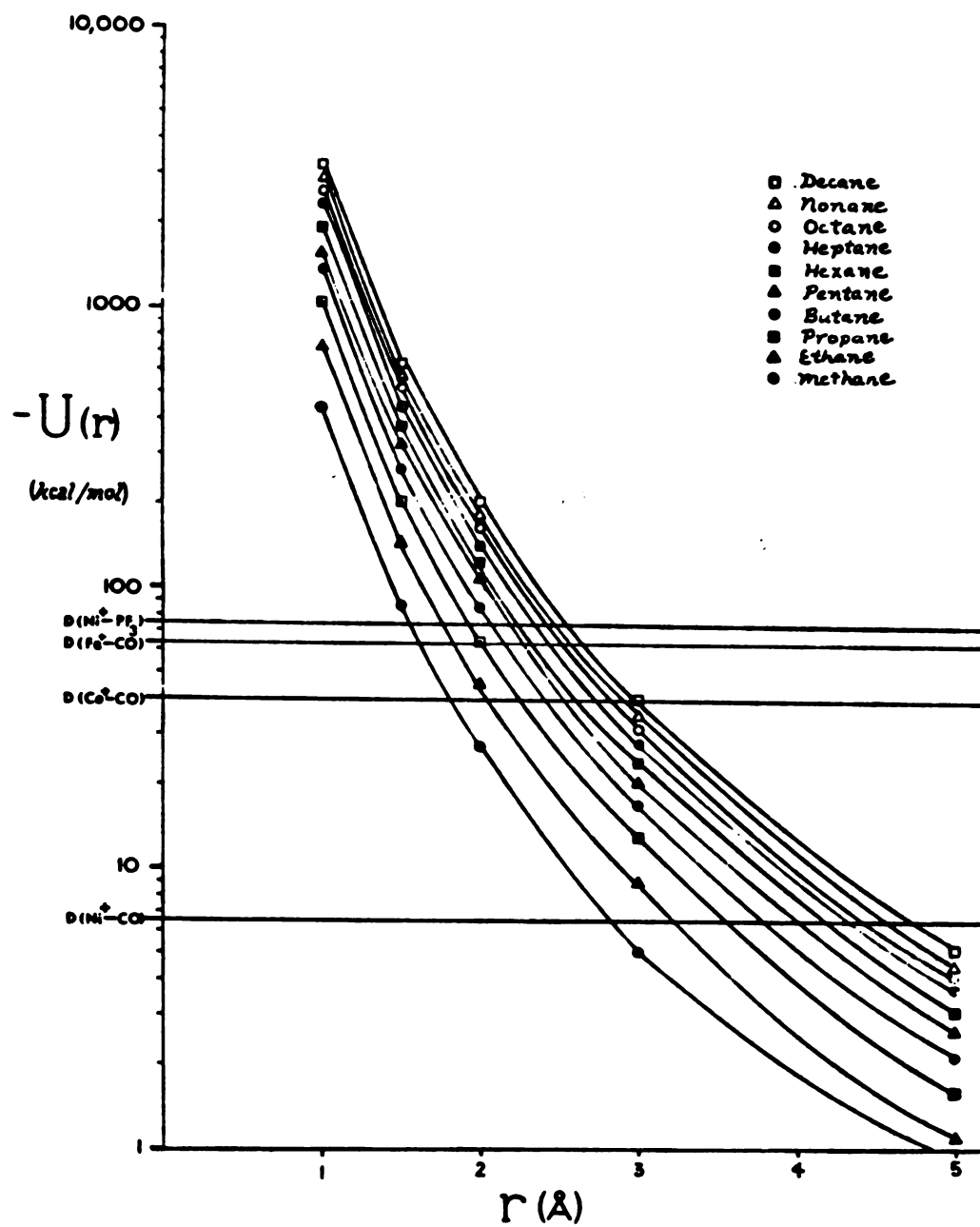


Figure 5. Plot of $U(r)$ vs. r , Including $D(M^+-L)$.

or PF_3 ligand on M^+ can be displaced by any alkane larger than propane at distances of separation of approximately 2\AA .

Unfortunately, the above analysis involves two major oversimplifications. First, an ion is not a dimensionless point charge. It has a radius which will limit its minimum distance of separation from an alkane. For example, the radius of Co^+ is approximately 0.7\AA ¹¹⁰ and that of hydrogen is at least 0.5\AA .¹¹¹ The sum of these radii would suggest that the minimum distance possible between Co^+ and a hydrogen atom in an alkane is $\sim 1.2\text{\AA}$. Therefore, the energies calculated for separations of 1\AA in Table 25 have little physical significance. Furthermore, alkanes larger than methane cannot realistically be represented as symmetrical polarizable spheres. Each alkane has a specific geometry associated with its lowest energy configuration. If we consider these geometries in three dimensional space, it is apparent that the distance between a "fixed" charge and the various portions of the alkane molecule cannot be represented by a single value. That is, a charge situated 2\AA away from a hydrogen located on a terminal carbon in hexane will be more than 2\AA away from the terminal carbon on the other end of the molecule. Therefore, to more realistically assess the energy involved in the interaction of an ion and an alkane, we need to evaluate the average molecular polarizability as a series of components, where each component represents the polarizability of a certain portion of the molecule. Then, the individual interactions of the charge with the various

polarizable parts of the molecule located at various distances from the charge can be calculated.

One method making this possible involves the calculation of the average molecular polarizability as a function of bond polarizabilities.¹⁰⁶ According to this method, each bond in the molecule has a specific polarizability associated with it. The polarizability of the bond in the direction perpendicular to the bond differs from the polarizability in the direction parallel to the bond. The parallel component of polarizability is represented by the symbol α_{\parallel} . α_{\perp} represents the perpendicular component of bond polarizability. α_{\parallel} and α_{\perp} have been reported by Denbigh for various bonds.¹¹² For example, α_{\parallel} for the C-C bond equals $1.13\text{cm}^3/\text{mol}$ and α_{\perp} equals $1.20 \times 10^{-2} \text{ cm}^3/\text{mol}$. If an electric field makes an angle θ with a chemical bond, the polarizability of the bond, α_{θ} , can be calculated using equation (17).

$$\alpha_{\theta} = \alpha_{\parallel} \cos^2 \theta + \alpha_{\perp} \sin^2 \theta \quad (17)$$

Averaging α_{θ} over all orientations leads to an average value of the bond polarizability, α :

$$\alpha = \frac{1}{3}(\alpha_{\parallel} + 2\alpha_{\perp}) \quad (18)$$

The average polarizability of the molecule is then taken as the sum of the average polarizabilities of its bonds. Note that the average polarizabilities obtained using this method¹¹² are in agreement with those calculated using equation (14).

One of the limitations of this method lies in the fact that it cannot be applied successfully to molecules involving resonance structures.

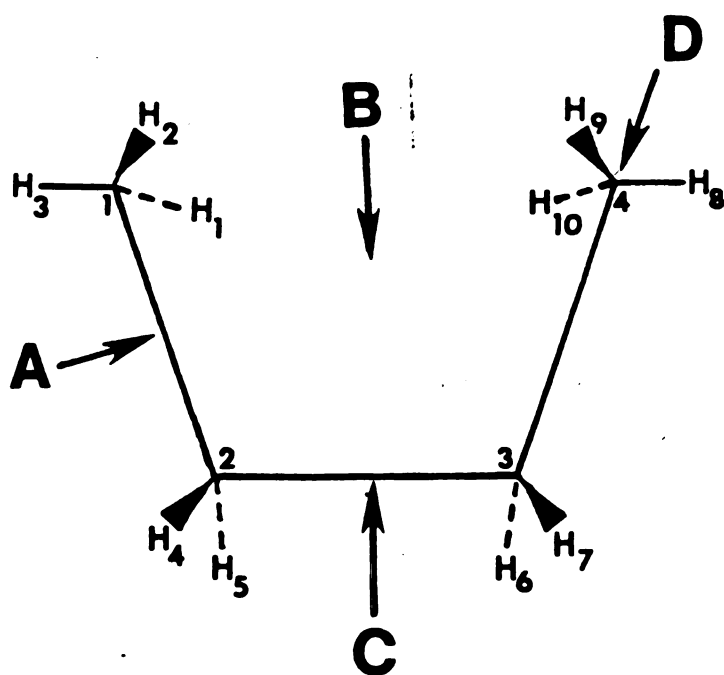
In the simplest application of this method, one can first imagine a molecule in three dimensional space and assign to each atom in the molecule three coordinates. Second, one can define the location of a charge, placed near the molecule, by three coordinates. Third, one can calculate the angle θ established by the field lines associated with the charge and the center of the polarizable bond. Once these angles are known, equation (17) can be used to calculate α_{θ} . Fourth, one

can calculate the various distances between the "fixed" charge and the various bonds of the molecule. These distances can be used in equation (15) along with the respective α_i 's to calculate the specific $U(r)$ associated with the charge and a particular bond. Finally, the sum of all of the $U(r)$'s can be obtained. This sum represents the total energy of interaction associated with that particular molecular configuration and charge location.

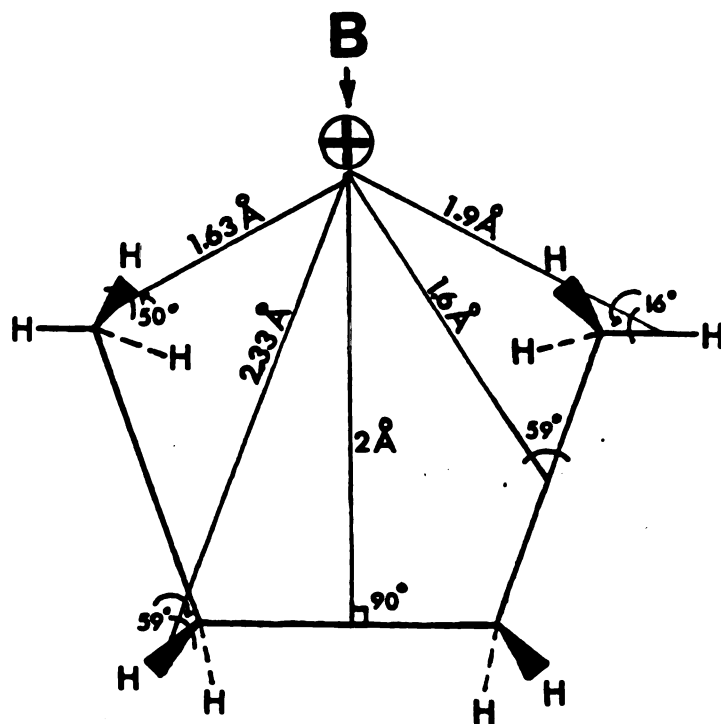
It is evident from the number of variables which must be defined in order to perform this calculation, that the larger the alkane, the more potentially complex this analysis. It was not within the scope of this study to perform exhaustive calculations. Rather, we wish to determine whether it is feasible for an intact alkane to displace a CO or PF₃ ligand from a metal ion. Thus, calculations were performed for various configurations of butane. Each alkane larger than butane consists of at least one "butane unit" plus additional C-C bonds. Thus, if the calculations reveal that it is theoretically possible for butane to displace L, then it will be assumed that alkanes larger than butane can also displace L.

The calculations were carried out assuming a "boat" configuration for butane. (Note that the "chair" configuration of butane actually corresponds to a lower energy configuration. However, we assumed that the energy barrier to rotation about the central C-C bond separating the "chair" from the "boat" configuration was approximately 3

kcal/mol. In using the chair configuration we were able to maximize the number of interactions between the charge and the six terminal C-H bonds of butane). According to Figure 6, the skeletal chain of butane is situated in the plane of the page. Furthermore, A, B, C and D represent four different locations in the plane of the paper where the positive charge can be placed. As a reference, the field lines set up by the charge at either location A, B, or C will make a 90° angle with the C-C bond directly in "front" of the charge. The field lines set up by the charge at point D will make a 0° angle to the C-C bond "below" it. The arrows in Figure 6 point to these respective C-C bonds. Each carbon and hydrogen atom is numbered for future reference. Calculations of $U(r)$ were carried out for "arrow lengths" of 1 or 2\AA . All other distances and angles were measured relative to these separations of 1 and 2\AA . For example, Figure 7 shows all of the angle and distance measurements pertinent to the calculation of $U(r)$ for a charge located at point B, 2\AA away from the internal C-C bond. (Recall that in actuality separations of 1\AA are physically impossible based on atomic and ionic radii. However, these calculations at short distances should serve as a gauge of interaction, i.e., if the energies calculated for these short distances are less than $D(M^+-L)$, then at longer distances there is no chance of an intact alkane displacing L). A breakdown of the energy of interaction between a charge located at either position A, B, C or D and the individual C-C and C-H bonds in butane is provided in Tables 27 and 28 for "arrow lengths" of 1 and 2\AA .



**Figure 6. Relationship between Charge Location
and C-C Bonds of Butane**



**Figure 7. Angle and Distance Measurements
For Charge Located at B**

Thus, if a charge is located at point B in Figure 7, its energy of interaction with either the C₁-C₂ or C₃-C₄ bonds of butane, according to Table 27 is -13.1 kcal/mol. However, its overall energy of interaction with all of the C-C and C-H bonds of butane is -124 Kcal/mol. It is evident from Tables 27 and 28 that the overall energies calculated at short distances are greater than the M⁺-L bond strengths provided in Table 26. However, once the charge is moved back an additional Angstrom, only one out of the four locations, B, provides for an interaction energy (124 kcal/mol) which is greater than the M⁺-L bond strengths indicated in Table 26. In general, a consideration of the energies associated with the interaction of M⁺ and the individual C-C and C-H bonds in Tables 27 and 28 reveals that the strongest interactions occur with the C-H bonds which are located closest to the charge.

In terms of the chemistry which is observed for butane, perhaps those bonds which experience the strongest interactions with M⁺ are weakened in the process thus facilitating their cleavage. Since C-C bonds are lower in energy than C-H bonds, let us consider the energy of interaction associated with the C-C bonds in butane using the values in Table 27. There are various approaches which could place the metal ion near the terminal or internal C-C bonds of butane. A, B, C and D represent these various approaches. The strongest interaction when the ion is

**Table 27. Bond by Bond Breakdown of $U(r)$
For "Arrow Length" of 1Å**

BOND	- $U(r)$ kcal/mol			
	A	B	C	D
C_1-C_2	3.3	4.6	18.9	0.2
C_2-C_3	19.0	3.3	3.3	1.5
C_3-C_4	0.8	4.6	18.9	33.2
C_1-H_1	72.4	10.5	1.3	0.9
C_1-H_2	21.6	15.9	1.3	0.9
C_1-H_3	21.6	15.9	1.3	0.9
C_2-H_4	21.6	18.7	28.0	0.6
C_2-H_5	21.6	18.7	28.0	0.6
C_3-H_6	1.4	18.7	28.0	1.7
C_3-H_7	1.4	18.7	28.0	1.7
C_4-H_8	0.6	10.5	1.3	120.7
C_4-H_9	0.6	15.9	1.3	120.7
C_4-H_{10}	0.6	15.9	1.3	120.7
Total $U(r)$	186.5	172	160.9	404.3

**Table 28. Bond by Bond Breakdown of $U(r)$
For "Arrow Length" of 2\AA**

BOND	- $U(r)$ kcal/mol			
	A	B	C	D
C_1-C_2	0.2	13.1	2.3	0.2
C_2-C_3	4.6	0.2	0.2	0.5
C_3-C_4	0.3	13.1	2.3	5.4
C_1-H_1	13.1	9.9	0.5	0.4
C_1-H_2	3.8	15.8	0.5	0.4
C_1-H_3	3.8	15.8	0.5	0.4
C_2-H_4	3.8	3.6	3.2	0.2
C_2-H_5	3.8	3.6	3.2	0.2
C_3-H_6	0.5	3.6	3.2	0.6
C_3-H_7	0.5	3.6	3.2	0.6
C_4-H_8	0.2	9.9	0.5	7.8
C_4-H_9	0.2	15.8	0.5	7.8
C_4-H_{10}	0.2	15.8	0.5	7.8
Total $U(r)$	35	124	20.6	32.3

located at point A occurs with the C₂-C₃ bond. Weakening of this bond may result in the formation of the [C₂H₅-M⁺-C₂H₅] insertion intermediate. This intermediate leads to ethane (or H₂) elimination in butane. When the ion is located at point B, there are no significant interactions with any of the C-C bonds. However, the ion interacts strongly with both the C₁-C₂ and C₃-C₄ bonds when located at point C. This interaction with both terminal bonds may cause a subsequent weakening in the C₂-C₃ bond leading to the formation of an insertion intermediate which again can be represented as [C₂H₅-M⁺-C₂H₅]. Finally, the strongest interaction that occurs with a C-C bond when a charge is located at point D occurs with the C₃-C₄ bond. Weakening of this bond may result in the formation of the [C₃H₇-M⁺-CH₃] insertion intermediate which can subsequently undergo a β-H shift and eliminate methane. However, at location D there is an even greater interaction between the charge and the three terminal C-H bonds closest to it. This interaction may facilitate the formation of an intermediate such as [C₄H₉-M⁺-H] which could undergo H₂ elimination.

Since D(C-H) is larger than D(C-C), a larger energy of interaction may be necessary to break the stronger C-H bond. Finally, we can use Table 27 to obtain the sums of the energies of interaction between the charge and all three of the C-C bonds in butane for a particular charge location. These results are summarized in Table 29. For example, when located at point A, the total energy of interaction between

**Table 29. Sum of the Energies of Interaction Between
a Charge and the three C-C Bonds of Butane**

<u>Location</u>	<u>Total Energy of Interaction Between Charge and C-C Bonds (kcal/mol)^a</u>
A	23.1
B	12.5
C	41.1
D	34.9

a. Based on values in Table 27.

the charge and the three C-C bonds of butane is 23.1 kcal/mol. A comparison of these sums reveals that location C provides for the largest energy of interaction. Recall that the insertion intermediate proposed earlier for this interaction was $[C_2H_5-M^+-C_2H_5]$. From Table 23 in chapter 6, the C-C bond most preferred by M^+ for insertion into butane is the internal C_2-C_3 bond. Location D provides for the next largest energy of interaction. The insertion intermediate proposed for this interaction is $[C_3H_7-M^+-CH_3]$. According to Table 23, the C_1-C_2 bond in butane was the next most preferred bond by M^+ for insertion. The interaction at point A is weaker than that at point D. Furthermore, location B provides for the weakest energy of interaction between the charge and the three C-C bonds of butane. Interestingly, these results suggest that there is a correlation between the bonds most preferred by M^+ for insertion (as presented in Table 23) and their energies of interaction.

Overall, these energy calculations, which take into account the size of the metal ion and the alkane molecule geometry, do suggest that it is feasible for an intact alkane larger than propane to complex with a metal ion and displace at least one CO or PF_3 ligand.

In addition to polarizability calculations, we note that the electron density associated with the carbon and hydrogen atoms of alkanes can be partitioned into charges on these atoms.¹¹³ Therefore, we must also assess the significance of the interaction between the charges of the atoms of the

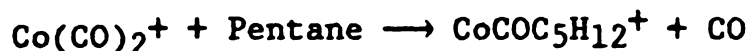
alkane (dipolar bonds) and the charge of the metal ion since ion-dipole interactions are longer range than ion-induced dipole interactions and could be of relatively high energy. Equation (19) can be used to calculate the potential energy, $U(r)$, between two charges separated by a distance, r (where

$$U(r) = \frac{Z_1 Z_2 e^2}{r} \quad (19)$$

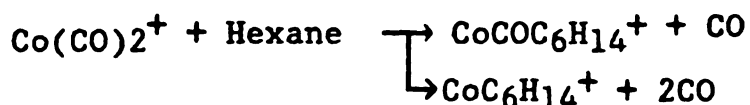
Z_1 is the charge of the carbon or hydrogen atom and Z_2 is the charge of the metal atom). Values for the atomic charges associated with a select set of alkanes can be found in the literature.¹¹³ These values are derived from ab initio calculations. A description of the methodology behind these ab initio calculations is beyond the scope of this discussion and will not be presented here. For our purposes, it is necessary to know that the atomic charge of a primary hydrogen in butane is -32.4 millielectrons (me) [1me = 10^{-3} electron] that of a primary carbon is +89.2 me, that of a secondary carbon is 84.8 me and that of a secondary H is -38.4 me.¹¹³ Using these values in equation (19), we can determine that the potential energy between a (+1) metal ion located at point B in Figure 7 and butane is 20.6 kcal/mol. The individual interaction energies between M^+ and the C and

H atoms of butane under these circumstances are presented in Table 30. The overall energy here represents a repulsive interaction in contrast to the polarizability results. Therefore, this model predicts that the approximate interaction energy of M^+ and butane in Figure 7 is 103.4 kcal/mol. Since 103.4 kcal/mol is greater than the M^+-L bond strengths in Table 26, it is still feasible for an alkane larger than propane to displace L while remaining intact.

Further evidence in support of the significance of alkane polarizabilities in these gas phase reactions can be found in the reactions of alkanes with ML_2^+ . Theoretically, if V_{σ} is sufficiently large, an intact alkane will be capable of displacing more than one ligand on the metal ion. Note, as the length of the alkyl chain increases, ligand substitution patterns for ML_2^+ change. Thus, alkanes larger than heptane always displace two L's. Alkanes smaller than hexane only displace one L. These results are presented graphically in Figure 8. For example, pentane reacts with $Co(CO)_2^+$ and displaces only one carbonyl ligand.



Apparently, the energy obtained in the interaction of pentane and $Co^+-(CO)_2$ is only large enough to cleave one Co^+-CO bond. However, when hexane reacts with $Co(CO)_2^+$, either one or two of the carbonyls are displaced.



Furthermore, when alkanes larger than hexane react with

Table 30. Interaction Energy Between M^+
and the Carbon and Hydrogen atoms of Butane

<u>ATOM</u>	<u>U(r) kcal/mol</u>
C ₁	21.1
C ₂	13.2
C ₃	13.2
C ₄	21.1
H ₁	-4.4
H ₂	-5.1
H ₃	-5.1
H ₄	-4.7
H ₅	-4.7
H ₆	-4.7
H ₇	-4.7
H ₈	-4.4
H ₉	-5.1
H ₁₀	<u>-5.1</u>

Total U(r) = 20.6

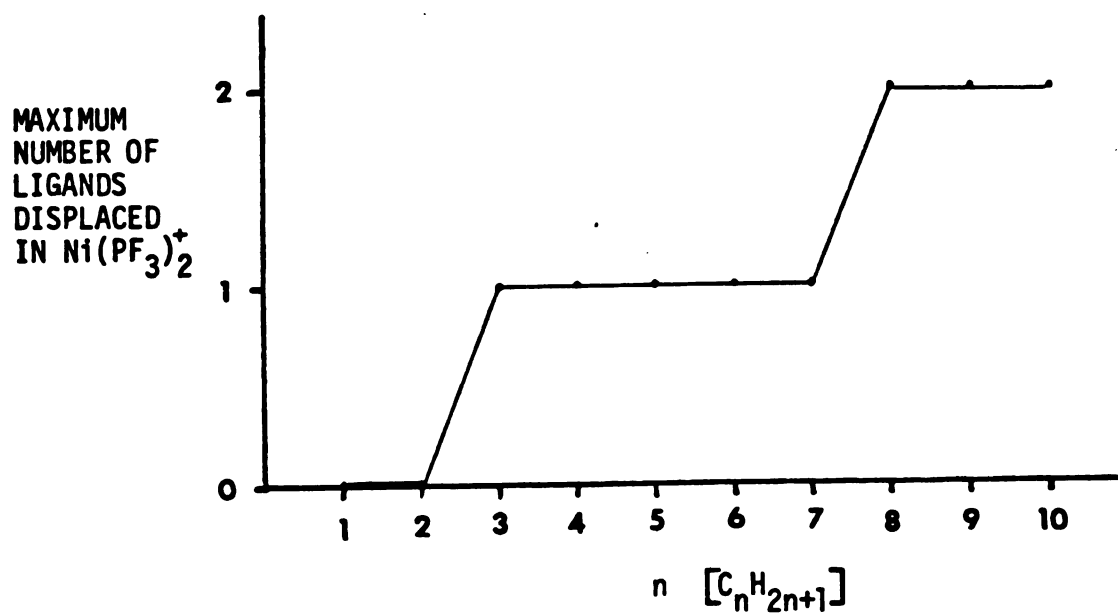
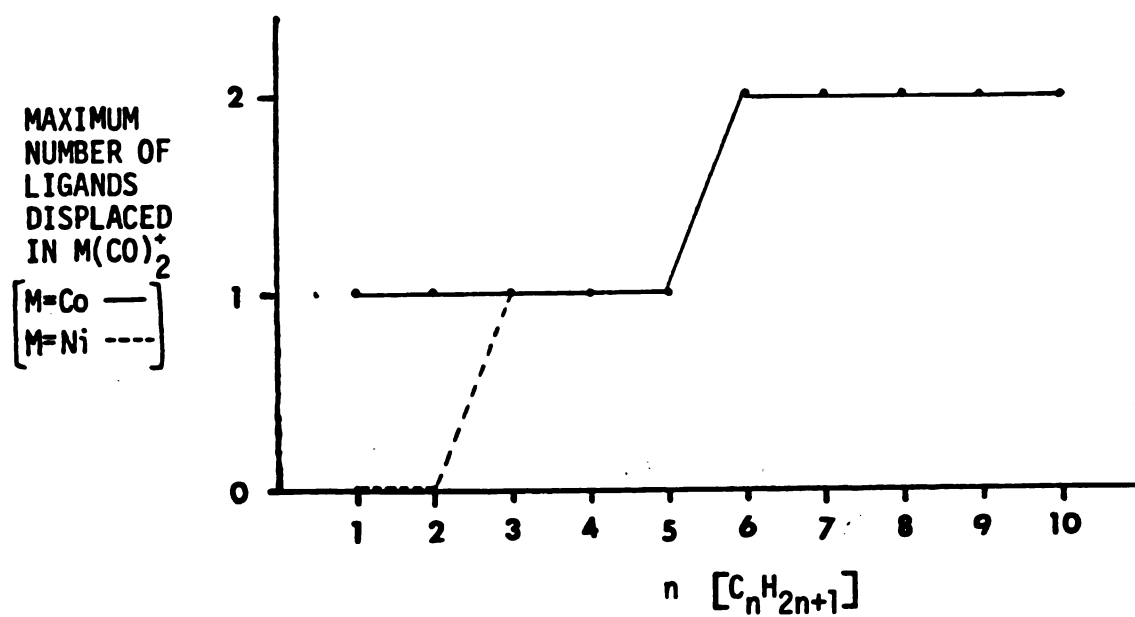
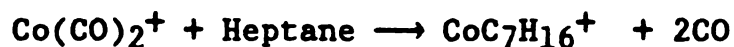
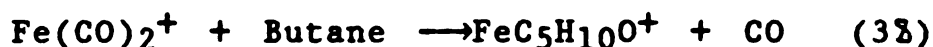


Figure 8. Ligand Substitution Patterns

$\text{Co}(\text{CO})_2^+$, loss of both carbonyls is observed.



These results suggest that the greater polarizability of a larger alkane allows for a stronger interaction with M^+ , resulting in a release of energy capable of breaking both Co^+-CO bonds. (Recall from Table 25 and Figure 5 that the average molecular polarizabilities of linear alkanes do increase as the alkyl chain length increases thus substantiating the above claim). Also, recent work reported by Larsen and Ridge suggests that the structure of the ligand substitution product formed in reaction (38)



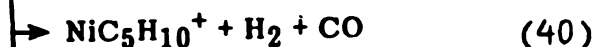
involves a Fe^+ , CO and an intact butane molecule. The major peaks they observed in the collision induced decomposition spectrum of $\text{FeC}_5\text{H}_{10}\text{O}^+$ correspond to Fe^+ , FeCO^+ and $\text{FeC}_4\text{H}_{10}^+$.⁶⁸ Thus, their results also suggest that an intact alkane can displace a ligand on the metal.

Metal ions containing more than two ligands are found to be totally unreactive in terms of cleaving bonds in the alkane. Perhaps the presence of three or more ligands on the metal center prohibits the metal center from getting sufficiently close to the alkane. Under these circumstances, the metal center and the alkane have no opportunity to interact. Note that similar reasoning has been used to explain the lack of reactivity observed for $\text{Fe}(\text{CO})_n^+$ [$n = 3-5$] and 12-crown-4.⁶⁰ In this case, Fe^+ , FeCO^+ and $\text{Fe}(\text{CO})_2^+$

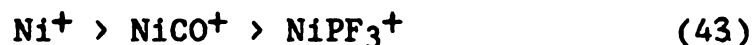
react with 12-crown-4 to form products whereas Fe(CO)_n^+ [$n = 3-5$] does not.

COMPARISON OF THE REACTIVITY OF M^+ AND ML^+

Now that we have determined that it is possible for an alkane to displace a CO or PF_3 ligand before metal ion insertion, let us compare the reactivity of M^+ and ML^+ in terms of the number of different products which are formed by each metal species to determine any steric effects which may be indicative of limited ML^+ insertion into alkanes. An inspection of Tables 4 through 21 reveals that the reactivity of ML^+ is less than that of M^+ . However, in the reactions where M^+ and ML^+ are precursors to the same product ions, it can be shown that ML^+ and M^+ exhibit the same preferences for the C-C bonds of alkanes using the same type of analysis presented in Chapter 6. Thus, Table 23 of chapter 6 which indicates the ordering of the preference of M^+ for the C-C bonds of linear alkanes also applies to ML^+ . The decrease in the reactivity of ML^+ can be attributed to the fact that the metal ion-alkane complex formed by ML^+ is lower in energy than the metal-ion alkane complex formed initially in the reaction of M^+ and an alkane by an amount equal to $D(\text{M}^+-\text{L})$. Thus, the data in Tables 4 through 21 further reveal that NiPF_3 is less reactive with alkanes than NiCO^+ . Reactions (39) through (42) with pentane serve to illustrate this point.



Thus, NiCO^+ forms three products and NiPF_3 is a precursor for only one product ion. In addition, according to Table 26, $D(\text{Ni}^+-\text{PF}_3)$ is greater than $D(\text{Ni}^+-\text{CO})$. These results suggest that there is a correlation between the reactivity of ML^+ and the M^+-L bond strength -- the stronger the M^+L bond, the less the reactivity of ML^+ relative to M^+ . Therefore, the Ni^+ -pentane complex formed by NiPF_3^+ is less energetic than the Ni^+ -pentane complex formed by NiCO^+ which is less energetic than the Ni^+ -pentane complex formed by Ni^+ . As a result, the following trend in reactivities is both expected and observed:



In general, the lack of obvious steric effects in these reactions may indicate that insertion of ML^+ into C-C bonds is a less favored process than insertion of M^+ into alkanes following the displacement of L by an alkane.

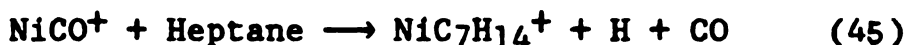
STERIC EFFECTS

One interesting trend which we do attribute to steric effects is observed in the reactions of MCO^+ and alkanes. MCO^+ reacts with alkanes larger than hexane to eliminate more H_2 than M^+ . For example, thirty-one per cent of NiCO^+ reacts with heptane to eliminate H_2 whereas only nine per cent of Ni^+ reacts to eliminate H_2 :

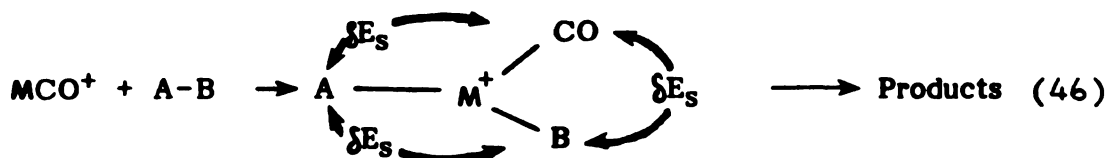
9%



31%



These results suggest that reactions (44) and (45) involve two different processes for H_2 elimination. We suggest that H_2 elimination in reaction (45) results from the initial insertion of MCO^+ into the terminal C-H bonds of these larger alkanes. This is unlike M^+ which preferentially inserts into C-C bonds. We believe that insertion into C-C bonds by MCO^+ is prohibited due to steric effects. Consider the following reaction:



In this reaction δE_s refers to the energy associated with the steric effects produced by two adjacent ligands. The energy, H insertion, required for insertion in reaction (46) can be written as:

$$H_{\text{insertion}} = D(A-B) - [D(M^+CO-A) + D(AM^+CO-B)] + E_s \quad (47)$$

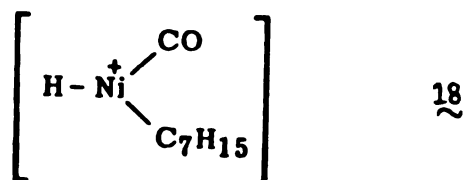
where $E_s = \sum \delta E_s$. [Note that reaction (47) involves the energy associated with bond making, bond breaking and the steric effects.] Based on chapter 6, if the thermodynamically most stable insertion intermediate is formed in reaction (46), M^+-C and M^+-H bond strengths suggest that insertion into C-C bonds is preferred. However, if the steric effects (E_s) associated with the C-C insertion intermediate are more significant than E_s associated with the C-H insertion intermediate, MCO^+ may show a preference for insertion into C-H bonds. Furthermore, insertion into a terminal C-H bond should minimize steric effects in the intermediate in reaction (46). Thus, for heptane, we suggest that Ni^+ insertion into C-C bonds leads to more stable intermediates than insertion into C-H bonds. Therefore, in terms of stability:

$$\Delta H_f(C_3H_7-Ni^+-C_4H_9) > \Delta H_f(H-Ni^+-C_7H_{15}) \quad (48)$$

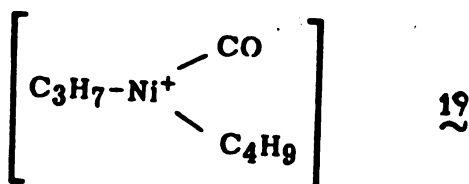
This implies:

$$[D(Ni^+-C_3H_7) + D(C_3H_7Ni^+-C_4H_9)] > [D(Ni^+-H) + D(HNi^+-C_7H_{15})]$$

NiCO^+ , on the other hand, reacts with heptane to form an intermediate which favors increased H_2 elimination. This suggests that the formation of intermediate 18



is preferred over the formation of intermediate 19



implying that $E_s(\text{18}) < E_s(\text{19})$ such that

$$[\text{D}(\text{Ni}^+\text{CO}-\text{H}) + \text{D}(\text{HNiCO}^+-\text{C}_7\text{H}_{15}) - E_s(\text{18})] >$$

$$[\text{D}(\text{Ni}^+\text{CO}-\text{C}_3\text{H}_7) + \text{D}(\text{C}_3\text{H}_7\text{Ni}^+-\text{COC}_4\text{H}_9) - E_s(\text{19})]$$

Experimentally, steric effects are assessed through bond strengths because ΔE_s cannot be determined individually. Thus, based on the results observed for Ni^+ and NiCO^+ with heptane we can write:

$$[\text{D}(\text{C}_3\text{H}_7-\text{Ni}^+-\text{H})] > [\text{D}(\text{C}_7\text{H}_{15}\text{CONi}^+-\text{H})]$$

and

$$[\text{D}(\text{C}_7\text{H}_{15}\text{Ni}^+-\text{H})] \approx [\text{D}(\text{C}_7\text{H}_{15}\text{CONi}^+-\text{H})]$$

These trends in bond strengths suggest that there is a

greater steric effect associated with the insertion of NiCO^+ into a C-C bond than into a C-H bond. Thus, we believe that MCO^+ preferentially inserts into the terminal C-H bonds of large alkanes to eliminate H_2 . There is only one large alkane that NiPF_3 reacts with to eliminate more H_2 than Ni^+ . This alkane is nonane. Thus, we suggest that insertion of NiPF_3^+ into the C-H bonds of alkanes may be less favored due to the steric effects which result when a bulky PF_3 ligand is adjacent to a bulky alkyl group on Ni^+ . Note that steric effects can be correlated with an easily measured parameter known as the cone angle θ .¹⁰⁴ The cone angle for symmetrical ligands is illustrated in Figure 9. θ is defined as the apex angle of a cylindrical cone which just touches the van der Waals radii of the outermost atoms in the ligand. For comparative purposes, the value of the ligand cone angle for PF_3 is 104° , whereas $\theta = 95^\circ$ for CO .¹¹⁴ Furthermore, for H, $\theta = 75^\circ$, for CH_3 , $\theta = 90^\circ$ and for C_2H_5 , the cone angle is 102° .¹¹⁴

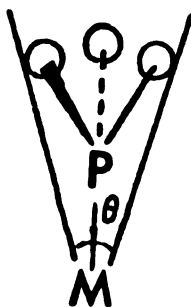


Figure 9. Definition of the Cone Angle

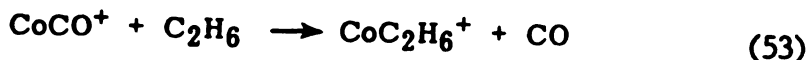
One interesting point raised by MCO^+ insertion is: why would MCO^+ insert into a C-H bond if calculations of the average molecular polarizability and $U(r)$ indicate that it should be easy to displace a CO before insertion? From Table 6 it is apparent that the energy of interaction $U(r)$, between M^+ and butane is dependent upon the location of M^+ relative to the C-C and C-H bonds of butane. Thus, certain locations of M^+ result only in weak interactions with the alkane which are too small to sufficiently compensate for the dissociation energy of the M^+-L bond. Under these circumstances it is possible for MCO^+ to remain "intact" and insert into a C-H bond. Interestingly, the gas phase reactions recently reported for MH^+ ⁵⁶ and MCH_3 and alkanes⁶³ indicate that these two metal ion-ligand complexes insert exclusively into the C-H bonds of alkanes unlike M^+ . For example, in the reaction of NiD^+ and ethane, NiC_2H_5^+ and HD are formed as the products (reaction (49)).



These results suggest that insertion of NiD^+ into a C-H bond occurs as a first step followed by the shift of a β -H onto the metal. HD is eliminated in the last step. Note that H_2 elimination is not observed in the reaction of Ni^+ and ethane. Apparently the presence of the H ligand on Ni^+ opens up new pathways for reaction just as the presence of CO on M^+ opens up new pathways for H_2 elimination.

Recall from chapter 5 that the possibility of CoCO^+

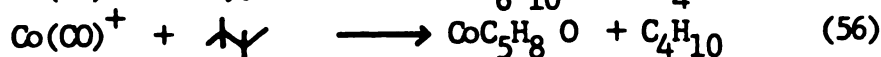
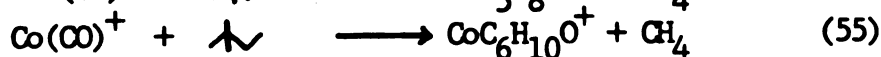
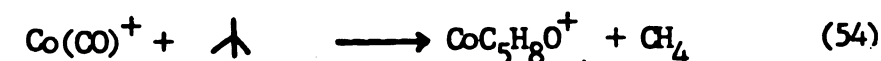
forming stronger bonds to amines than Co^+ was raised. Similarly, MCO^+ may form stronger bonds to alkanes than M^+ making insertion into the higher energy C-H bond favorable. [Note that $D(\text{C-H}) = 103 \text{ kcal/mol}$ and $D(\text{C-C}) = 85 \text{ kcal/mol}$].⁸² Promotion energies⁹⁰ indicate the amount of energy required by M^+ to achieve an electron configuration conducive to two-bond formation. Perhaps less promotion energy is required for MCO^+ relative to M^+ due to the presence of the ligand which causes the electron configuration of MCO^+ to be "inherently" more conducive towards bonding to other ligands. This might explain why CoCO^+ reacts with methane and ethane (Tables 2 and 3) and Co^+ does not react at all. The ionic products of reactions (51) and (53) may involve a Co^+ bonded to an H and an alkyl group.



Furthermore, perhaps the concept of promotion energy can be used to explain the lack of reactivity observed for CoNO^+ and alkanes.

Interestingly, 2,2-dimethylpropane, 2,2 dimethylbutane and 2,2,4,4-tetramethylbutane all react with CoCO^+ to form a product in which the CO ligand is retained while a smaller

neutral alkane is eliminated. These are the only examples in which CO retention in the product ion is observed. Each of these branched alkanes contains at least one neopentyl group. These results suggest that it is possible for CoCO^+ to insert into the C-C bond of branched alkanes containing a neopentyl group.



Thus, once CoCO^+ inserts into a C-C bond, a β -hydrogen shifts, followed by the elimination of a small neutral alkane. Note that Co^+ reacts with these branched alkanes to eliminate the same small neutral alkanes as CoCO^+ does.

RELATIVE RATES

Reactivity can also be considered in terms of relative rates. Here we will define the reactivity of ML_n^+ [$n = 0-2$] in terms of the relative rate at which they react (as opposed to defining reactivity as the number of different products ML_n^+ can form). The relative rates calculated for M^+ , ML^+ , and ML_2^+ in 2:1 mixtures of alkane to metal compound are presented in Tables 30 through 32. These relative rates, K , were estimated from the relative abundances of the reactant product ion, I (Product), in the mass spectra of the reaction mixtures using equation (20):

**Table 31. Relative Reaction Rates
in 2:1 Mixtures of Alkanes to $\text{Co}(\text{CO})_3\text{NO}$**

$\text{Co}(\text{CO})_n^+ +$	<u>n=0</u>	<u>n=1</u>	<u>n=2</u>
Methane	0	1.0	0
Ethane	0	1.0	0
Propane	0.14	1.0	0
Butane	1.0	0.27	0.65
Pentane	0.95	0.78	1.0
Hexane	1.0	0.70	0.71
Heptane	1.0	0.93	0.12
Octane	0.28	0.21	1.0
Nonane	1.0	0.92	0.76
Decane	0.90	1.0	0.71
2-Methylpropane	1.0	0.19	0.74
2,2-Dimethylpropane	0.89	0.69	1.0
2-Methylbutane	0.89	0.71	1.0
2,2-Dimethylbutane	0.56	1.0	0
2,3-Dimethylbutane	1.0	0.91	0
2,2,3,3-Tetramethylbutane	0.48	1.0	0.79
3-Methylpentane	0.32	1.0	0
2,4-Dimethylpentane	0.38	0.55	1.0
2,2,4-Trimethylpentane	0.67	1.0	0.45
2,3,4-Trimethylpentane	0.67	1.0	0.17

**Table 32. Relative Reaction Rates
in 2:1 Mixtures of Alkanes to $\text{Ni}(\text{CO})_4$**

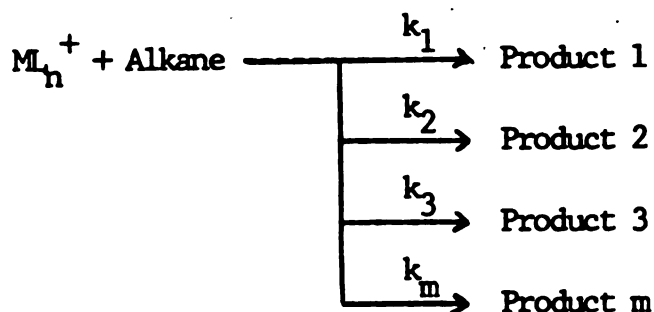
$\text{Ni}(\text{CO})_n^+ +$		<u>n=0</u>	<u>n=1</u>	<u>n=2</u>
	Methane	0	0	0
	Ethane	0	0	0
	Propane	1.0	0.24	0.14
	Butane	1.0	0.37	0.05
	Pentane	0.32	1.0	0.81
	Hexane	1.0	0.87	0.77
	Heptane	1.0	0.95	0.58
	Octane	1.0	0.19	0.08
	Nonane	0.91	1.0	0.53
	Decane	1.0	0.82	0.89
	2-Methylpropane	0.15	0.19	1.0
	2,2-Dimethylpropane	0.93	1.0	0.88
	2-Methylbutane	0.76	1.0	0.82
	2,2-Dimethylbutane	1.0	0.94	0.44
	2,3-Dimethylbutane	0.75	1.0	0.48
	2,2,3,3-Tetramethylbutane	0.49	1.0	0
	3-Methylpentane	0.42	1.0	0.50
	2,4-Dimethylpentane	0.63	0.77	1.0
	2,2,4-Trimethylpentane	0.62	1.0	0
	2,3,4-Trimethylpentane	0.99	1.0	0.05

**Table 33. Relative Reaction Rates
in 2:1 Mixtures of Alkanes to $\text{Ni}(\text{PF}_3)_4$**

$\text{Ni}(\text{PF}_3)_n^+$ +	<u>n=0</u>	<u>n=1</u>	<u>n=2</u>
Methane	0	0	0
Ethane	0	0	0
Propane	0.10	1.0	0.49
Butane	0.38	1.0	0.43
Pentane	1.0	0.70	0
Hexane	0.44	1.0	0.33
Heptane	0.40	1.0	0
Octane	0.61	1.0	0.52
Nonane	1.0	0.88	0.85
Decane	0.45	0.51	1.0
2-Methylpropane	0.24	1.0	0.90
2,2-Dimethylpropane	0.72	1.0	0.97
2-Methylbutane	0.61	1.0	0.93
2,2-Dimethylbutane	1.0	0	0
2,3-Dimethylbutane	0.62	0.72	1.0
2,2,3,3-Tetramethylbutane	0.66	1.0	0
3-Methylpentane	0.54	1.0	0.93
2,4-Dimethylpentane	0.47	1.0	0.85
2,2,4-Trimethylpentane	0.32	1.0	0.12
2,3,4-Trimethylpentane	0.29	1.0	0.91

$$K \propto \frac{\sum_{i=1}^m I(\text{Product } i)}{I(\text{ML}_n^+) + \sum_{i=1}^m I(\text{Product } i)} \quad (20)$$

The fastest reactions are arbitrarily assigned a magnitude of 1.0 in Tables 30 through 32. These results suggest the following trends in reactivity for cobalt- and nickel-containing ions for ML_n^+ reacting with an alkane:



$$K(\text{Co}^+) \cong K(\text{CoCO}^+) > K(\text{Co}(\text{CO})_2^+) \quad (57)$$

$$K(\text{Ni}^+) \cong K(\text{NiCO}^+) > K(\text{Ni}(\text{CO})_2^+) \quad (58)$$

$$K(\text{NiPF}_3^+) > K(\text{Ni}^+) > K(\text{Ni}(\text{PF}_3)_2^+) \quad (59)$$

$$\text{where } K \cong \sum_{i=1}^m k_i$$

From reactions (58) and (59), it follows that

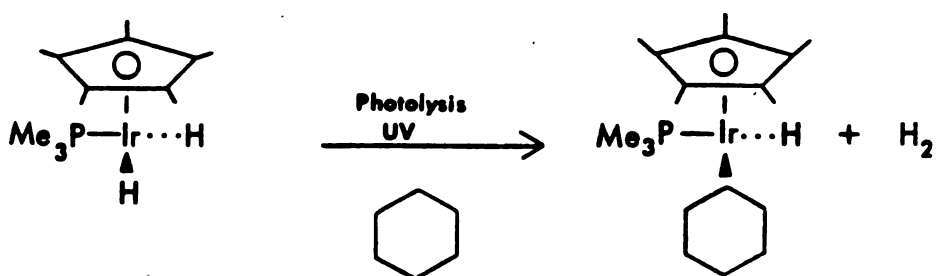
$$K(\text{NiPF}_3^+) > K(\text{Ni}^+) \cong K(\text{NiCO}^+)$$

Overall, the M^+ and MCO^+ ions react at approximately the same rate with alkanes. However, when a PF_3 ligand is present on Ni^+ , NiPF_3^+ is found to react faster than Ni^+ . In all cases, ML_2^+ reacts most slowly with alkanes.

SOLUTION CHEMISTRY PARALLELS

Compared to other chemically active molecules containing multiple bonds or lone pairs of electrons, alkanes, which consist of stable C-C and C-H σ bonds, have been found to be relatively inert in condensed phase chemistry. However, since alkanes are of fundamental importance in the chemical industry, recently there has been a drive towards devising systems capable of selectively activating the C-H or C-C bonds of alkanes. Many examples of the activation of C-H bonds in polar organic molecules by metal complexes in solution can be found.¹⁰⁴ Apparently, polar substituents make facile activation of the C-H bonds in these molecules possible.^{104,115} Alkanes obviously contain no polar substituents. However, the oxidative addition of a metal to the C-H bonds of alkanes has been reported recently in the literature. For example, Crabtree et al. reported the stoichiometric and selective dehydrogenation of cyclic alkanes. Apparently, the two acetone ligands in an iridium complex (which also contained two hydride and two triphenylphosphine ligands) are so weakly bound to Ir, they can easily be displaced by a hydrocarbon molecule. Crabtree suggests that the initial step in this reaction involves the insertion of Ir into a C-H bond of the alkane.⁸⁷ This reaction is carried out in 1,2-dichloroethane, a noncoordinating solvent. In addition, Bergman et al. have

reported the discovery of another iridium complex which adds oxidatively to the C-H bonds in saturated hydrocarbons leading to the formation of stable hydridoalkyl-metal complexes. This reaction proceeds at room temperature in a homogeneous solution. This process is illustrated for cyclohexane in reaction (60):⁸⁶



Note that this iridium complex only involves four ligands. Bergman suggests that upon photolysis the metal complex loses both of its hydrides as dihydrogen. As a result, the iridium complex is coordinatively unsaturated and capable of inserting into a C-H bond of cyclohexane. Furthermore, Bergman has recently reported that a similar rhenium complex

activates the C-H bonds in alkanes.¹¹⁶ As these examples may suggest, in solution the C-H bonds of alkanes are found to be preferentially activated over the C-C bonds by metal complexes. Apparently, the activation of C-C bonds is unfavored due to the steric hindrance that would result from the interaction of a metal complex and a C-C bond.¹¹⁵ Recall that similar reasoning was used to explain the preferential insertion of MCO^+ into C-H bonds in alkanes in the gas phase.

Furthermore, Poliakoff and Turner¹¹⁷ suggest that upon photolysis of $\text{Fe}(\text{CO})_5$ in a low-temperature methane matrix, $\text{Fe}(\text{CO})_5\text{CH}_4$ is formed. Their data indicate that the methane ligand in this metal complex is intact. These results are similar to those we presented earlier for the reactions of ML_2^+ and alkanes in which we suggested that intact alkanes were capable of displacing L.

Furthermore, in a study of the correlation between the activity of platinum crystal surfaces and the catalytic reactions of hydrocarbons, Somorjai et al. reported¹¹⁸ that highly coordinated atoms are the key components of catalysis with high turnover rates. Interestingly, their results suggest that metal-ligand catalysts will break and form H-H and C-H bonds quite readily. However, unlike a highly uncoordinated atom in a metallic cluster, metal ligand catalysts lack the ability to break C-C bonds.¹¹⁸

Thus, preferential attack of C-H bonds in alkanes by metal-ligand complexes is observed on platinum surfaces. In addition, Somorjai suggests that highly uncoordinated metal

atoms in metal clusters are capable of breaking C-C bonds. These results parallel those observed in the gas phase reactions of bare metal ions and alkanes where C-C bonds are preferentially attacked.

Other examples of the activation of C-C bonds by uncoordinated metal atoms can be found in the literature. For example, zirconium atoms have been reported to add oxidatively to the C-C (and C-H) bonds of methane, ethane, propene, and propane at cryogenic temperatures.¹¹⁹ Furthermore, cleavage of the C-C bonds in pentane by nickel clusters at low temperatures has been reported by Davis and Klabunde.¹⁰² Thus parallels between the observed reactions for M^+ in the gas phase and the reactions observed for metal atoms in condensed phases can also be made.

CONCLUSION

In conclusion, the ligand effects presented in this chapter have yielded some interesting insights into the gas phase chemistry of ML_n^+ ($n = 0,1,2$) and alkanes. Evidence indicating that intact alkanes are capable of displacing CO or PF_3 ligands was presented and rationalized on the basis of ion-induced dipole and energetic calculations. Also, the preferential insertion of ML^+ into C-H bonds resulting in H_2 elimination was discussed in terms of steric effects and

contrasted to the gas phase chemistry observed for M^+ . Finally condensed phase reactions, paralleling the gas phase reactions, were presented.

Note that, up to this point in time, work in the area of organometallic gas phase chemistry has centered on the characterization of the reactions occurring between various metal-containing ions and organic molecules. The purpose of this study has been to go beyond characterizing reactions by gaining new insights into the nature of the interaction occurring between metal ions and organic molecules in the gas phase. However, caution must be used in interpreting the results of the energetic calculations due to the numerous assumptions (already cited in the text) associated with this analysis. Furthermore, the author notes that in this analysis, no consideration of the dynamics associated with these ion/molecule reactions has been made.

CHAPTER 8

CONCLUSION

Chemical Ionization (CI) mass spectrometry is a technique in which sample molecules undergo ion/molecule reactions with reagent ions and thus become ionized. Since the energy transferred to the sample molecule in an ion/molecule reaction is less than that transferred upon ionization via conventional 70eV electron impact, CI is considered a "soft" ionization technique. As a result, the analyte molecule is found to undergo less fragmentation. Usually the molecular weight of the analyte can be readily determined from CI mass spectra. Furthermore, unlike the 70eV non-selective electrons in electron impact ionization reagent ions which react specifically with analyte molecules can be chosen for study. Thus CI reactions frequently yield structural information concerning the analyte molecule.

Previously in the area of gas phase organometallic chemistry, the focus has been on the characterization of the reactions of metal and metal-containing ions with organic molecules. A mechanism involving a metal ion insertion/ β -hydrogen shift/competitive ligand loss sequence has been used to explain the formation of the

majority of the product ions observed in these reactions. If each step in this mechanism were fully understood, products and branching ratios could be predicted a priori making metal ions ideal CI reagents. The metal insertion step appears to be most important in determining final product distributions.⁴³ However, it is the least understood step of this mechanism. Thus, although previous studies have provided useful insights into organometallic gas phase chemistry by revealing that metal ions react specifically with organic molecules, there is still much that is not understood about the nature of the interactions between metal ions and organic molecules. The purpose of this study was to gain a better understanding of the nature of this interaction.

The first part of the discussion, Chapter 5, provided a characterization of the gas phase reactions of cobalt and cobalt-containing ions with secondary and tertiary amines. This chapter illustrated the utility of $\text{Co}(\text{CO})_3\text{NO}$ as a CI reagent. It was shown that Co^+ produced from 70eV electron impact reacted specifically with amines. The mechanism consistent with the formation of product ions involved the oxidative addition of Co^+ to C-C and C-H bonds followed by a β -hydrogen atom transfer to the metal and then the elimination of a small neutral molecule such as H_2 or C_2H_6 . Knowledge of this mechanism allowed one to interpret the mass spectra of amines assigning structures to all of the

product peaks. Thus, specific structural information could be formulated since the observed chemistry depended upon the structures of the reactant amines. Furthermore, a characteristic series of ligand substitution reactions was observed yielding molecular weight information.

Metal and metal-containing ions were also found to react specifically with alkanes. Analogous to the amine chemistry, the observed product ions in alkane mixtures were indicative of initial metal ion insertion into C-C and C-H bonds. The data suggested that metal ions preferentially inserted into the C-C bonds of alkanes rather than into C-H bonds.

The purpose of Chapter 6 was to gain a better understanding of the insertion process as it occurs in alkanes. (Note that the functional group, X, in polar molecules, RX, may have a strong effect in "directing" the site of attack of the metal ion to certain skeletal bonds which may not be attacked in the corresponding alkane (RH).¹⁹ In the gas phase chemistry of M^+ ($M=Fe, Co, Ni$) with alkanes, the metal ion can insert into a number of C-C bonds to form intermediates of the type $R-M^+-R'$. As indicated by the product distributions, insertion into certain C-C bonds is preferred over others. To explain this observation, a correlation between the preference by M^+ for insertion into a particular skeletal bond and the ionization potentials of the alkyl radicals formed upon

insertion was noted. This correlation suggests an inverse relationship between $IP(C_nH_{2n+1})$ and $D(M^+-C_nH_{2n+1})$, i.e., IP decreases and bond energy increases as n increases. A similar relationship between IP and bond strengths of alkyl radicals to other cations such as Hg^+ was presented supporting this suggestion. Thus, this correlation may suggest that the preferred intermediates resulting from M^+ insertion into the C-C bonds of alkanes involve those in which the (M^+-R) bonds which are formed are the strongest.

Finally in Chapter 7, ligand effects observed in the reactions of metal-containing ions and alkanes were discussed. With the addition of one or two ligands, three types of behavior were observed:

1. Ligand acted as a "spectator" and ML^+ reacted with an alkane just as M^+ did.
2. As the number of ligands on the metal exceeded one, ligand substitution products were favored.
3. The amount of H_2 elimination increased for MCO^+ as the size of the alkane increased implying that insertion into C-H bonds is favored by MCO^+ .

Differences in the chemistry of M^+ and ML_n^+ ($n=1,2$) with alkanes was explained on the basis of steric effects. Furthermore, evidence indicating that intact alkanes are capable of displacing CO or PF_3 ligands was presented and rationalized on the basis of ion/induced dipole energetic calculations. Parallels to condensed phase chemistry were made.

List of References

List of References

1. J. Allison, D.P. Ridge, J. Am. Chem. Soc., 101, 4998 (1979).
2. P.B. Armentrout, J.L. Beauchamp, J. Chem. Phys., 74, 2819 (1981).
3. R.W. Jones, R.H. Staley, J. Phys. Chem., 86, 1387 (1982).
4. C.J. Cassady, B.S. Freiser, J. Am. Chem. Soc., 107, 1566 (1985).
5. A. Tsarbopoulos, J. Allison, Organometallica, 3, 86 (1984).
6. J. Allison, D.P. Ridge, J. Am. Chem. Soc., 98, 7445 (1976).
7. J. Allison, D.P. Ridge, J. Organometal. Chem., 99, (C11 (1975)).
8. P.B. Armentrout, J.L. Beauchamp, J. Am. Chem. Soc., 102, 1736 (1980).
9. B.D. Radecki, Master's Thesis, Michigan State University, 1982.
10. M.F. Lappert, P.P. Power, A.R. Sanger, R.C. Srivastava, "Metal and Metalloid Amides;" Ellis Horwood Limited; West Sussex, England, 1980.
11. J.L. Beauchamp, Ann. Rev. Phys. Chem., 22, 527 (1971)
12. T.A. Lehman, M.M. Bursey, "Ion Cyclotron Resonance Spectroscopy," J. Wiley and Sons, New York (1976).
13. J.D. Baldeschwieler, Science, 159, 263 (1968).
14. J.D. Baldeschwieler, S. S. Woodgate, Acc. Chem. Res., 4, 114 (1971).
15. C.J. Drewery, G.C. Goode, K.R. Jennings, "Ion Cyclotron Mass Spectrometry, "MTP International Review of Science-Physical Chemistry," Series One, Volume Five, Mass Spectrometry, A. Macoll, Ed., University Park Press, Baltimore, 183 (1972).
16. J.M.S. Henis, "Ion Cyclotron Resonance Spectrometry," Ion-Molecule Reactions, Vol. 2, J. L. Franklin, Ed., Plenum Press, New York, 395 (1972).
17. G.C. Goode, A.J. Ferrer-Correia, K.R. Jennings, Int. J. Mass Spec. Ion Phys., 5, 229 (1970).
18. G.A. Junk, H.J. Svec, Z. Naturforsch., 23, 1 (1968).
19. R.E. Winters, R.W. Kiser, J. Inorg. Chem., 3, 699 (1964).

20. E. Schumacher, R. Taubenest, *Helv. Chim. Acta*, 47, 1525 (1964).
21. J. Muller, "Ion Molecule Reactions of Organometallic Complexes," *Advances in Mass Spectrometry*, Vol. 6, A. R. West, Ed., Appl. Sci. Publishers, Ltd. England, 823 (1974).
22. R.C. Dunbar, J.F. Ennever, J.P. Fackler, *Inorg. Chem.*, 12, 2734 (1973).
23. M.S. Foster, J.L. Beauchamp, *J. Am. Chem. Soc.*, 93, 4924 (1971).
24. M.S. Foster and J.L. Beauchamp, *J. Amer. Chem. Soc.*, 97, 4808 (1975).
25. M.S. Foster and J.L. Beauchamp, *J. Amer. Chem. Soc.*, 97, 4814 (1975).
26. R.R. Corderman and J.L. Beauchamp, *Inorg. Chem.*, 15, 665 (1976).
27. R.R. Corderman and J.L. Beauchamp, *J. Amer. Chem. Soc.*, 98, 5700 (1976).
28. R.D. Bach, A.T. Weibel, J. Patane and L. Kevan, *J. Amer. Chem. Soc.*, 98, 6237 (1976).
29. R. V. Hodges and J. L. Beauchamp, *Anal. Chem.*, 48, 825 (1976).
30. J. Allison, D.P. Ridge, *J. Am. Chem. Soc.*, 99, 35 (1977).
31. G.H. Weddle, J. Allison, D.P. Ridge, *J. Amer. Chem. Soc.*, 99, 105 (1977).
32. G. Dietz, D.S. Chatelier, D.P. Ridge, *J. Am. Chem. Soc.*, 100, 4905 (1978).
33. J. Allison and D.P. Ridge, *J. Am. Chem. Soc.*, 100, 163 (1978).
34. J. Allison, R. Kinser, T.G. Dietz, M. deAngelis, D.P. Ridge, *J. Amer. Chem. Soc.*, 100, 2706 (1978).
35. R.C. Burnier, T.J. Carlin, W.D. Reents, Jr., R.B. Cody, R.K. Lengel, B.S. Freiser, *J. Am. Chem. Soc.*, 101, 7127 (1979).
36. J. Allison, R.B. Freas, D.P. Ridge, *J. Amer. Chem. Soc.*, 101, 1332 (1979).
37. J.L. Beauchamp, A.E. Stevens, R.R. Corderman, *Pure & Appl. Chem.*, 51, 967 (1979).
38. R.C. Burnier, G.D. Byrd, B.S. Freiser, *Anal. Chem.*, 52, 1641 (1980).

39. P.B. Armentrout, J.L. Beauchamp, Chem. Phys., 50, 37 (1980).
40. R.W. Jones and R.H. Staley, J. Am. Chem. Soc., 102, 3794 (1980).
41. J.S. Uppal, R.H. Staley, J. Am. Chem. Soc., 102, 4144 (1980).
42. L.F. Halle, P.B. Armentrout, J.L. Beauchamp, J. Am. Chem. Soc., 103, 962 (1981).
43. P.B. Armentrout, J.L. Beauchamp, J. Am. Chem. Soc., 103, 784 (1981).
44. A.E. Stevens, J.L. Beauchamp, J. Am. Chem. Soc., 103, 190 (1981).
45. P.B. Armentrout, L.F. Halle, J.L. Beauchamp, J. Am. Chem. Soc., 103, 6624 (1981).
46. P.B. Armentrout, J.L. Beauchamp, J. Am. Chem. Soc., 103, 6628 (1981).
47. J.S. Uppal, D.E. Johnson, R.H. Staley, J. Am. Chem. Soc., 103, 508 (1981).
48. C. Burnier, G.D. Byrd, B.S. Freiser, J. Am. Chem. Soc., 103, 4360 (1981).
49. G.D. Byrd, R.C. Burnier, B.S. Freiser, J. Am. Chem. Soc., 104, 3565 (1982).
50. G.D. Byrd, B.S. Freiser, J. Am. Chem. Soc., 104, 5944 (1982).
51. L.F. Halle, R. Houriet, M.M. Kappes, R.H. Staley, J.L. Beauchamp, J. Am. Chem. Soc. 104, 6293 (1982).
52. L.F. Halle, P.B. Armentrout, J.L. Beauchamp, Organometallics, 1, 963 (1982).
53. R. Houriet, L.F. Halle, J.L. Beauchamp, Organometallics, 2, 1818 (1983).
54. D.B. Jacobson, B.S. Freiser, J. Am. Chem. Soc., 105, 7492 (1983).
55. D.B. Jacobson, B.S. Freiser, J. Am. Chem. Soc., 105, 7484 (1983).
56. T.J. Carlin, L. Sallans, C.J. Cassady, D.B. Jacobson, B.S. Freiser, J. Am. Chem. Soc., 105, 6320 (1983).
57. D.B. Jacobson, B.S. Freiser, J. Am. Chem. Soc., 105, 5197 (1983).

58. D.B. Jacobson, B.S. Freiser, J. Am. Chem. Soc., 105, 736 (1983).
59. M. Lombarski, J. Allison, Int. J. Mass Spectron. Ion Phys., 49, 281 (1983).
60. S.K. Huang, J. Allison, Organometallics, 2, 883 (1983).
61. C.J. Cassady, B.S. Freiser, J. Am. Chem. Soc., 106, 6176 (1984).
62. D.B. Jacobson, B.S. Freiser, J. Am. Chem. Soc., 106, 5351 (1984).
63. D.B. Jacobson, B.S. Freiser, J. Am. Chem. Soc., 106, 3891 (1984).
64. D.B. Jacobson, B.S. Freiser, J. Am. Chem. Soc., 106, 3900 (1984).
65. D.B. Jacobson, B.S. Freiser, Organometallics, 3, 13 (1984).
66. T.C. Jackson, D.B. Jacobson, B.S. Freiser, J. Am. Chem. Soc., 106, 1252 (1984).
67. D.B. Jacobson, G.D. Byrd, B.S. Freiser, Inorg. Chem., 23, 553 (1984).
68. B.S. Larsen, D.P. Ridge, J. Am. Chem. Soc., 106, 1912 (1984).
69. R.B. Freas, D.P. Ridge, J. Am. Chem. Soc., 106, 825 (1984).
70. J. Wronka, D.P. Ridge, J. Am. Chem. Soc., 106, 67 (1984).
71. B.D. Radecki, J. Allison, J. Am. Chem. Soc., 106, 946 (1984).
72. C.J. Cassady, B.S. Freiser, S.W. McElvany, J. Allison, J. Am. Chem. Soc., 106, 125 (1984).
73. M.B. Wise, D.B. Jacobson, B.S. Freiser, J. Am. Chem. Soc., 105, 1590 (1985).
74. C.J. Cassady, B.S. Freiser, J. Am. Chem. Soc., 107, 1566 (1985).
75. D.B. Jacobson, B.S. Freiser, J. Am. Chem. Soc., 107, 1581 (1985).
76. J. Halpern, in "Organotransition Chemistry," Y. Ishii and M. Tsutsui, Plenum Press, New York, p. 109, 1975.
77. P.B. Armentrout, L.F. Halle, J.L. Beauchamp, J. Am. Chem. Soc., 103, 190 (1981).
78. A.E. Stevens, J.L. Beauchamp, J. Am. Chem. Soc., 103, 190 (1981).

79. R.R. Corderman, J.L. Beauchamp, J. Am. Chem. Soc., 98, 3998 (1976).
80. J. Muller, W. Goll, Chem. Ber., 106, 1129 (1973).
81. J. Muller, W. Holzinger, W. Kalbfus, J. Organomet. Chem., 97, 213 (1975).
82. Bond strengths calculated by using the data from:
a) J.L. Franklin, J.G. Dillard, H.M. Rosenstock, J.T. Herron, K. Draxl, Nat. Stand. Ref. Data Ser., Nat. Bur. Stand., 26 (1969). b) H.M. Rosenstock, K. Draxl, B.W. Steiner, J.T. Herron, J. Phys. Chem. Ref. Data, 6 (1977). c) D.P. McMillen, D.M. Golden, Ann. Rev. Phys. Chem. 33, 493 (1982). d) J.D. Cox, G. Pilcher, "Thermochemistry of organic and Organometallic Compounds," Academic Press, New York (1970).
83. D.A. Aue, M.T. Bowers, "Gas Phase Ion Chemistry," v. 2, M.T. Bowers, Ed., Academic Press, New York (1979).
84. D. Wobschall, "Ion Cyclotron Resonance Spectrometer," Rev. Sci. Instr., 36, 466 (1965).
85. A. Warnick, L.R. Anders, T.E. Sharp, Rev. Sci. Instr., 45, 929 (1974).
86. A.H. Janowicz, R.G. Bergman, J. Am. Chem. Soc., 104, 3521 (1982).
87. R.H. Crabtree, J. Quirk, J. Mihelcic, J. Am. Chem. Soc., 104, 107 (1982).
88. See, for example: a) P.B. Armentrout, J.L. Beauchamp, J. Am. Chem. Soc., 102, 1736 (1980). b) J.A. Connor in "Topics in Current Chemistry. No. 71. Inorganic/Chemistry/Metal Carbonyl Chemistry," F.L. Boschke, Ed., Springer-Verlag, New York (1977).
89. J.B. Hendrickson, D.J. Cram, G.S. Hammond, "Organic Chemistry," McGraw-Hill Book Company, New York (1970).
90. S.J. Babinec, J. Allison, J. Am. Chem. Soc., 106, 7718 (1984).
91. P.B. Armentrout, N. Aristov, R. Georgiadis, L. Sunderlin, "33rd Annual Conference on Mass Spectrometry and Allied Topics," San Diego, 1985, paper ROA5.
92. F.A. Houle, J.L. Beauchamp, J. Am. Chem. Soc., 101, 4067 (1979).
93. J.M. Williams, W.H. Hamill, J. Chem. Phys., 49, 4467 (1968).
94. F.P. Lossing, A. Maccoll, Can. J. Chem., 54, 990 (1976).

95. A. Tsarbopoulos, B.D. Radecki, J. Allison, "32nd Annual Conference on Mass Spectrometry and Allied topics," San Antonio, 1984, paper TOD 10.
96. I. Fleming, "Frontier Orbitals and Organic Chemical Reactions," John Wiley and Sons, New York, 1976.
97. M.J. Wax, J.M. Stryker, J.M. Buchanan, C.A. Kovac, R.G. Bergman, J. Am. Chem. Soc., 106, 1121 (1984).
98. G.W. Parshall, Acc. Chem. Res., 8, 113 (1975).
99. T.H. Tulip, J.A. Ibers, J. Am. Chem. Soc., 101, 4201 (1979).
100. H.F. Schaefer, Acc. Chem. Res., 10, 287 (1977).
101. L. Abis, A. Sen, J. Halpern, J. Am. Chem. Soc., 100, 2915 (1978).
102. S.C. Davis, K.J. Klabunde, J. Am. Chem. Soc., 100, 5973 (1978).
103. P.L. Watson, D.C. Roe, J. Am. Chem. Soc., 104, 6471 (1982).
104. F.A. Cotton, G. Wilkinson, "Advanced Inorganic Chemistry," John-Wiley & Sons, New York, (1980).
105. K.J. Miller, J.A. Savcik, J. Am. Chem. Soc., 101, 7206 (1979).
106. J.O. Hirschfelder, C.F. Curtiss, R.B. Bird, "Molecular Theory of Gases and Liquids," John-Wiley & Sons, New York (1964).
107. S.W. Benson, "The Foundation of Chemical Kinetics," McGraw-Hill Book Company, Inc., New York (1960).
108. L.F. Halle, W.E. Crowe, P.B. Armentrout, J.L. Beauchamp, Organometallics, 3, 1694 (1984).
109. R.W. Kiser, M.S. Krassol, J. Am. Chem. Soc., 89, (1967).
110. J.E. Huheey, "Inorganic Chemistry," Harper and Row, Publishers, New York (1978).
111. F. Daniels, R.A. Alberty, "Physical Chemistry," John-Wiley & Sons, Inc., New York (1975).
112. K.G. Denbigh, Trans. Faraday Soc., 36, 936 (1940).
113. S. Fliszar, "Charge Distributions and Chemical Effects," Springer-Verlag, New York (1983).
114. C.A. Tolman, Chem. Rev., 77, 313 (1977).
115. A.E. Shilov, "Activation of Saturated Hydrocarbons by Transition Metal Complexes," D. Reidel Publishing Company, Boston (1984).

- 116. R.G. Bergman, P.F. Seidler, T.T. Wenzel, J. Am. Chem. Soc., 107, 4358 (1985).
- 117. M. Poliakoff, J.J. Turner, J.C.S. Dalton, 2277 (1974).
- 118. G.A. Somorjai, D.W. Blakely, Nature, 258, 580 (1975).
- 119. R.J. Remick, T.A. Asunta, P.S. Skell, J. Am. Chem. Soc., 101, 1320 (1979).